The role of actin cytoskeleton downstream of the Src oncogene in the earlier events of breast tumour progression

Sandra Raquel de Oliveira Tavares

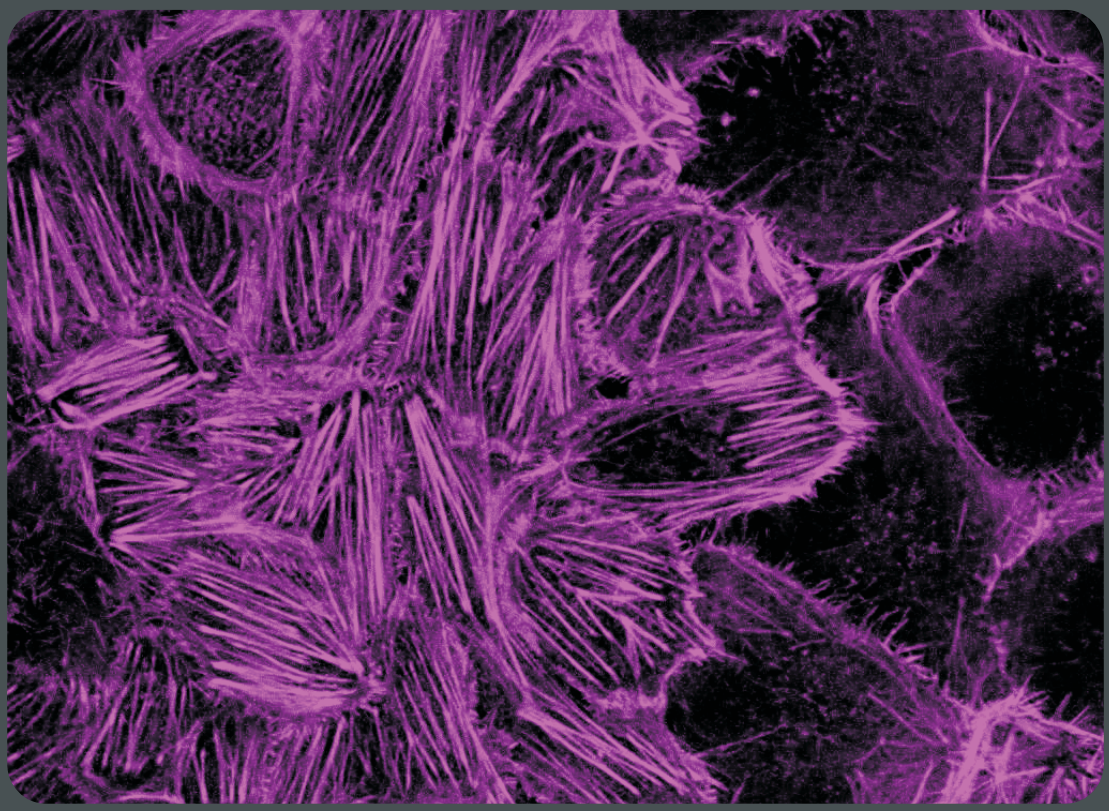

Dissertation presented to obtain the Ph.D degree in Cell Biology

Instituto de Tecnologia Química e Biológica António Xavier | Universidade Nova de Lisboa

Oeiras,
November, 2016

UNIVERSIDADE NOVA DE LISBOA

The role of actin cytoskeleton downstream of the Src oncogene in the earlier events of breast tumour progression

Sandra Raquel de Oliveira Tavares

Dissertation presented to obtain the Ph.D degree in Cell Biology
Instituto de Tecnologia Química e Biológica António Xavier | Universidade Nova de Lisboa

Research work coordinated by:

INSTITUTO GULBENKIAN DE CIÊNCIA

Oeiras, November, 2016

Declaração/ Declaration

Declaro que esta dissertação é o resultado do meu próprio trabalho desenvolvido entre Abril 2012 e Janeiro 2016 no laboratório da Dra. Florence Janody, Instituto Gulbenkian de Ciência, Oeiras, Portugal. Este doutoramento foi realizado no âmbito do Programa Gulbenkian de Doutoramento (edição 2011-2012). Os capítulos 2, 3 e 4 estão incluídos num manuscrito submetido para publicação com autoria de Sandra Tavares, André Vieira, Anna Verena Taubenberger, Nuno Pimpão Santos Martins; Catarina Brás-Pereira; Margarida Araújo, António Polónia, Joana Vaz, José Pereira Leal, Jochen Guck, Joana Paredes e Florence Janody.

I declare that this dissertation is a result of my own reserach carried out between April 2012 e January 2016 in the laboratory of Dr. Florence Janody, Instituto Gulbenkian de Ciência, Oeiras, Portugal. Chapters 2, 3 and 4 are part of a manuscript submitted for publication authored by Sandra Tavares, André Vieira, Anna Verena Taubenberger, Nuno Pimpão Santos Martins; Catarina Brás-Pereira; Margarida Araújo, António Polónia, Joana Vaz, José Pereira Leal, Jochen Guck, Joana Paredes and Florence Janody.

Apoio Financeiro/ Financial Support

Esta dissertação teve o apoio financeiro da FCT, no âmbito do Quadro Comunitário de Apoio, bolsa de doutoramento #SFRH/BD/51884/2012, da Fundação Calouste Gulbenkian e Liga Portuguesa contra o Cancro/Pfizer.

This dissertation had the financial support from FCT through the Quadro Comunitário de Apoio, doctoral fellowship #SFRH/BD/51884/2012, Fundação Calouste Gulbenkian and Liga Portuguesa contra o Cancro/Pfizer.

Acknowledgements

What an exciting ride it was!

I guess that is due to the beauty and magic of IGC. There is so much more besides science in these corridors. So many smiles exchanged between people that the only thing they share is the passion for science. Knowledge is our aim and we are happy pursuing it. Well, at least that was how I felt during these 5 years. IGC, the geek wonderland. It didn´t take me long to realize that I had found "my place".

The main person responsible for this was obviously my supervisor, Florence. You gave me exactly what I was looking for without even knowing it. I said this at the beginning and it is still true. Florence, you gave me the support I needed in tough moments. You were such a cool supervisor that you laughed at most of my jokes, even the ones that were not appropriate between supervisor and student (*You really shouldn´t support this kind of behaviour!*). Besides giving me the chance to do really cool science, I must say that you taught me something much more inspiring. You showed me the strength and commitment that it takes to stand up for our values. Fighting for our convictions is not just for young teenagers, it's a feature of courageous adults.

The opportunity to work at the Institute was given to me by Thiago Carvalho and Prof. António Coutinho. I couldn´t thank you more and I hope I have fulfilled your expectations. I must acknowledge the directors of the programme, Élio, and the institute, Jonathan and Jorge. Élio, thank you for keeping our programme up and running; Jonathan, in your own way, you stimulated my most pro-active side and, I thank Jorge for the informal conversations, but most of all, for the consideration and respect that you always had for me, my ideas and my projects.

My dear Communication Team, I had so much fun collaborating with you! Because of you, I met amazing people and had extraordinary experiences

talking about science. If someone would tell me, back in 2011, that I would teach cell biology to Catarina Furtado, I would laugh so hard… For sure, Science sounds better with you!!!

Now, the friends…

Sofia, my ebony goddess, your generosity and devotion to IGC was to me the first evidence that I was in a special place. I wasn´t wrong! You are the glue that keeps us all together and under your embrace we thrive. Looking back and thinking in the way you took care of me gets me so emotional... Fomos primas, somos primas. Adoro-te muito.

There is no way I can thank in the right measure to Bea and Catarina. If I was so happy doing this PhD, is a lot due to you two. You showed me what a group is. It is really hard to thank you. You brought so much to my life that I have no idea how to thank you. For sure I thank you for the laughter and concern. But saying "Thank you for the Friendship" is too vague, "Thank you for the advices" is too short and "Thank you for the patience" is too obvious…

To my dear CCR's: Carla, Paulo Duarte and Ana Rita Marques. It was fun to be part of your gang. I'll never forget the advices in times of trouble. Listening to me during this last year was not easy, I know, for this reason, my dear Isa, a big thanks! To my other friends spread across the institute, Marta, Rita, Filipe, Barroso, Catarina Júlio, Inês and Cláudia Bispo; and to the ones that already left IGC: Rui Gardner, Sara, Alex, Ânia, and Cláudia Andrade. You were the walls of "my IGC", with you I always felt at home.

André and Anna, thank you for being so much more than collaborators. Your help and commitment for this project were crucial. I was really fortunate for having you as partners in this journey. Thank you for teaching me so much and for making me feel like part of your teams! Sweet Margarida, it was a pleasure to work with someone so devoted and enthusiastic as you are.

To my closest family that has always believed in me. You gave me the motivation to do this PhD, even being so far away from you all. I have missed you tremendously, but you made it better with your kind words and support. Obrigada por tornarem a distância mais fácil de suportar.

Finally, to my beloved Ricardo. You have been my rock. Accepting to come with me, to the lab at midnight with a storm alert, it's something that only a true partner in life would be up for. Can't wait to be with you again.

If I loved you less, I might be able to talk about it more.

Jane Austen, *Emma*

Sumário

A tumorigénese é um processo em que as células progressivamente adquirem alterações genéticas e epigenéticas em genes promotores e supressores tumorais, promovendo a vantagem de crescimento e proliferação das mesmas. Alterações posteriores poderão condenar essas células pré-malignas à transição a malignas com capacidades invasivas e metastáticas. Proto-oncogenes da família das cínases Src foram ligados à tumorigénese, e a sua sobre-expressão e sobre-activação foi descrita em cancro da mama. O aumento da actividade de Src foi associado a aumento de proliferação celular, sobrevivência, transição epitélio-mesênquima, migração, invasão e matástases. Apesar de Src ser bem conhecido no despoletar de motilidade de células cancerígenas, migração e invasão, pela regulação de actina filamentosa (F-actina); ainda não se sabe Src também utiliza a F-actina para promover proliferação e sobrevivência de células tumorais em estádios pré-malignos. Em 2013, o nosso laboratório demonstrou que Src promove a acumulação de F-actina apical no epitélio de *Drosophila*. Por sua vez, a F-actina limita a apoptose ou o crescimento descontrolado de tecido induzidos por Src.

O principal objectivo deste estudo foi investigar se a F-actina desempenha um papel subsequente à activação de Src, na promoção da aquisição de características de cancro da mama pré-maligno. De acordo com a esta hipótese, eu observei que a expressão de genes codificantes de proteínas que se ligam à actina está predominantemente afectada em lesões benignas da mama. Entre estas, Ena/VASP-like (EVL) e cinco outras proteínas também se encontravam

desreguladas numa linha celular indutível por tratamento com tamoxifeno, MCF10A-ER-Src. Adicionalmente, estas também se encontravam envolvidas no crescimento descontrolado de tecido induzido por Src, em *Drosophila melanogaster.* As minhas observações alegam que muito cedo na progressão do cancro da mama, Src afecta a expressão destas seis proteínas que se ligam à actina e que por sua vez, estas controlam o crescimento tumoral pela regulação de redes de F-actina especializadas (Capitulo 2).

Depois utilizando a linha celular de mama, humana e que através de tratamento com tamoxifeno possibilita a reconstituição *in vitro,* do percurso natural de cancro da mama induzido por Src (MCF10A-ER-Src), mostrei que a transformação celular pode ser dividida em duas fases. No início da transformação celular, baixos níveis de activação de Src promovem a polimerização transiente de fibras de actina polarizadas, levando a um aumento da rigidez celular e estando associados a capacidade de crescimento independente de factores de crescimento. Posteriormente, a fibras de actina são dissociadas, a células perdem rigidez e adquirem características malignas. Assim, enquanto a perda de rigidez celular permite a invasão celular/metástases, o meu trabalho revela que o enrijecimento das células mediado por fibras de actina poderá levar ao crescimento tumoral durante os estádios pré-malignos (Capitulo 3).

Por fim, eu observei que durante o início da transformação celular da linha celular MCF10A-Er-Src, Src induz o aumento transiente de EVL e a sua mobilização para as extremidades das fibras de actina dependentes de Src. A polarização destas fibras, realizada por EVL, é necessária para a promoção de rigidez celular, proliferação e progressão para o fenótipo maligno. Assim, eu mostro que níveis elevados de EVL são predominantemente encontrados em tumores de mama pré-malignos e estão associados ao sub-tipo molecular Luminal A (Capitulo 4).

Nesta tese, eu demonstro que a F-actina também desempenha um papel consequente à activação de Src, para a promoção da aquisição de características pré-malignas em cancro da mama. Em suma, as minhas observações estão de

acordo com um modelo no qual no inicio da progressão tumoral, baixos níveis de activação de Src promovem a agregação de fibras polarizadas e enrijecimento celular para sustentar a expansão de lesões precursoras de cancro da mama. Enquanto em estádios mais avançados, níveis elevados de Src reduzem a rigidez celular para permitir a invasão de células cancerígenas. Acredito, portanto, que estas observações poderão ter um impacto significativo no desenvolvimento de novas ferramentas de diagnóstico em estádios precoces de cancro da mama.

Summary

Tumorigenesis is a multistep process, by which cells acquire genetic and epigenetic alterations in oncogenes and tumour suppressor genes, which provide growth and/or survival advantage. Subsequent alterations may condemn these pre-malignant cells into malignant ones with invasive and metastatic abilities. Proto-oncogenes of the Src-family kinases have been linked to tumorigenesis and their over-expression and activation described in breast cancer. Increased Src activity has been associated with increased cell proliferation, survival, epithelial-mesenchymal transition (EMT), migration, invasion and metastasis. Although Src is well-known to trigger cancer cell mobility, migration and invasion, through regulation of filamentous actin (F-actin), whether it also uses F-actin to promote proliferation and survival of tumour cells at pre-malignant stages remains unknown. Our lab has demonstrated that Src promotes apical F-actin accumulation in *Drosophila* epithelia. In turn, F-actin limits Src-induced apoptosis or tissue overgrowth.

The main goal of this study was to investigate if F-actin plays a role downstream of Src activation to promote the acquisition of pre-malignant breast cancer features. In agreement with this hypothesis, I found that the expression of genes encoding for actin binding proteins (ABPs) is predominantly affected in benign breast lesions. Among those, Ena/VASP-like (EVL), in addition to 5 others ABPs were also misregulated in the Tamoxifen (TAM)-inducible MCF10A-ER-Src cell line, and involved in Src-induced tissue overgrowth in *Drosophila*

melanogaster. My observations argue that early during breast tumour progression, Src affects the expression of these 6 ABPs that control tumour growth via the regulation of specialized F-actin networks (Chapter 2).

Then, using the Src inducible mammary epithelial cell line MCF10A-ER-Src, which recapitulates the natural history of Src-induced breast cancer, I showed that transformation can be divided into two distinct phases. Early during cellular transformation, low Src induction promotes the transient polymerization of polarized acto-myosin stress fibres that correlate with an increase in cell stiffness and the acquisition of self-sufficiency in growth properties. Following this phase, the acto-myosin stress fibres disassemble, cell soften and acquire malignant features. Thus, while cell softening allows for cell invasion/metastasis, my work reveals that stress fibre-mediated cell stiffening could drive tumour growth during the pre-malignant stage (Chapter 3).

Lastly, I found that early during transformation of the TAM-induced MCF10A-Er-Src cell line, Src induces the transient upregulation of EVL and its mobilization to the tips of the transient Src-dependent acto-myosin stress fibres. Polarization of these fibres by EVL is required to promote cell stiffening, cell growth and the progression toward a malignant phenotype. Accordingly, I show that high EVL levels is predominantly found in pre-malignant breast tumour samples and correlate with the Luminal A breast molecular subtype (Chapter 4).

In this thesis, I demonstrate that F-actin also plays a role downstream of Src activation to drive the acquisition of pre-malignant breast cancer features. All together, my observations are in agreement with a model by which early during breast tumour progression, low Src activity could promote the assembly of polarized stress fibres and cell stiffening to sustain the expansion of cancer precursors, while at later stages of carcinogenesis, higher Src activity reduces stress fibre-mediated cell stiffening to allow for cancer cell invasion. I believe that these findings can have a significant impact for the development of new diagnostic tools in early stages of breast cancer.

List of Abbreviations

Actin Binding Proteins	ABPs
Adenosine DiPhosphate	ADP
Adenosine Triphosphate	ATP
Adherens Junctions	AJ
Aldehyde dehydrogenase	ALDH
Atomic Force Microscopy	AFM
Atypical Ductal Hyperplasia	ADH
Bromodeoxyuridine	BrdU
Cancer Stem Cell	CSC
c-Jun N-terminal kinase	c-JNK
Crk-Associated Substrate	CAS
C-terminal Src kinase	CSK
Cytokeratin 5	CK5
Diaminobenzidine	DAB
Diaphanous-Related Formins	DRFs
Differentially Expressed	DE
Ductal Carcinoma In Situ	DCIS
Ena/VASP-Like	EVL
Enabled	Ena
Enhanced Chemi-Luminescence	ECL

Epidermal Growth Factor	EGF
Epidermal Growth Factor Receptor	EGFR
Epithelial-Mesenchymal Transition	EMT
Ethanol	EtOH
EVL knock-down	EVL KD
Extent	E
Extra-Cellular Matrix	ECM
Extracellular-signal Regulated Kinase/Mitogen-Activated Protein Kinase	ERK/MAPK
F-actin Binding	FAB
Filamentous Actin	F-actin
Filamin	FLN
Focal Adhesion	FA
Focal Adhesion kinase	FAK
frozen Robust Multi-Array Average	fRMA
G-actin Binding	GAB
Gene Expression Omnibus	GEO
Globular Actin	G-actin
Human Epidermal growth factor Receptor 2	HER2
Interleukin 6	IL6
Invasive Ductal Carcinoma	IDC
MCF10A-ER-Src	ER-Src
MCF10A-PBabe	PBabe
Metalloproteinases	MMPs
Mitogen-activated protein kinases	MAPK
National Center for Biotechnology Information	NCBI
N-terminal Ena/VASP Homology 1	EVH1
Nucleation Promoting Factors	NPFs
Oestrogen Receptor ,	ER
Oestrogen Receptor negative	ER-

Oestrogen Receptor positive	ER+
P-cadherin	P-cad
Phosphate Buffer Solution	PBS
phospho-Myosin Light Chain	pMLC
Progesterone Receptor	PR
Propidium Iodide	PI
Protein Tyrosine Phosphatase 1B	PTP1B
Receptor Tyrosine Kinases	RTKs
Retinoblastoma	RB
Signal Transducer and Activator of Transcription 3	STAT3
Src Family of non-receptor tyrosine Kinases	SFK's
Tamoxifen	TAM
Terminal Duct-Lobular Units	TDLU
Three-Dimensional	3D
Tris-buffered saline	TBS
Tropomyosins	TM
Tumour Initiating Cells	TICs
α-Cardiac Actin	α-CAA
α-Skeletal Actin	α-SKA

Contents

Chapter 1

General Introduction

"Para além da curva da estrada
Talvez haja um poço, e talvez um castelo,
E talvez apenas a continuação da estrada.
Não sei nem pergunto.
Enquanto vou na estrada antes da curva
Só olho para a estrada antes da curva,
Porque não posso ver senão a estrada antes da curva.
De nada me serviria estar olhando para outro lado
E para aquilo que não vejo.
Importemo-nos apenas com o lugar onde estamos.
Há beleza bastante em estar aqui e não noutra parte qualquer.
Se há alguém para além da curva da estrada,
Esses que se preocupem com o que há para além da curva da estrada.
Essa é que é a estrada para eles.
Se nós tivermos que chegar lá, quando lá chegarmos saberemos.
Por ora só sabemos que lá não estamos.
Aqui há só a estrada antes da curva, e antes da curva
Há a estrada sem curva nenhuma."

Alberto Caeiro, "Poemas Inconjuntos"

1.1 TUMOURS OF THE BREAST

1.1.1 BREAST ANATOMY AND PHYSIOLOGY

The female breast is a heterogeneous structure that serves as the mammary gland, producing and secreting milk. The mammary gland comprises several branching duct systems built from a series of polarized, bi-layered epithelial ducts. Each duct system drains through an individual lactiferous sinus. Lobules, the functional units of the mammary parenchyma, consist of a cluster of epithelium-lined ductules or acini that arise from proliferation of distal terminal ducts. Each terminal duct and its acini compose the terminal duct-lobular units (TDLU) (Masood & Kameh 2005; Boudreau et al. 2012) (Figure 1.1.A).

The duct systems reside in a complex microenvironment comprised by a laminin-rich basement membrane, that establishes the separation between a collagenous extracellular matrix and a variety of stromal cells types, such as adipocytes, mesenchymal stem cells, etc. (Masood & Kameh 2005; Gudjonsson et al. 2005; Boudreau et al. 2012). The ductal network is composed of two epithelial cell types: an inner layer of cuboidal to low columnar, polarized luminal cells, surrounded by an outer, discontinuous layer of myoepithelial cells, enclosed by the basement membrane. Both cell types are derived from breast epithelial precursor cells positioned within the luminal epithelial compartment (Masood & Kameh 2005; Gudjonsson et al. 2005) (Figure 1.1.B).

The most common form of breast cancer arises in the inner luminal epithelial cells within the TDLU (Masood & Kameh 2005; Gudjonsson et al. 2005).

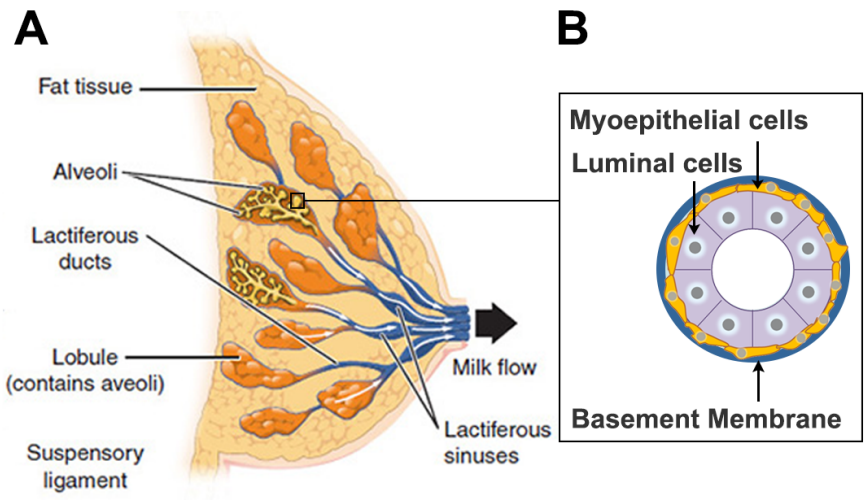

Figure 1.1: Normal adult female breast anatomy and histology. (A) The human Normal breast architecture is based on a branching ductal network. **(B)** Each terminal duct and its acini compose the TDLU. TDLU is lined by luminal epithelial cells, surrounded by myoepithelial cells and basement membrane. Adapted from www.thevisualmd.com.

1.1.2 BREAST CANCER EPIDEMIOLOGY

Breast cancer is the second most common cancer in the world after lung cancer, and by far the most frequent cancer among women. In 2012, a quarter of all cancers diagnosed were from the breast (Ferlay et al. 2014). In Portugal, as in the European Union, the incidence of female breast cancer has been increasing since 1975. On the contrary, the mortality has been decreasing. Although the survival rates were more favourable in Portugal than in the majority of European countries (Figure 1.2.A), breast cancer still stands as the major cause of death from cancer, representing 16.9% from a total of 10.600 cancer-related deaths (Ferlay et al. 2014).

Like most epithelial cancers, invasive breast carcinoma incidence increases rapidly with age. A worldwide age-standardized analysis has shown that there is a significant variation in the distribution of breast cancer, suggesting that there are several causes for breast cancer, besides aging (Figure 1.2.B). The aetiology of breast cancer is multi-factorial and involves diet and diet-related

factors; hormones and reproductive factors; exposure to ionizing radiation; family history of breast cancer; and benign breast disease (Ellis et al. 2003).

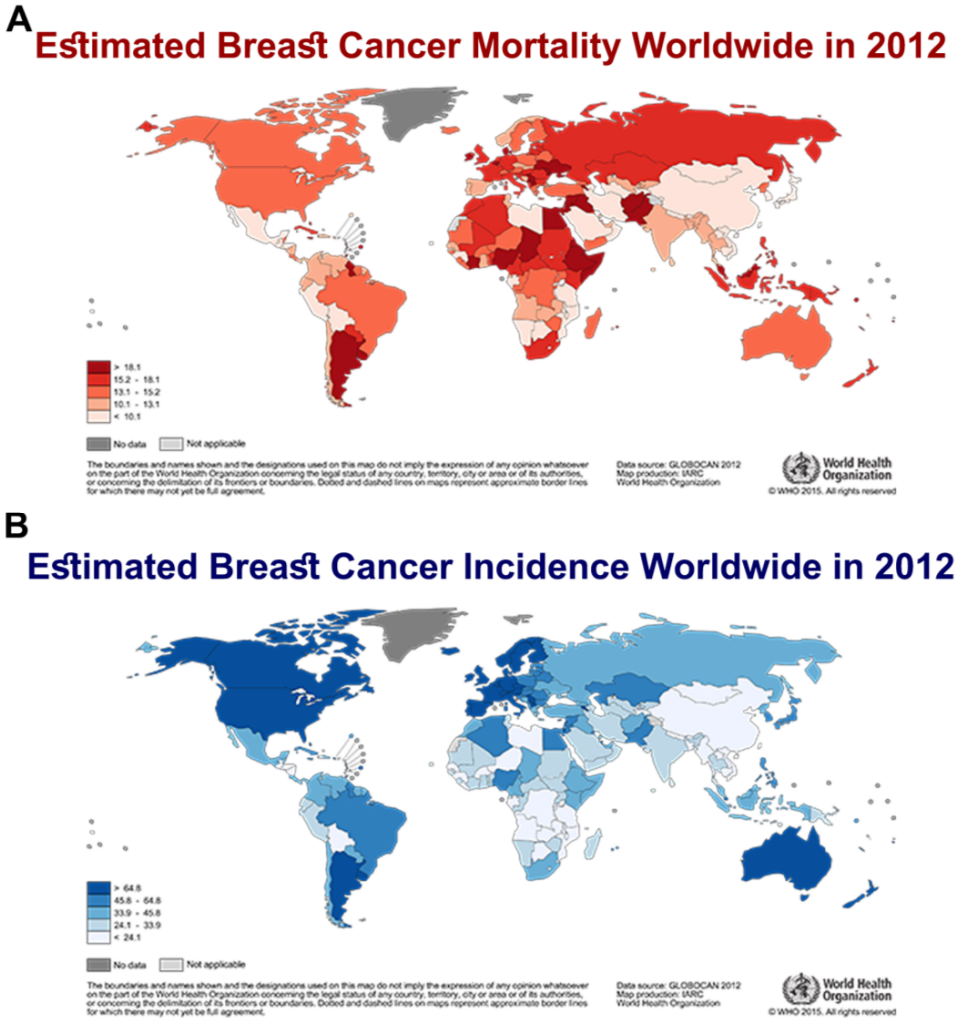

Figure 1.2: Global incidence (A) and mortality (B) rates of breast cancer. Age-standardized rates per 100.000 population. From Globocan 2012.

1.1.3 BREAST CANCER PATHOLOGY

Breast cancer is a complex and heterogeneous disease at molecular and clinical levels. It encompasses different entities with different risk factors, histological features, clinical behaviour and response to therapy. The commonest type of breast carcinoma is the Invasive Ductal Carcinoma, with a 45-70% incidence (Ellis et al. 2003). Unlike invasive breast cancer, which has been extensively studied, the molecular alterations that lead to the development and progression of breast cancer precursors remain poorly understood (Lopez-Garcia et al. 2010; Polyak 2007).

Breast Cancer progression

A benign lesion is defined by the epithelial growth that is confined to a specific site within a tissue and that has not penetrated through the basement membrane. On the contrary, in malignant lesions (cancer) there is evidence of invasion locally, and there is a possibility of metastasis (Weinberg Robert A. 2007). There are specific morphological and cytological patterns that were consistently associated with distinctive lesions and/or clinical outcomes. These patterns are called "histological types" (Weigelt et al. 2010) and are used to classify tumours.

Benign proliferative lesions of the breast have been reported to be associated with increased risk of breast cancer development. Some of these lesions show neoplastic proliferation with histological, immunohistochemical and molecular features identical to those of matched invasive breast cancers. Lesions that fulfil these criteria are considered breast cancer precursors (Lopez-Garcia et al. 2010).

Different models have been proposed to describe the tumour progression of Invasive Ductal Carcinomas (IDCs) (Ellis et al. 2003; Bombonati & Sgroi 2011). It is believed that these lesions follow a classical mode of progression, in which the normal breast tissue develops atypical ductal hyperplasia (ADH). This type of lesions is characterized by multifocal small clonal populations with monomorphic

cells and generally ovoid to rounded nuclei (Masood & Kameh 2005; Ellis et al. 2003). ADH is associated with risks of 8-10 folds to develop Ductal Carcinoma *in Situ* (DCIS) and 4-5 folds to evolve to IDC, (Ellis et al. 2003; Hartmann et al. 2005). DCIS is a neoplastic proliferative lesion with complete replacement of normal ducts by atypical cells, confined within spaces bordered by myoepithelium and basement membrane. Considered a precursor lesion (obligate or non-obligate), DCIS has a relative risk of 8-11 folds to acquire malignant features and evolve to IDC. IDC's are defined by the invasion of the surrounding stroma and a marked tendency to metastasize to distant organs (Lopez-Garcia et al. 2010; Bombonati & Sgroi 2011; Ellis et al. 2003) (Figure 1.3).

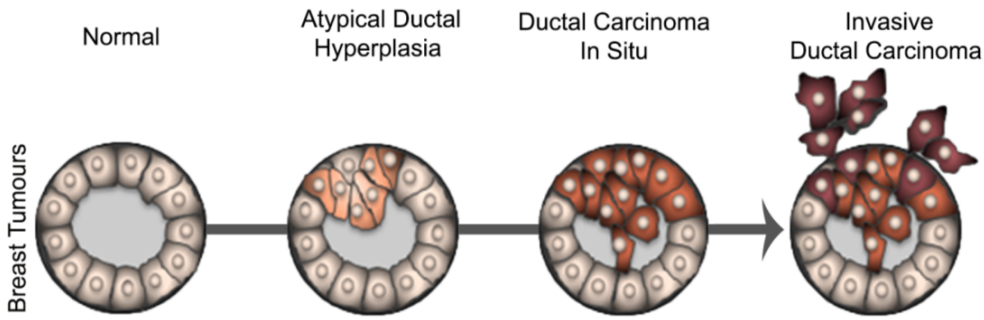

Figure 1.3: Classical model of breast cancer progression. Schematic view of Normal, Atypical Ductal Hyperplasia, Ductal Carcinoma *in Situ* and Invasive Ductal Carcinoma progression based on morphological and molecular features.

Histological grades

Besides the histological type, breast cancers can be classified into biologically and clinically meaningful subgroups according to histological grade. IDCs are routinely graded based on the assessment of their levels of differentiation (tubule formation), their cell morphology (nuclear pleomorphism) and their proliferation rate (mitotic activity). When evaluating tubule formation, only structures exhibiting clear central lumina are counted. Nuclear pleomorphism is assessed by comparing the regularity of nuclear size and shape using normal epithelial cells in adjacent breast tissue as reference. Mitotic activity is evaluated by counting well-defined mitotic figures (Ellis et al. 2003; Lopez-Garcia et al. 2010). Many studies have demonstrated a significant association

between histological grade and patients' survival. Precursor lesions and a range of invasive lesions may be classified as low (Grade I), intermediate (Grade II) or high grade (Grade III), being the worst prognosis attributed to the highest histological grade (poor differentiation) (Lopez-Garcia et al. 2010; Elston & Ellis 1991; Ellis et al. 2003).

Molecular subtypes

Several transcriptional profiling studies have been applied to the study of breast cancer to unravel the biological and clinical heterogeneity of IDCs but also to our understanding of breast cancer progression. To better understand breast cancer heterogeneity at the molecular level, Perou and colleagues performed cDNA microarray analysis. From this study, they observed the existence of two major classes: oestrogen receptor positive (ER+) and oestrogen receptor negative (ER-) breast cancer. Additionally, they described different molecular subtypes of breast cancer: luminal, HER2 and basal-like (Perou et al. 2000). Posteriorly, the same group showed that ER+ group can be sub-divided into two different groups, luminal A and luminal B, that present different clinical outcomes (Sørlie et al. 2001). Since the existence of these molecular subtypes was confirmed (Sorlie et al. 2003; Hu et al. 2006), the expression status of a set of receptors that includes oestrogen receptor (ER), progesterone receptor (PR) and Human Epidermal growth factor Receptor 2 (HER2) has been used to define the different subtypes (Table 1.1).

Luminal A and luminal B are the most common subtypes, usually representing low- to intermediate-grade tumours characterized by a pattern of expression reminiscent of normal ductal epithelial cells. Lesions up-regulating ER also present increased expression of low molecular weight cytokeratins 8/18 and high levels of expression of genes related to ER and PR (Weigelt et al. 2010). Luminal A lesions present low levels of proliferation genes and lack of expression of HER2. Usually these tumours are of low histological grade and associated with good outcome (Lopez-Garcia et al. 2010; Bombonati & Sgroi 2011; Weigelt et al.

2010). In contrast, Luminal B lesions are frequently associated with higher histological grade, present higher proliferation rates and significant worse prognosis. At the molecular level, these tumours show milder overexpression of ER, over-expression of HER2 and higher expression of proliferation-related genes (Weigelt et al. 2010).

ER+ or ER- tumours are profoundly distinct diseases (Lopez-Garcia et al. 2010). The ER- group is more heterogeneous and comprise the remaining molecular subtypes, HER2 and basal-like (Sørlie et al. 2001; Perou et al. 2000). HER2 tumours are high-grade tumours associated with an aggressive clinical behaviour. Molecularly, these tumours are characterized by the expression of HER2 and HER2 pathway-associated genes, and by the lack of expression of ER and PR. The basal-like subtype expresses cytokeratins and other markers, e.g. P-cadherin, CD44, Epidermal Growth Factor Receptor (EGFR), etc. associated with basal/myoepithelial cells and lack expression of ER, PR and HER2. Basal-like carcinomas are usually of high histological grade, present high proliferation rates and display necrosis and lymphocytic infiltrate (Bombonati & Sgroi 2011; Weigelt et al. 2010; Lopez-Garcia et al. 2010). The association between histological grading and molecular subtypes shows that the tumour grades reflect divergent biological and clinical behaviours (Table 1.1).

Table 1.1: Characteristics of breast cancer molecular subtypes.

Molecular Subtype	ER, PR, HER2	Histology Grade	Proliferation Rate	Incidence*
Luminal A	ER+/PR+/HER2-	Low	Low	73%
Luminal B	ER+/PR+/HER2+	Intermediate	High	10%
HER2	ER-/PR-/HER2+	High	High	5%
Basal-like	ER-/PR-/HER2-	High	High	10–20 %

ER: Oestrogen receptor; PR: progesterone receptor; HER2: Human Epidermal growth factor Receptor 2; -: negative; +: positive. *Anderson et al. 2014

The identification of the molecular subtypes of breast cancers raised the hypothesis of breast cancers can initiate in different cell types, leading to the

emergence of a new area of research, the biology of breast cancer stem cells (CSCs) (Stingl & Caldas 2007).

CSCs were isolated and characterized as tumour initiating cells in several common malignancies. Tumours generated with a subset of cancer cells expressing $CD44^{high}/CD24^{low}$ cells are able to recapitulate the histopathology of the initial tumour demonstrating the ability of these cells to regenerate the full range of tumour heterogeneity. Additionally, CSCs retain their self-renewal ability, generating tumours after serial passages. Notably, higher content of CSCs has been associated with high tumour histological grade and basal-like molecular sub-type. Since, Breast CSCs are also able to resist radiation- and chemotherapy-induced cell death, allowing them to cause tumour recurrence they are also associated with poor clinical outcome (Malhotra et al. 2010; Phillips et al. 2006; Li et al. 2008).

1.2 HALLMARKS OF CANCER

The histological progression from breast cancer initiation to metastasis results from the tumourigenic process. Cancer progression of tissues from epithelial origins involves the stepwise acquisition of a number of traits that enable cells to become tumorigenic and ultimately malignant. The set of biological capabilities acquired by tumoural cells includes sustaining proliferative signalling, evading growth suppressors, resisting cell death, enabling replicative immortality, inducing angiogenesis, and activating invasion and metastasis (Figure 1.4) (Hanahan & Weinberg 2011).

Figure 1.4: The hallmarks of cancer. The hallmarks of cancer comprise distinct biological capabilities acquired by tumour cells. The hallmarks enable cells to survive, multiply and invade distant tissues. They include sustaining proliferative signalling, evading growth suppressors, resisting cell death, enabling replicative immortality, inducing angiogenesis, and activating invasion and metastasis (adapted from Hanahan & Weinberg 2011).

The most fundamental feature of cancer cells is the ability to become self-sufficient in growth. Normal tissues exert a tight control on the production and release of growth-promoting signals to ensure tissue homeostasis, while cancer cells use different strategies to deregulate these signals and overcome this control. The acquisition of sustained proliferative signalling can be achieved by self-production of growth factors, resulting in autocrine stimulation. Alternatively, cells can signal neighbour cells. In turn, these cells will synthetize and secrete growth factors. The deregulation of growth signalling pathways can be induce through increasing levels of receptors or by altering their structural conformation, facilitating their direct interaction with ligands. Additionally, constitutive activation of these pathways, through gain of function mutations in

downstream effectors can lead to self-sufficiency in growth (Hanahan & Weinberg 2011).

In addition to sustaining proliferative signalling, cancer cells must also counteract tumour suppressor mechanisms that negatively regulate cell proliferation and tissue growth. Loss of suppressors of proliferation as TP53 and RB (Retinoblastoma) is the most common strategy to overcome these mechanisms. These proteins act as central nodes that control two alternative cell fates, proliferation or activation of senescence and apoptotic programs. Apoptosis, a natural barrier to cancer development, can be triggered by different stresses, including high levels of oncogene signalling and DNA damage associated to over-proliferation. So, tumours that progressed to high-grade malignancy not only have high levels of proliferation rates but also attenuated apoptosis (Hanahan & Weinberg 2011).

Most normal cell lineages undergo a limited number of successive cell divisions. After this number has been reached, cells enter into a non-proliferative viable state, called senescence, or into crisis, characterized by their elimination via cell death. On the contrary, cancer cells acquire an unlimited replicative potential, enabling the development of tumours. In most cases, this trait is attributed to the up-regulation of telomerase, that maintains telomeric DNA length, avoiding senescence or crisis (Hanahan & Weinberg 2011).

To sustain their proliferative status, masses of cancer cells also require access to nutrients and oxygen, as well as get ride of metabolic waste and carbon dioxide. These needs are facilitated by the ability of cancer cells to promote the development of neo-vasculature irrigating the tumour, through an angiogenic process. Another of the key step for malignant transformation is the ability of cancer cells to undergo an epithelial-to-mesenchymal transition (EMT). During EMT, epithelial cells change shape and gene expression programs, acquiring features of mesenchymal cells. This transition is believed to favour cell migration and invasion (Ref). In addition, a large number of evidence suggest that EMT is also involved in the development and maintenance of breast cancer stem cells

(CSCs) or tumour initiating cells (TICs) (Hanahan & Weinberg 2011; Kotiyal & Bhattacharya 2014). Breast CSCs define a small population of cancer cells that share important features with mammary stem cells, namely their ability to self-renew, resist apoptosis, allowing them to survive and cause tumour recurrence. Thus CSCs have been associated with primary tumour initiation and maintenance but also with the seeding and establishment of metastasis at distant sites (May et al. 2011). These cancer cells would also exhibit impaired adhesion to neighbour cells. At this stage, carcinomas had progressed to high pathological grades (Hanahan & Weinberg 2011).

Since 2000, two additional hallmarks of cancer were suggested. The first is the deregulation of cellular energetics to better support neoplastic proliferation. The second is the ability of cancer cells to evade immunological destruction. Additionally, both genomic instability and inflammation facilitate the acquisition of core and emerging hallmarks (Hanahan & Weinberg 2011).

1.3 THE SRC PROTO-ONCOGENE

Alteration in the regulation of genes or pathways involved in cancer progression can lead to the acquisition of at least one hallmark of cancer. If the loss or gain-of-function mutations of these genes leads to the acquisition of one or more malignant traits, these genes are called tumour suppressor genes or oncogenes, respectively. The cooperative interaction between these classes of genes are likely to be in the foundation of most carcinomas (Hanahan & Weinberg 2011). Src is one of the oncogenes.

1.3.1 HISTORICAL PERSPECTIVE

More than a century has passed, since Peyton Rous has described for the first time an agent that could cause transmissible growth of solid tumours in birds (Rous 1911). 60 years later, the emergence of molecular biology and genetic technics made possible the identification of *v-Src* in the genome of the Rous sarcoma virus, as the oncogene responsible for cellular transformation. Shortly after, Bishop and Varmus demonstrated that *v-Src* has a counterpart in human cells, *c-Src* (Src) (Aleshin & Finn 2010; Yeatman 2004). Src was the first confirmed proto-oncogene ever described and since its discovery, it became the most well studied member of the Src family of non-receptor tyrosine kinases (SFK's), that includes eight other members: FYN, LYN, LCK, HCK, FGR, BLK, YRK and YES. Besides being the oldest, Src is also the SFK most frequently implicated in cancer (Aleshin & Finn 2010; Yeatman 2004).

1.3.2 SRC AND CANCER

Src encodes a non-receptor tyrosine kinase, whose increased activity has been associated with the acquisition of several Hallmarks of Cancer (Yeatman 2004; Aleshin & Finn 2010). So far, it has been established that Src is involved in cellular proliferation and EMT, and it also acts as a trigger of cancer cell migration and invasion. In colorectal cancer, low or high levels of Src over-activity are associated with proliferation or invasiveness, respectively. Because overexpressing Src does not provide additional growth potential to the colon cell line KM12C but alters its adhesive properties, it has been proposed that early during tumour progression, low Src activation promotes tumour growth, while, at later stages, higher Src over-activation would promote invasiveness (Yeatman 2004; M S Talamonti et al. 1993; Jones et al. 2002). However, despite strong evidences that Src is implicated in cancer, the mechanism by which Src promotes tumourigenesis is still poorly understood.

Over-expression and specific activation of Src-family kinases have been described in several human solid cancers, including mammary carcinomas (Irby & Yeatman 2000). The clinical significance of Src expression, activation and localization in breast carcinomas has been explored in several translational studies. In the study performed by Elsberger and her colleagues, the assessment of Src mRNA levels showed no differences between normal, non-malignant and malignant tissues. Interestingly, when the analysis was performed considering ER status, a higher expression of Src was correlated with a decreased disease-specific survival, but only when ER was also being over-expressed (Elsberger et al. 2010). Regarding Src activation and localization, different studies have shown a clear correlation between Src kinase activation and poorer survival outcome (Elsberger et al. 2010; Elsberger et al. 2009; Kanomata et al. 2011). In DCIS, moderate to high levels of activated Src were found in 80% of the cases. Additionally, activated Src was associated with HER2 positivity, high tumour grade and elevated proliferation (Wilson et al. 2006). Two distinct studies showed that ER+ breast cancers, presenting a gene expression signature associated with an increase in Src activity, show worse survival rates (Zhang et al. 2009; Bild et al. 2006). Using different cohorts of patients it has also been shown that different cellular localizations of activated Src are correlated with different clinico-pathological features (Elsberger et al. 2009). For instance, cytoplasmic Src was associated with shorter disease-specific survival, increasing grade, tumour size, ER negativity and HER2 positivity (Elsberger et al. 2009; Elsberger et al. 2010). On the contrary, nuclear Src correlates with ER positivity and with the Ki67 proliferation index (Elsberger et al. 2010). Altogether, these studies suggest that Src has distinct functions when localized a specific cellular localization, which affects diverse aspects of tumorigenesis.

1.3.3 SRC REGULATION AND ACTIVATION

Proteins in the Src family have a conserved organization composed of four Src homology (SH) domains and a C-terminal tail containing a negative-regulatory tyrosine residue (Y530 – human and Y427 - chicken) and a unique amino-terminal domain (Figure 1.5.A). Src exists in two conformations open (active) and closed (inactive). The C-terminal tail and the SH2 and SH3 domains are involved in the negative regulation of Src. Phosphorylation at position Y530 promotes the interaction between the C-terminus and the SH2 domains that leads to a closed conformation. Additional interactions between the SH3 and the kinase domains stabilize this close conformation, reduced its ability to interact with its substrates. Transition from a close inactive to open active conformations is achieved by the dephosphorylation at position Y530 and further autophosphorylation within the catalytic domain at position Y419. Unlike, human c-Src, v-Src is constitutively active, because it lacks the C-terminal tail containing the negative-regulatory tyrosine residue. The absence of this region enables v-Src transformation properties, even when its protein levels are low (Yeatman 2004; Aleshin & Finn 2010) (Figure 1.5.B).

The intramolecular activity of Src is regulated by a balance between kinases and phosphatases. Negative regulation of Src, via Y530 phosphorylation is performed by C-terminal Src kinase (CSK). This phosphorylation event can be reverted by the action of specific phosphatases, such as protein tyrosine phosphatase 1B (PTP1B). On the contrary, Src can be activated by direct binding of focal-adhesion kinase (FAK) or its molecular partner Crk-associated substrate (CAS) to the SH2 and SH3 domains. CAS, FAK interaction with Src disrupts the inhibitory intramolecular interactions, leading to its open active conformation. Both FAK and CAS are principal regulators of focal adhesion (FA) complex formation and actin cytoskeleton dynamics (Yeatman 2004; Aleshin & Finn 2010). In addition, Src activation can be triggered by several routes, through integrins, interleukin-6 receptor, amongst others, turning on crucial signalling pathways involved in malignant transformation.

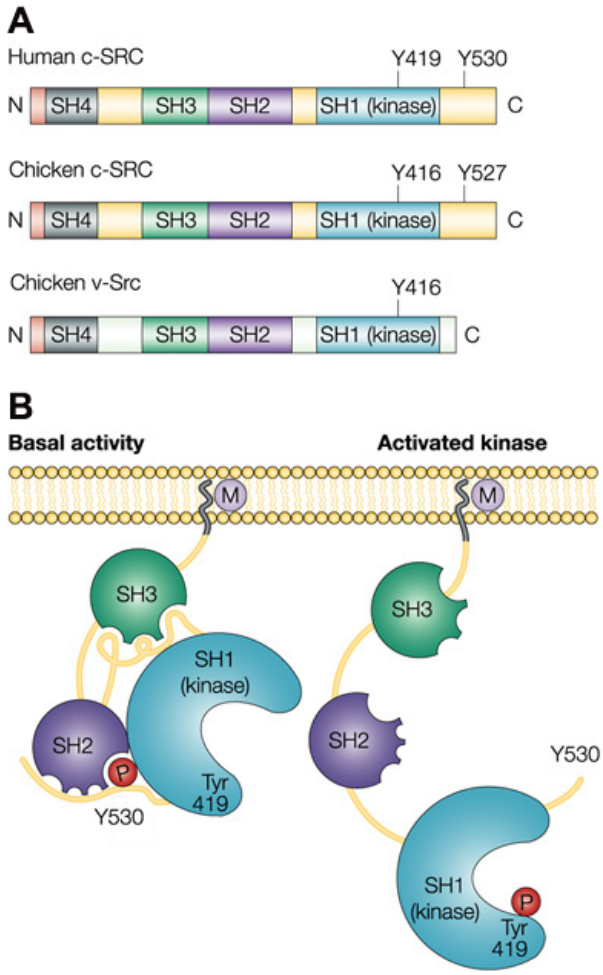

Figure 1.5: Structure and activation of SRC proteins. (A) Structures of human c-SRC, chicken c-SRC and chicken v-Src. All proteins have four SRC homology (SH) domains. The SH1 domain holds the kinase domain and a residue involved in autophosphorylation (Y419 – human and Y416 - chicken). Chicken *v-Src* lacks the C-terminal containing a negative regulatory tyrosine residue (Y530). **(B)** Phosphorylation of Y530 leads to a closed and inactive conformational state, stabilized by the interactions between C-terminal and SH2, and the interaction between SH3 and the kinase domain. Dephosphorylation of Y530 displaces thr inhibitory intramolecular interactions, leading to an open conformation of Src. Its full activation occurs with the autophosphorylation of Tyr419. M indicates myristoylation; P indicates phosphorylation.

1.3.4 SRC FUNCTIONS

The basic function of Src is the transmission of external signals to the cell interior. The control of Src subcellular localization and its co-localization with molecular partners and potential substrates is critical to regulate its activity (Biscardi et al. 2000). Upon activation, Src is translocated to the plasma membrane, where it phosphorylates tyrosine residues on substrates mainly involved in receptor tyrosine kinases (RTKs) signalling and adhesion signalling (Bjorge et al. 2000). RTKs and integrins can act together in several biological processes, such as cell survival, proliferation, cytoskeleton reorganization and invasion (Huveneers & Danen 2009; McLean et al. 2005).

One of the RTKs which its overexpression is associated with Src activity is the epidermal growth factor receptor (EGFR) (Biscardi et al. 2000). The resulting synergistic mitogenicity results from the activation of the Grb2/Sos/Ras/Raf/MEK/MAPK and PI3K/Akt signalling cascades (Belsches et al. 1997; Cantley 2002; Lu et al. 2003; Biscardi et al. 2000). The first pathway, the Ras/MAPK pathway leads to changes in gene expression through the activation of transcription factors responsible for the stimulation of mitosis, survival, and expression of matrix-degrading proteases (Abram & Courtneidge 2000). Src also can act through the activation of PI3K/Akt pathway. The increased activation of Akt leads to the inhibition of pro-apoptotic mediators, protecting cells from death during tumour growth, invasion, and metastasis (Fincham et al. 2000). RTK-induced stimulation of Src results in activation of signal transducers and activators of transcription (STAT) 3. STAT family members are associated with contribute to oncogenesis mainly by promoting cell cycle progression and cell survival. STAT3, in particular, contributes to the Myc mitogenic pathway (Bromann et al. 2004).

The action of Src on substrates involved in migration, invasion and metastasis is a dynamic process, tightly regulated temporally and spatially by cell adhesion and F-actin regulation (Guarino 2010).

1.3.5 SRC PHENOTYPES

Transfection of untransformed cells with *v-Src* produces striking cellular morphological effects, characterized by the acquisition of elongated, fusiform shape or, in more extreme scenarios, rounding-up and disaggregation. These morphological phenotypes result from the deregulation of cell adhesion complexes that mediate contacts between cells - adherens junctions (AJ) - and with the ECM - focal adhesions (FA). Src plays a pivotal role in the regulation of the assembly and disassembly of these complexes (Figure 1.6). When cells are transformed with Src, they suffer a reduction in FA number (Tarone et al. 1985; Winograd-Katz et al. 2011; Frame et al. 2002), affecting cell shape and mechanics (Yeatman 2004). In addition, Src weakens AJ's through the phosphorylation of E-cadherin, β-catenin and other AJ proteins, which, in turn, disrupts cell:cell contacts (Frame et al. 2002).

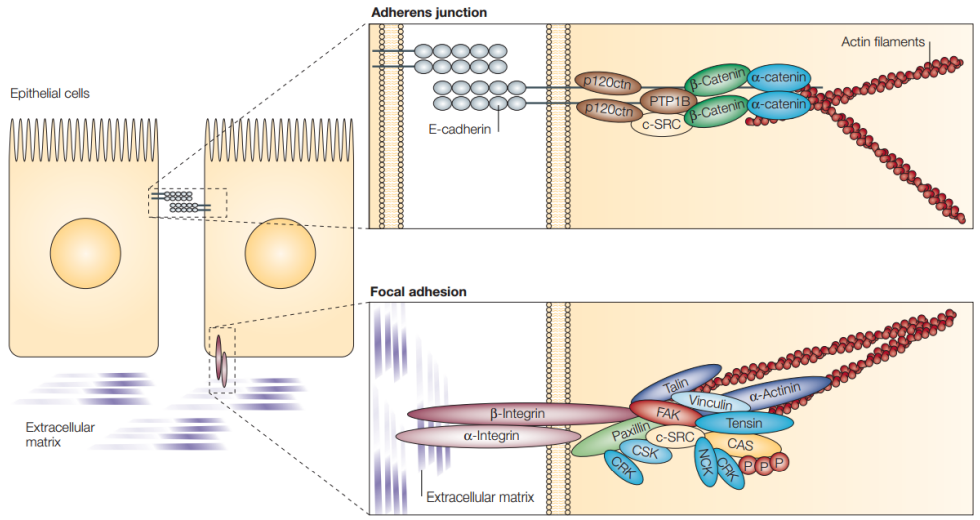

Figure 1.6: Schematic representation of adherens junction and focal adhesion complexes. There are two main types of adhesion complexes in epithelial cells — AJ and FA. Adherens junctions facilitate cell–cell adhesion through binding between E-cadherin molecules on adjacent cells. A cytoplasmic complex consisting of α-catenin, β-catenin and p120 catenin (p120ctn) links E-cadherin homodimers to the actin cytoskeleton. Src associates with this complex and, when activated, is able to promote the disruption of the AJ. At focal adhesions, integrin heterodimers bind to the extracellular matrix. Their cytoplasmic domains bind to protein complexes which connect integrins to the actin cytoskeleton. Several signalling molecules also associate with this complex, including focal-adhesion kinase (FAK) and Src, which can promote the turnover of the focal adhesion when activated, to promote cellular motility. Adapted from (Yeatman 2004)

Src over-expression has been associated with cell cycle progression, particularly in the transition from G2 and M phase. Increased proliferation rates were connected to reduced doubling times and nutrient requirements (Yeatman 2004). Regarding later stages of cancer, high levels of Src activity contribute to the metastatic phenotype mainly through the deregulation of cells adhesion, migration and invasion (Frame et al. 2002; Yeatman 2004). Since these three cellular processes are interconnected and all rely on actin, the Src-mediated acquisition of malignant traits is accompanied by massive changes in organization of the actin cytoskeleton (Winograd-Katz et al. 2011).

1.4 THE ACTIN CYTOSKELETON

The cytoskeleton of eukaryotic cells is built of three different types of protein filaments: microfilaments (actin filaments), microtubules and intermediate filaments. The cytoskeleton is responsible for establishing cell shape and their mechanical properties, cell locomotion, chromosome segregation, and intracellular transport of organelles (Uzman et al. 2000). In vertebrates, 6 genes encode for distinct actins, called isoforms (Dugina et al. 2009): two striated muscle actins (α-skeletal, (α-SKA) and α-cardiac, (α-CAA)), two smooth muscle actins (α- and ɣ-SMA) and two cytoplasmic actins (β- ɣ-CYA) (Dugina et al. 2009; Baranwal et al. 2012). The 6 actin isoforms share high levels of sequence conservation, with only a few differences in amino-acid at their N-terminus. Particularly, the two cytoplasmic isoforms only differ by four amino acids. Although highly similar, β- and ɣ-actins have different patterns of cellular distribution and contribute differently in the organization of cell morphology, polarity and motility (Dugina et al. 2009).

1.4.1 REGULATION OF THE ACTIN CYTOSKELETON

Actin filaments are built from the assembly of actin monomers, the glomerular actin (G-actin) that polymerize into filamentous actin (F-actin). Actin filaments are polarized, resembling an arrowhead, with a "barbed end" or fast growing end and a "pointed end" or slow growing end. F-actin polymerization occurs in vitro and can be divided into 3 steps. First, actin monomers slowly associate to form a dimer, followed by the formation of a stable trimmer. This trimmer constitutes the nucleus of polymerization. During the elongation phase, actin monomers bound to adenosine diphosphate (ADP) are charged to form G-actin bound to adenosine triphosphate (ATP). Those can rapidly be added to the growing end of the filament. As the filament ages, ATP decays to ADP+Pi, and then to ADP. Finally, near the pointed end, depolymerisation occurs through dissociation of ADP-bound G-actins from the filament, which can then be reincorporated in a new filament after addition of a phosphate to ADP. The unidirectional growth of filaments due to actin monomers flow from pointed to barbed ends is called "treadmilling" (Figure 1.7). Through these processes, F-actin is in a continuous state of assembly/disassembly (Dos Remedios et al. 2003).

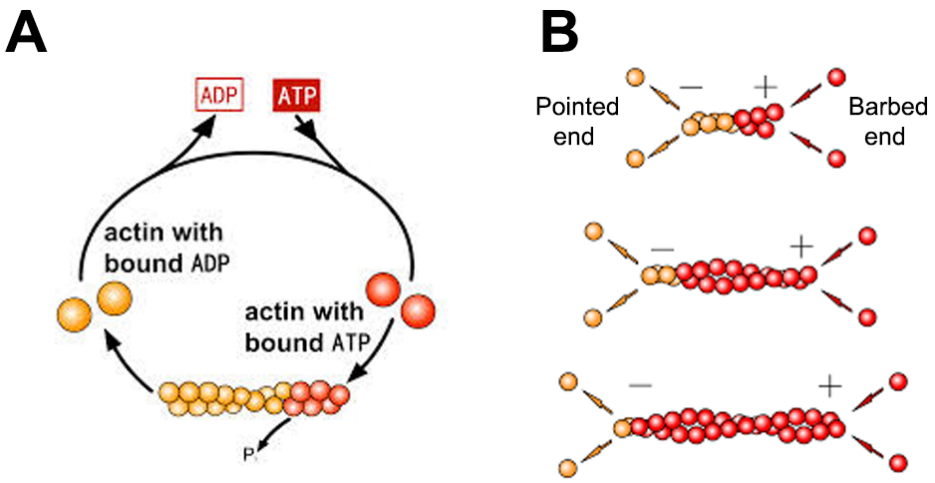

Figure 1.7: Schematic of actin filament treadmilling mechanism. (A) Dynamic equilibrium between the G-Actin and F-actin pools, which is regulated by ATP hydrolysis and G-actin concentration. At physiological concentrations, ATP-bound G-actin-ATP associates with the barbed end of F-actin (Red), while ADP-bound G-actin dissociates from the pointed end of F-actin (yellow). **(B)** The double-helical actin filament is structurally and kinetically asymmetric, leading to what is known as actin filament threadmilling. Thus, the barbed (or +) end (red) is characterized by net incorporation of actin monomers, while the pointed (or –) end (yellow) is characterized by net dissociation of actin monomers. The oldest subunits of the filaments are in the highest proximity to pointed end (adapted from the webpage of Sichuan University http://cc.scu.edu.cn/G2S).

In vivo, formation of small actin oligomers is an energetically unfavourable event. This is in part due to the presence of proteins, which directly interact with actin to control actin filament polymerization, depolymerisation and organization into distinct ordered networks. These Actin Binding Proteins (ABPs) can be grouped in six functional classes, based on their action on actin. Some 1) promote nucleation and elongation of filaments (e.g., Arp2/3, Ena/Vasp). Others 2) inhibit polymerization or stabilize them (e.g., CapZ, Tropomyosin). In addition, some ABPs 3) depolymerize or sever F-actin (e.g., Destrin, Cofilin). The remaining 3 groups of ABPs 4) promote the cross-linking or bundling of filaments with each other (e.g., Filamin), or 5), or use actin as a trail (e.g., Myosin) or 6), or play a scaffolding role by promoting interactions between actin filaments and cytoplasmic targets (e.g., Cortactin) (Dos Remedios et al. 2003; Michelot & Drubin 2011)

Nucleation and elongation of filaments

The transition from G- to F-actin is tightly regulated in time and space, in response to physical and chemical extracellular stimuli. Actin polymerization can be triggered by one or more mechanisms, including *de novo* nucleation of actin filaments, resulting from the uncapping of existing barbed ends, or following severing of existing filaments that create new barbed ends. In addition, actin filament nucleation can arise at the side of pre-existing filaments (Wear et al. 2000).

ARP2/3 complex

The ARP2/3 complex is a multimeric complex, which consists of seven subunits: two actin-related proteins Arp2 and Arp3 and five additional subunits ARPC1-5 (Lee & Dominguez 2010). While the Arp2, ARPC2, ARPC3 and ARPC4 subunits are encoded by one gene in vertebrates, Arp3, ARPC1 and ARPC5 are encoded by two genes and appear to have different properties on actin (Abella et al. 2015). ARP2/3 forms stable nucleation centres for new filaments, and assemble a "daughter" filament at an angle of 70° from the side of a pre-existing "mother" filament. Thus, ARP2/3 is localized at the branching point (Y-junction), connecting the pointed end of the newly formed filament with the mother filament, leaving the barbed end of the "daughter" filament available for elongation (Dos Remedios et al. 2003; Lee & Dominguez 2010). By itself, the ARP2/3 complex has very low nucleation activity; in consequence, ARP2/3 complex requires activation by nucleation promoting factors (NPFs). These factors, in addition to bind the first actin subunit of the new filament, promote the conformational change of the ARP2/3 complex and consequently enhance its actin nucleating activity. The most studied NPFs are the Wiskott-Aldrich syndrome protein family (WASP) and WASP and Verprolin homologous protein (WAVE). ARP2/3 complex together with its NFPs plays several functional roles during phagocytosis, cell junction assembly, endocytic structures, membrane

ruffling and lamellipodia dynamics, filopodia formation, and Golgi and tubulovesicular membrane dynamics. The role of WASP/WAVE proteins is critical for cytoplasmic organization during the development in *Drosophila* and in mammalian cells (Campellone & Welch 2010; Dos Remedios et al. 2003).

It has been shown that the metastatic process correlates with changes in the expression of Arp2/3 complex components. In particular, some studies show that higher levels of some members of the complex in breasts carcinomas, including ARPC2 and ARPC5, are associated with the rise in invasiveness and metastatic potential. Moreover, observations in breast cancer cell lines indicate that ARPC2 and ARPC5 are involved in both cell migration and invasion (Gross 2013).

Formins

Unlike ARP2/3 complex, formins are involved in the elongation of unbranched actin networks, like filopodia and stress fibres. Formins are a large family of proteins, characterized by the presence of the formin homology 1 and 2 (FH1 and FH2) domains. These domains are involved in regulation, dimerization, auto-inhibition, and actin nucleation/elongation. Most formins attach to the growing barbed ends through their FH2 domain and protect them from capping. This way they promote filament elongation (Lee & Dominguez 2010; Ridley 2011; Blanchoin et al. 2014). The most well studied formins are the diaphanous-related formins (DRFs), which include mDia. As most of the cytoskeletal proteins, these are multidomain and multifunctional proteins (Lee & Dominguez 2010).

Ena/VASP proteins

The Ena/VASP (enabled/vasodilator stimulated phosphoprotein) family of proteins comprises three members: Mena, VASP and EVL (Ena/VASP-Like) (Barzik et al. 2005). Ena/VASP proteins have been implicated in several cellular functions such as axon guidance and the migration of cancer cells. Like most

cytoskeletal proteins, Ena/VASP proteins are modular, containing N-terminal Ena/VASP Homology 1 (EVH1) domain, the central proline-rich domain and the C-terminal EVH2 domain. Functional EVH1 domain binds to several important regulators of the actin cytoskeleton, including other ABPs like zyxin, ActA and vinculin (Gentry et al. 2012; Bear & Gertler 2009) (Figure 1.8). The proline-rich domain interacts with SH3-domain–containing proteins, and with profilin (Figure 1.8). This interaction promotes the addition of profilin-actin complexes and is required for filaments barbed end association (Bear & Gertler 2009; Hansen & Mullins 2010; Gentry et al. 2012). The EVH2 domain is the responsible for the interaction with actin. This domain has a G- and an F-actin binding site, GAB and FAB, respectively. Additionally, it mediates the tetramerization of Ena/VASP proteins (Figure 1.8). Interaction between EVH2 and growing ends of actin filaments are required for efficient targeting of Ena/VASP proteins to lamellipodia and filopodia.

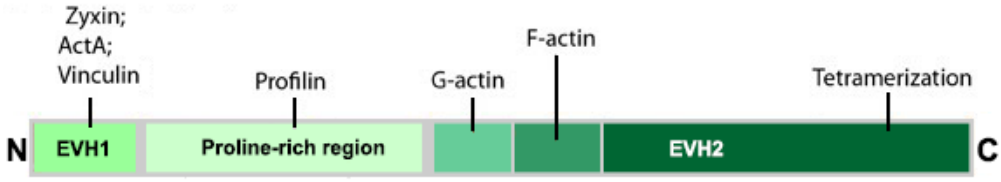

Figure 1.8: Domain structure of Ena/VASP proteins. The EVH1 and EVH2 domains and proline-rich region are indicated. EVH1 mediates protein:protein interactions EVH1 domain binds to several other ABPs like zyxin, ActA and vinculin. The proline-rich region harbours binding sites for profilin. The EVH2 domain contains a G-actin-binding site (GAB), an F-actin-binding site (FAB) and a coiled-coil at the very C-terminus that mediates tetramerization.

In vitro experiments have shown that the enrichment of Ena/VASP protein results in long and unbranched filaments, through their anti-capping activity (Winkelman et al. 2014; Barzik et al. 2005) and by delivering actin monomers to the filaments barbed ends (Figure 1.9). In contrast, the depletion of Ena/VASP protein from their normal locations promoted formation of dense actin networks with short, highly branched filaments (Bear et al. 2002; Lebrand et al. 2004; Barzik et al. 2005). The synchronized elongation of filaments by Ena/VASP against the plasma membrane is associated with filopodia tips, lamellipodia , cell-

cell contacts and focal adhesions (Figure 1.9) (Stevenson et al. 2012). Besides the anti-capping activity, other biochemical activities have been attributed to Ena/VASP proteins. Enabled (Ena) (the sole *Drosophila* family member) has the ability to promote the clustering of filaments at their polymerizing ends (Figure 1.9) (Winkelman et al. 2014; Lanier et al. 1999). This favours the bundling along actin filament length by fascin (Bear & Gertler 2009). In addition, Ena/VASP proteins appear to display anti-branching activity. Some groups have observed that Ena/VASP proteins reduce the frequency of branches in actin filaments, in an anti-capping independent manner (Bear et al. 2002). This effect has been proposed to result from a competition for actin monomers between Ena/VASP at the barbed ends, and the ARP2/3 complex at the side of the "mother" filaments. Alternatively, Ena/VASP might inhibit directly the docking of the ARP2/3 complex to the side of the "mother" filament. It has also been suggested that Ena/VASP has a catalytic debranching effect of ARP2/3 branches (Bear & Gertler 2009). Although it has not been validated *in vivo*, Ena/VASP proteins have the ability to nucleate actin filaments *in vitro*. Altogether, these mechanisms promote the formation of longer, less-branched networks.

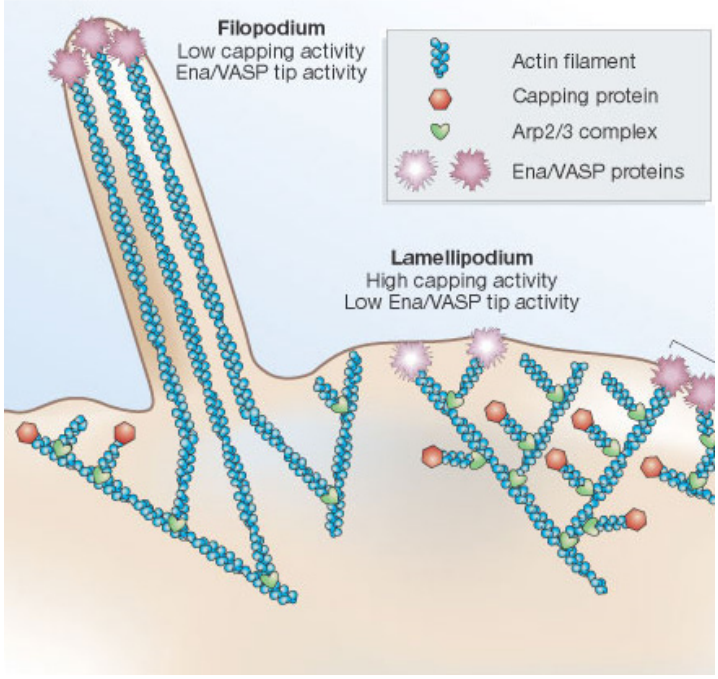

Figure 1.9: Schematic model for the role of Ena/VASP mediated actin polymerization on cellular protrusions. Actin filaments polymerize at their barbed ends near the plasma membrane. Filopodia formation result from the elongation of filaments by Ena/VASP proteins, which inhibit the capping of actin barbed ends locally by Capping protein. If the capping activity is high at the barbed-end, capped filaments stop growing and remain short. This favours an actin filament network that is most efficient for lamellipodium expansion (adapted from Schafer 2004).

The Ena/VASP family members have been implicated in cancer progression, in particular the mammalian homologue, Mena, and EVL. Four splice variants of Mena were described and associated with different stages of cancer progression. Mena^{11a} is present in primary tumour cells but lost in invasive ones (Di Modugno et al. 2012). Concomitantly, Mena INV (or Mena^{++}) and Mena^{+++} become upregulated in these invasive lesions and potentiate carcinoma cell metastasis (Di Modugno et al. 2012). Mena INV was found to be overexpressed in breast and colorectal cancers. Another isoform, MenaΔv6, is restricted to invasive cancer cells (Di Modugno et al. 2012). Mena deficiency decreases invasion, metastasis and tumour progression and impairs normal breast development. EVL has also been shown up-regulated in IDCs (Hu et al. 2008). However, in contrast to Mena, high EVL protein levels are inversely correlated with high invasiveness

and poor prognosis in IDC lesions (Mouneimne et al. 2012). Moreover, it has been proposed that EVL-mediated actin bundling suppressed the invasive abilities of breast cancer cells (Mouneimne et al. 2012).

Inhibition of polymerization or stabilization of filaments

The length and number of actin filaments has to be tightly controlled when total actin concentration is constant. Proteins that are in the best position to regulate actin polymerization and treadmilling dynamics are the ones that cap the barbed ends of filaments. The most abundant barbed-end capping protein is the capping protein heterodimer (CAPZ), composed of an α (CapZA) and β (CapZB) subunits (Dos Remedios et al. 2003). In addition to regulate the assembly of actin monomers at the barbed ends of filaments, CapZ captures pre-existing filaments and controls the correct assembly of filaments at the Z-line, in muscle cells (Dos Remedios et al. 2003). Capping protein does not affect the rate of filament fragmentation, instead it binds to F-actin barbed ends with high affinity and blocks the polymerization of short branched F-actin networks mediated by the ARP2/3 complex (Cooper & Sept 2008). In the absence of capping protein, uncapped filaments incorporate G-actin monomers and elongate freely at their barbed ends (Dos Remedios et al. 2003; Cooper & Sept 2008). F-actin networks built by ARP2/3 and capping protein have been associated with lamellipodial protrusions, membrane ruffles formation and endocytosis (Cooper & Sept 2008).

Other ABPs, such as Tropomyosins (TM) stabilize and prevent the depolymerisation of actin filaments (Dos Remedios et al. 2003). This family of ABPs is composed of a large number of isoforms, which results from 1) the existence of four genes encoding for TMs, 2) the presence of multiple alternative splicing, leading to different gene products and, 3) isoform-specific post-translational modifications (Lindberg et al. 2008; Gunning et al. 2015).

TMs are dimeric, coiled-coil structures, which can associate in a head-to-tail fashion, forming co-polymers with actin filaments. TMs mechanically

stabilize actin filaments, promoting the formation of longer actin filaments by protecting them from being severed by gelsolin and cofilin during elongation (Lindberg et al. 2008; Gunning et al. 2015). In addition, TMs decreases the rate of depolymerization at the pointed end of the actin filament and collaborates with tropomodulins to further stabilize the pointed end of filaments (Gunning et al. 2015). TMs provide to actin filaments different properties, in term of their ability to cross-link, to be severed and to interact with myosin proteins (Gunning et al. 2015). This is especially important for building distinct actin networks with specific functions in complex cellular processes.

The association of different TM with different actin functions is reflected in differential expression of TM isoforms during oncogenic transformation (Helfman et al. 2008). For instance, high molecular weight (HMW) TMs, TM1-3, protect actin filaments from severing proteins gelsolin and cofilin better than low molecular weight (LMW) TMs. Specifically, only TM1-3 are decreased during tumourigenesis. These changes in TMs expression appear to contribute to the disruption of stress fibres and focal adhesions, thereby contributing to the invasive and metastatic properties of cancer cells (Helfman et al. 2008).

Depolymerisation or severing of F-actin

To ensure the consistent supply of actin monomers, actin filaments have to be depolymerized. This task is performed by a class of ABPs that break existing filaments to recycle G-actin for polymerization into new filaments. Actin depolymerizing-factor (ADF)/ Cofilin is a family of proteins expressed in all eukaryotic cells and includes destrin (destroys F-actin) and cofilin (co-sediments with filamentous actin) (Dos Remedios et al. 2003; Insall & Machesky 2009). Although their names suggest that destrin depolymerizes F-actin and cofilin severs F-actin, both can increase the pool of G-actin. Cofilin not only severs and depolymerizes F-actin at the pointed ends of old actin filaments, but also has the ability to debranch networks (Insall & Machesky 2009). Cofilin is associated with

membrane ruffling, cytokinesis, advancing of neuronal growth cones and myofibrillogenesis (Insall & Machesky 2009; Dos Remedios et al. 2003).

Cross-linking or bundling

Cross-linked actin networks are complex networks built by specialized proteins that establish the connection between already polymerized actin filaments (Blanchoin et al. 2014). Filamin (FLN) A was the first cross-linking protein identified in non-muscle cells (Nakamura et al. 2011). It belongs to a family that comprises 3 different proteins, encoded by three highly conserved genes, *FLNA*, *FLNB* and *FLNC*. These proteins interact directly with F-actin but also with proteins involved in signal transduction and gene expression (Popowicz et al. 2006). FLN-partner interactions depend on: mechanical forces, phosphorylation, proteolysis, and competition between binding partners (Nakamura et al. 2011). While other bundling proteins, like α-actinin and spectrin form parallel actin networks, FLN binding to F-actin induces both parallel actin bundles and high-angle orthogonal networks, depending on its concentration (Popowicz et al. 2006; Feng & Walsh 2004).

FLN is particularly important to control the physical properties of actin networks. In the absence of FLN-mediated cross-linking, a larger number of filaments would be required to achieve the elasticity and viscosity provided by FLN. The flexible and orthogonal actin branches are able to adapt to morphological changes, making FLN ideally suited for mechanical signal transduction (Nakamura et al. 2011; Popowicz et al. 2006). In agreement with this, FLNs stabilize stress fibres and the actin cytoskeleton linkages to focal adhesions and membranes (Lynch et al. 2011). Moreover, FLNA is necessary for mechanosensing behaviour of cells and tissue generation (Nakamura et al. 2011).

Although mutations in the FLN genes are common in human breast and colon cancers (Nakamura et al. 2011), the effects of most of them require further studies. Still, there has been described a dual role of FLN in cancer. On one side,

FLN are critical for cell migration and deficiency of FLN may impair tumour invasion; in another aspect, FLN inhibit MMP activity that may suppress tumour invasion. The dual role of FLN in tumour invasion may depend on the stages of tumour progression or work coordinately in regulating tumour metastasis (Bandaru et al. 2014).

Motor

Motor proteins are proteins that use F-actin as a track upon which to move. The first motor protein identified was skeletal muscle myosin, involved in muscle contraction (Alberts et al. 2002). Myosins move along the actin filament by coupling the hydrolysis of ATP to conformational changes (Uzman et al. 2000).

Thirteen members of the myosin gene superfamily have been identified by genomic analysis. The most abundant isoforms, Myosin I and Myosin II, are present in nearly all eukaryotic cells. Although the specific activities of myosins differ, they all function as motor proteins, moving toward the plus end of the actin filaments, although they do so at different speeds. The exception is myosin VI, which moves toward the minus end (Alberts et al. 2002). Myosin II powers muscle contraction and cytokinesis, whereas Myosins I and V are involved in intracellular organization and cytoskeleton-membrane interactions such as the transport of membrane vesicles (Alberts et al. 2002; Uzman et al. 2000).

Scaffolding

The role of scaffolding ABPs is to promote the interaction between actin filaments and cytoplasmic targets. Among those, cortactin links dynamic actin networks to membrane trafficking and signalling proteins (Kirkbride et al. 2011).

Cortactin is a prominent substrate of Src kinases, which has been shown to act as a NPF for the Arp2/3 complex, stabilizing branched actin networks (MacGrath & Koleske 2012; Kirkbride et al. 2011). In cells, cortactin has been associated with cell motility, through several mechanisms: promotion of

lamellipodial persistence, FA assembly, cellular signalling, endocytosis and secretion of metalloproteinases (MMPs) (Kirkbride et al. 2011). The important role of cortactin in all these processes placed it in a central position in the development and maturation of invadopodia. In agreement, cortactin gene *CTTN* is overexpressed in many cancers, including breast cancer, colorectal cancer and melanoma (MacGrath & Koleske 2012). Besides the impact of cortactin overexpression in cell migration, it also promotes cell cycle progression and inhibits the degradation of EGF receptor, increasing the pro-mitotic receptor signalling. Overall, cortactin is an important marker for aggressive cancers (Kirkbride et al. 2011; MacGrath & Koleske 2012).

1.4.2 The Diversity of Actin-Filament-Based structures

The constant cycles of polymerization and disassembly of actin filaments allows cells to remodel their actin cytoskeleton, in order to change their shape, and to use it as a force-generating system in complex cellular processes, such as: cell motility, cell adhesion, exo- and endocytosis, and cytokinesis. To perform all these functions, actin filaments are organized into distinct networks, at precise locations in the cytoplasm. Each of these F-actin-based structures is able to perform specific cellular functions. In animal cells, 15 distinct F-actin networks have been described (Michelot & Drubin 2011). Among those, the best studied ones are the actin cortex, the lamellipodium, filopodia and stress fibres (Blanchoin et al. 2014; Michelot & Drubin 2011).

The cell cortex is a thin actin shell attached the inner face of the plasma membrane. It is composed of a mix of branched and bundled straight filaments, with contractile properties due to the presence of myosin. Acto-myosin contractility of the cortex is important for cell shape changes and movement (Blanchoin et al. 2014).

Although, lamellipodia and filopodia induce protrusions of the cell membrane through actin polymerization pushing the membrane, these structures

constitute distinct actin networks, regulated by different signalling pathways and exerting different cell functions. The lamellipodium is a sheet-like protrusion, localizes at the leading edge of migrating cells, and associated with intracellular organelles. The formation of lamellipodia is driven by the polymerization of dense ARP2/3-dependent branched actin networks (Ridley 2011). Their main cellular function is to direct cell migration (Vignjevic & Montagnac 2008). In contrast, filopodia are finger-like protrusions at the leading edge of cells involved in sensing the cellular environments, promoting cell-cell signalling and cell guidance toward chemoattractants. Filopodia contain unbranched, bundled arrays of actin filaments with their barbed ends towards the plasma membrane (Michelot & Drubin 2011; Blanchoin et al. 2014). Combination of filopodia and lamellipodia enables directed cell migration (Vignjevic & Montagnac 2008).

The set of ABPs that regulate the lamellum is distinct from the ones that control lamellipodia formation (Michelot & Drubin 2011). The lamellum is composed mainly of stress fibres, which are the major contractile structures in animal cells. They are highly enriched for myosin to form acto-myosin structures, responsible for contraction. Phosphorylation of myosin light chain, on Thr18 and Ser19, increases contractility of stress fibres through two different pathways: Ca^{2+}/calmodulin dependent, which leads to a rapid response; and through the activation of Rho pathway resulting in a sustained response. In non-motile cells, stress fibres are thick and stable. On the contrary in motile cells stress fibres are thinner and less frequent (Tojkander et al. 2012). Although all stress fibres are composed of bundles of anti-parallel filaments, they can vary their morphology and origin, depending of whether they emerge from the lamellipodium or from FAs. Based on their properties, stress fibres can be grouped in four different groups: 1) perinuclear actin cap, 2) transverse arcs, 3) dorsal and 4) ventral stress fibres (Tojkander et al. 2012; Blanchoin et al. 2014). The perinuclear cap is defined as a group of actin stress fibres positioned above the nucleus, whose main function is to control nuclear shape in interphase cells. Additionally, they might act as mechano-sensors, transmitting force from the environment to the nucleus

(Tojkander et al. 2011). Transverse arcs are curved actin filament bundles with contractile properties. Although they are not attached to FAs, they transmit contractile force from the environment through their connection with other stress fibres (Figure 1.10) (Tojkander et al. 2012). In motile cells, transverse arcs show typical flow from the leading cell edge towards the cell centre (Hotulainen & Lappalainen 2006). Dorsal stress fibres, which are anchored to FAs at their distal ends, are used as a platform for assembly of other stress fibres (Figure 1.10). These fibres are not decorated with myosin II, therefore they do not possess contractile ability (Tojkander et al. 2012; Hotulainen & Lappalainen 2006). In contrast, ventral stress fibres are contractile actin filament bundles, attached to FAs at both ends (Figure 1.10) (Hotulainen & Lappalainen 2006; Tojkander et al. 2012). They represent the major contractile machinery in interphase cells, promoting cell movement through cell adhesion and contraction (Tojkander et al. 2012; Hotulainen & Lappalainen 2006).

Stress fibres have important roles in mechano-sensing and in translating physical cues from the environment into biochemical signals. It has been shown that the actin cytoskeleton behaves as a fluid-like material on soft substrates or as a solid-like material on stiff condition. Moreover, different substrate stiffness induces different cell responses via F-actin regulation (Gupta et al. 2015). Alteration in actin cytoskeleton rigidity is determined by changes in the organization, abundance and structure of stress fibres (Tojkander et al. 2012).

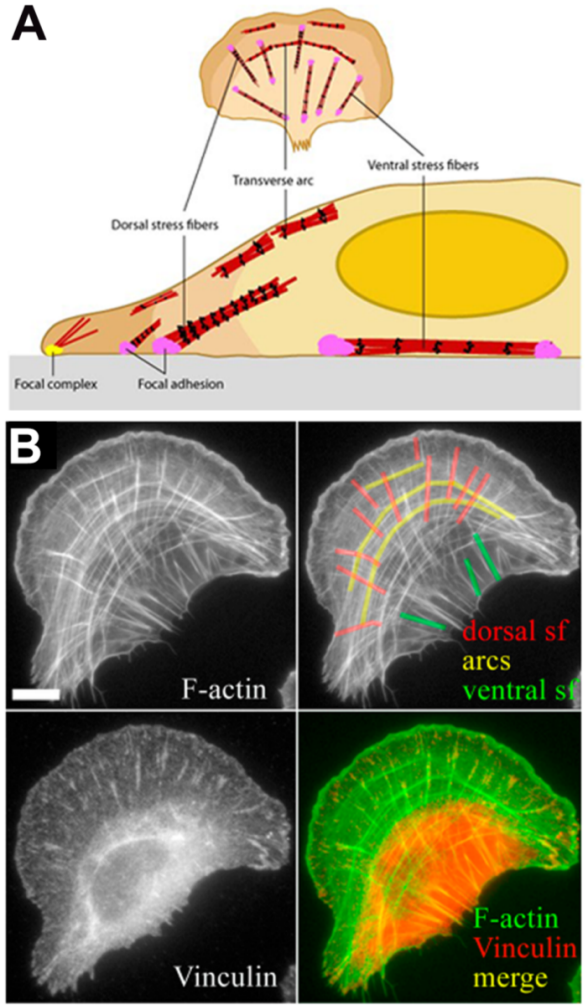

Figure 1.10: Actin stress fibres network in motile animal cells. (A) Schematic presentation of distinct stress fibre networks in motile animal cells. These cells can contain at least three categories of stress fibres involved in cell movement: 1) dorsal stress fibres are anchored to FAs at their distal end; 2) transverse arcs are curved bundles, typically connected to FAs through interactions with dorsal stress fibres; 3) ventral stress fibres are acto-myosin bundles anchored to FAs at both ends, **(B)** The three categories of contractile actin fibres are highlighted: dorsal stress fibres (red), arcs (yellow) and ventral stress fibres (green).. Scale bar, 10 μm. Figure adapted from Tojkander et al. 2012 and Hotulainen & Lappalainen 2006

1.4.3 F-ACTIN MECHANICS

The actin cytoskeleton determines the mechanical properties of cells. Alterations in cell stiffness/elasticity induced by remodelling of the actin cytoskeleton have emerged as key features for various normal biological processes and for progression of certain diseases. For instance, cancer cells possess specific mechanical and actin cytoskeleton features that are different from normal stromal cells (Haghparast et al. 2013). In the recent years, several papers showed that cancer cells are softer than their normal counterparts (Xu et al. 2012; Remmerbach et al. 2009). Understanding how actin network dynamics affects cell behaviour is fundamental to better comprehend the molecular basis of actin-based pathologies.

To assess the mechanical properties of cells, these are subjected to "rheology" experiments, where the cells are submitted to a force per unit of surface or a pressure and the consequent deformations are analysed. Elastic materials show a proportional change between the deformation (strain) and the applied force per unit area (stress). If the material does not recover its original shape, there is a viscous component present in the system. The ratio between stress and strain is called elastic modulus (Stricker et al. 2010; Blanchoin et al. 2014; Nakamura et al. 2011). Biopolymers, such as actin filaments, usually present mechanical properties between the elastic and viscous states, and thus are said "viscoelastic". Atomic Force microscopy (AFM) is one of the methodologies used to determine the elastic properties of biological samples (Vinckier & Semenza 1998).

Distinct F-actin networks generate different force levels, due to their biochemical composition and actin organization. The presence of cross-linkers on actin networks increases the elastic modulus and decreases viscosity (Blanchoin et al. 2014; Stricker et al. 2010), in simple terms, these networks get stiffer. Networks with low F-actin density and low level of cross-linking soften at large strains. In contrast, dense networks with high content of cross-linkers stiffen at intermediate strains followed by a dramatic softening at larger strains (Blanchoin

et al. 2014; Stricker et al. 2010). The tight control of the mechanical properties of actin networks, enables stress fibres and FAs to act as interface platforms, regulating the mechanical response to force inside the cells and the transmission of forces to the ECM (Stricker et al. 2010).

1.5 SRC AND THE ACTIN CYTOSKELETON

As described in the previous section, Src is a key player in cytoskeletal rearrangements, cell adhesion and migration. Src acts on cytoskeleton dynamics through its regulation of Rho GTPases activity. In particular, Src regulates both guanine nucleotide-exchange factors (GEFs) and GTPase-activating proteins (GAPs) which respectively enhance and decrease the activity of Rho GTPases (Huveneers & Danen 2009). The Rho-family GTPases Rac, Cdc42, and Rho are the major regulators of adhesion and cytoskeleton dynamics, controlling the assembly/disassembly of both cell–matrix adhesions and actin-based cytoskeletal structures (Huveneers & Danen 2009).

In late events of tumourigenesis, suppression of Rho–dependent cell-matrix adhesions due to increased levels of activated Src leads to stress fibres disassembly. Simultaneously, Src promotes the formation of actin filament clusters with adhesive properties, capable of degrading the ECM (Winograd-Katz et al. 2011). These actin structures, that seem to be specific to cancer cells and commonly called invadopodia, promote cell migration and invasion, and ultimately tumour metastasis (Finn 2008; Murphy & Courtneidge 2011).

For the first time, in 2014, our lab has demonstrated that in *Drosophila* epithelia, the pro-growth function of Src is also control by the actin cytoskeleton. We have shown that the hyperproliferation of Src-overexpressing tissues was associated to an accumulation of F-actin. However, overexpressing actin capping protein could inhibit Src-induced apoptosis or tissue overgrowth through the control of F-actin. Based on the high level of functional conservation in genes

between flies and human, these observations suggested that early during tumour progression, Src promotes tumour growth through F-actin accumulation (Fernández et al. 2013). However, despite decades of research on Src, a role of F-actin downstream of Src in promoting the acquisition of pre-malignant cancer hallmarks at early stages of breast cancer progression remained to be explored.

1.6 *DROSOPHILA* AS A MODEL SYSTEM TO STUDY TUMOURIGENESIS

Model organisms are widely used to study human biology, as they make possible to execute a broad set of experimental approaches. To be considered a model for human biology, the process studied has to be similar enough in the model organism and in human to make possible extrapolation. *Drosophila melanogaster* fulfils both criteria. First, more than 50% of the proteins that cause human diseases including cancer, have functional orthologues in *D. melanogaster* (Gonzalez 2013). Misregulation of oncogenes and tumour suppressor genes in the fruit fly triggers several hallmarks of cancer, including evasion of apoptosis, sustained proliferation, prolonged survival, genome instability and metabolic reprogramming. In several cases, the identification of the key cancer-associated genes in *D. melanogaster* initiated their discovery in the human cancer context. The discovery of the Notch, Hippo and JAK-STAT pathways, as well as cell competition mechanisms are classical examples of the recognition of the fruit fly as an good model organism to study basic processes of carcinogenesis (Gonzalez 2013; Tipping & Perrimon 2014). Second, *D. melanogaster* allows sophisticated functional and genome-wide assays to tackle signalling pathways interactions and to identify disease-related genes. Although, as in humans, fruit flies can also develop tumours naturally, these can be induced experimentally through genetic manipulations, using the thousands of mutants, enhancer and protein traps and

transgenic animals expressing gain of function or nearly genome-wide double stranded RNAs (dsRNA) for RNA degradation available in stock collections (Gonzalez 2013). The variety of genetic tools associated with low genetic redundancy makes *D. melanogaster* a powerful organism for cancer research.

The role of tumour suppressor genes or oncogenes in tumourigenesis can be explored using the available genetic tools in experiments of gain or loss of function. Tumours generated can go from benign hyperplasia tissue overgrowth with cells maintaining a monolayer organization, to neoplasia. In neoplastic tumours, cells lose their epithelial morphology, round-up and tissue architecture is affected, ultimately leading to organism death. Different larval tissues are currently used to model human cancer of different origins. Among those, larval imaginal discs are used to model epithelial tumours, larval glia is used to study glioblastoma, and muscle to study rhabdomyosarcoma (Gonzalez 2013).

There are other important advantages that support *D. melanogaster* as a useful model system. Flies are easy and inexpensive to keep in laboratory conditions, have a much shorter generation time and have a highly prolific nature. Their anatomy, histology and cell types have been extensively described in the literature. But as for any model organism, *Drosophila* has limitations. The lack of adaptive immune system and blood, as well as the existence of an open circulatory system prevent the study of late stages processes of cancer progression, such as metastatic intra- and extravasation (Gonzalez 2013).

The wing imaginal disc has a relatively simple epithelial structure. At the beginning of the first instar larva, these discs are composed of about 30 cells, Because these tissues are highly proliferative, at the end of third instar larvae, 4 days later, each wing disc reaches nearly 50,000 cells (Milan et al. 1996). Their simple organization, tight control of cell proliferation and accessibility for genetic manipulations, makes this tissue an excellent model to study how cells evade apoptosis and proliferation in the context of epithelial tissue. For example, using *Drosophila* as a model, it has been shown that slightly elevated levels of Src leads to higher proliferation, and anti-apoptotic signals resulting in tissue overgrowth.

Further increase of Src signalling induces apoptosis and cooperates with oncogenic mutations such as Ras^{V12} to induce metastasis and invasion (Vidal et al. 2007). Additionally, our lab showed that increased Src-activity induces tissue overgrowth through the control of F-actin (Figure 1.11) (Fernández et al. 2013).

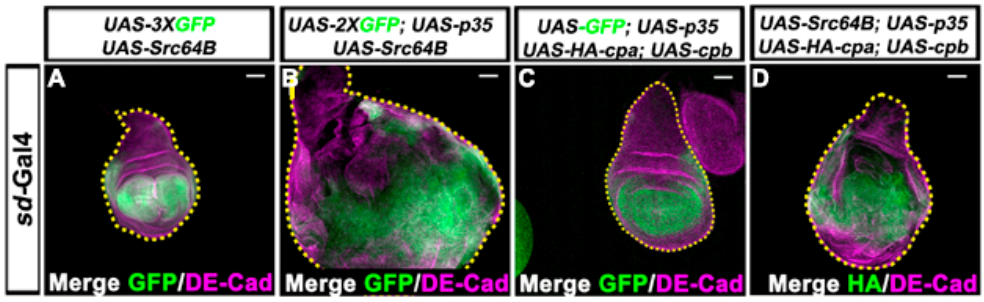

Figure 1.11: Actin-capping protein prevents the overgrowth of wing imaginal disc size overexpressing *Drosophila Src64B* and *p35*. All panels show third instar wing imaginal discs with dorsal up in which scalloped (sd)-Gal4 drives the expression of **(A)** UAS-*GFP* (green) and UAS-*Src64B* or (B) UAS-*GFP* (green) UAS-*Src64B* and UAS-*p35* or **(C)** UAS-*GFP* (green) UAS-*p35*, UAS-*HA-cpa* (CapZA in human) and UAS-*cpb* (CpaZB in human) or **(D)** UAS-*GFP* (green) UAS-*Src64B*, UAS-*p35*, UAS-*HA-cpa* and UAS-*cpb* When Src overexpressing cells are kept alive by expression of the caspase inhibitor P35 the FDP-expressing tissue overgrowth **(Compare B with A)**. Although overexpressing both capping protein subunits has no impact on tissue size **(C)**, their overexpression suppresses the overgrowth of *Src,p35*-expressing wing discs **(D).** Adapted from Fernández et al. 2013.

1.7 THE MCF10A ER-SRC AS A MODEL SYSTEM TO STUDY THE EFFECT OF SRC ON TUMORIGENESIS

Studies in patient's tumour tissue and cancer cell lines have provided over the years extremely important information regarding human cancer genetics and cellular processes driving malignant phenotypes. But their major limitation is their inability to provide insight on the biochemical and cell biological pathways involved in the early stages of tumourigenesis. This flaw can be overcome by the use of inducible cell line, as MCF10-ER-Src.

MCF10A cells derived from human fibrocystic mammary tissue. The isolation and establishment of this cell line had occurred spontaneously, after extended cultivation in low calcium concentration and without treatments with pro-carcinogen (Soule et al. 1990). MCF10A cells do not show any characteristics of invasiveness and are considered to be a normal-like breast epithelial cell line. These cells (a) show lack of tumorigenicity in nude mice; (b) grow in polarized three-dimensionally acini in collagen and (c) require growth factors to proliferate. Their karyotype is near-diploid with minimal rearrangement. Because these cells fail to express the three most common hormonal receptors, including the ER receptor (Soule et al. 1990; Kao et al. 2009), MCF10A stable cell lines carrying oncogenes fused to the oestrogen binding domain can be conditionally induced through treatment with the oestrogen analogue Tamoxifen (TAM). The MCF10A-ER-Src (ER-Src) cell line were stably transfected with a construct encoding a fusion protein between the Schmidt Rupin A form of v-Src and the hormone binding domain of the human oestrogen receptor. This fusion protein is maintained inactivated in the absence of ligand-binding to the ER-binding domain. However, in the presence of TAM, TAM binds to the ER-binding domain and triggers an active conformational change of the ER-Src fusion protein and its activation. TAM treatment of the ER-Src cell line for 36 hours is able to trigger full phenotypic transformation. The transformation process is triggered by a transient inflammatory response mediated by NF-κB activation. This inflammatory response induces an epigenetic switch that activates a positive feedback, involving PTEN and STAT3 (Iliopoulos et al. 2009). ER-Src transformed cells form multiple colonies in soft agar, self-renewing mammospheres in non-adherent conditions and tumours upon injection into nude mice (Iliopoulos et al. 2009; Hirsch et al. 2010; Hirsch et al. 2009).

Another great advantage of the ER-Src cell line is its ability to grow as monolayer but also in three-dimensional culture. Culture of MCF10A cells in reconstituted basement membrane results in formation of polarized, growth-arrested acini-like spheroids that recapitulate several aspects of glandular

architecture *in vivo* (Debnath et al. 2002; Muthuswamy et al. 2001). So, these cells enable proper studies on cellular processes, like apoptosis, proliferation and differentiation, in normal state and during early tumour formation. Thus, this *in vitro* model with conditional Src activation gives the rare opportunity to follow and study, in 2D and in 3D, the timely ordered events that lead to full malignant transformation (Iliopoulos et al. 2009).

1.8 AIMS AND THESIS SCOPE

Tumourigenesis is a multistep process, in which several alterations in oncogenes and tumour suppressor genes condemn normal cells to sustain proliferative signalling, evade growth suppressors, resist cell death and finally invade distant tissues (Hanahan & Weinberg 2011). The first oncogene ever described was the c-Src non-receptor tyrosine kinase. Over more than one century, it became the most investigated proto-oncogene. Its overexpression and/or over-activation was described in several human cancers, including those of the breast (Zhang & Yu 2012). Basal Src activity, which occurs early during tumour progression, is believed to sustain proliferative signalling and survival of pre-malignant cells. Later, further Src activation may facilitate cell migration, adhesion and invasion of malignant cells via F-actin regulation (Zhang & Yu 2012). Our previous observations in *Drosophila* epithelia argue that Src also sustains proliferative signalling and survival of pre-malignant cells via the control of the actin cytoskeleton (Jezowska et al. 2011; Fernández et al. 2011).

In this thesis, I investigated if F-actin plays a role downstream of Src activation, in the earlier events of tumour progression. To answer this question I first investigate if pre-malignant breast tumours display alterations in the expression of genes encoding direct regulators of the actin cytoskeleton. To search for genes specifically associated with Src-induced tumourigenesis, I identified ABPs commonly deregulated in pre-malignant human breast tumours

and in the inducible ER-Src cell model. Those were then tested for a role in Src-induced tissue overgrowth in the *in vivo* model *Drosophila melanogaster*. To determine if the sustaining self-sufficiency in growth provided by Src activation is associated with alterations in the actin networks, I investigated the transformation features acquired during the multistep development of Src-induced cellular transformation and the dynamic changes in the actin cytoskeleton. Last, to determine if alterations in F-actin associated to the early events of Src-mediated malignant transformation were required for transformation, I studied in the inducible ER-Src cell model the role of one of the ABP deregulated in pre-malignant human breast tumours, as well as in the inducible ER-Src cell model and required for Src-induced tissue overgrowth in the fly. Finally, I have investigated the expression of this ABP in different breast cancer stages and molecular subtypes.

Chapter 2

Microarray analysis identified Actin cytoskeletal regulators associated with early breast tumours and involved in Src-mediated tissue overgrowth.

"Se podes olhar, vê. Se podes ver, repara."

José Saramago, Ensaio sobre a Cegueira

My contribution for this chapter was the bioinformatic analysis of patient's tumour microarray raw data. Additionally, I performed the pathway analysis and functional classification of actin binding proteins. All this work was performed under the supervision of Joana Vaz.

Florence Janody performed all the fly genetics experiments.

2.1 SUMMARY

Tumourigenesis is a multistep process, in which several alterations in cell physiology condemn normal cell to malignant transformation. Src-family kinases have been linked to tumourigenesis and their over-expression and activation described in breast cancer. Increased Src activity has been associated to increased cell proliferation and epithelial-mesenchymal transition (EMT). Although, Src has a well-known role in triggering cancer cell mobility, migration and invasion, through regulation of filamentous actin (F-actin), less is known regarding its partnership with the actin cytoskeleton in non-invasive stages. In *Drosophila* epithelia, Florence Janody's lab has observed that Src promotes apical F-actin accumulation. Additionally, they have shown that the control of F-actin by actin-Capping Protein limits Src-induced apoptosis or tissue overgrowth.

To evaluate the role of F-actin dynamics in Src-mediated proliferation, I searched for actin binding proteins differentially expressed during cellular transformation of the Tamoxifen (TAM)-inducible MCF10A-ER-Src cell line (ER-Src) and during breast carcinogenesis using available microarrays datasets. I found that the expression of actin cytoskeleton genes is predominantly affected in benign lesions, atypical hyperplasia (ADH) and ductal carcinoma *in situ* (DCIS). In addition, classification of the actin binding proteins (ABPs) mis-regulated into functional categories reveals that while malignant lesions are enriched for proteins that depolymerize F-actin, pre-malignant lesions are poorly enriched for this class of actin binding proteins, suggesting that distinct actin networks are involved in promoting the pre-malignant and malignant phenotypes. Among the 27 ABP's differentially expressed in ADH and DCIS, 6 were also misregulated in the same direction during transformation of the ER-Src cell line and there *Drosophila* orthologue were involved in Src-induced tissue overgrowth. These observations argue that early during breast tumour progression Src affect the expression of 6 ABPs that control tumour growth via the regulation of specialized F-actin networks.

2.2 INTRODUCTION

Breast cancer is the most common carcinoma worldwide and the second most frequent cancer-related cause of death. Particularly in women, the disease stands as the major responsible for deaths caused by cancer (Ferlay et al. 2014). Cancer of the breast is a highly complex and heterogeneous disease that presents a spectrum of several types of lesions. Each pathological entity has associated different risk factors, histological characteristics, clinical behaviours and prognosis (Lopez-Garcia et al. 2010). The expression status of a set of receptors that includes oestrogen receptor (ER), progesterone receptor (PR) and Human Epidermal growth factor Receptor 2 (HER2) has been used to classify the different breast lesions. In particular, it has been demonstrated that oestrogen receptor positive (ER+) or oestrogen receptor negative (ER-) tumours are profoundly distinct diseases (Lopez-Garcia et al. 2010). Lesions up-regulating ER also present increased expression of low molecular weight cytokeratins 8/18 and genes associated with the ER pathway (Weigelt et al. 2010). However, based on gene expression profiling, ER+ lesions can be separated in two distinct molecular subtypes: Luminal A and Luminal B that present different clinical outcomes (Sørlie et al. 2001). Luminal A lesions present low levels of proliferation genes associated with good outcome. In contrast, Luminal B lesions frequently present higher proliferation rates and significant worse prognosis (Weigelt et al. 2010). The ER- group is more heterogeneous and comprise the remaining molecular subtypes, normal breast-like HER2 and basal-like (Sørlie et al. 2001; Perou et al. 2000).

The majority of breast cancers originate from the lactiferous ducts (Invasive Ductal Carcinoma), with a 45-70%incidence (Ellis et al. 2003). Several models of progression have been proposed to describe the tumour progression of ER+ Invasive Ductal Carcinomas (IDCs) that represent 80% of all IDCs (Ellis et al. 2003). It is believed that these lesions follow a classical mode of progression, in which the normal breast tissue develops atypical ductal hyperplasia (ADH), a

neoplastic intraductal lesion in which cells present uniform nuclei and occasional mild atypia. This type of lesion is associated with an increased risk of Ductal Carcinoma *In Situ* (DCIS) development. DCIS is a neoplastic proliferative lesion with marked atypia, confined within spaces bordered by myoepithelium and basement membrane. DCIS tumours have an inherent potential to acquire malignant features and evolve to Invasive Ductal Carcinoma (IDC) through the invasion of the surrounding stroma (Lopez-Garcia et al. 2010; Bombonati & Sgroi 2011; Ellis et al. 2003). Precursor lesions and a range of invasive lesions may be histologically classified as low (indolent), intermediate or high grade (aggressive) (Lopez-Garcia et al. 2010). These grades (Grade I, II and III) can be defined by the assessment of differentiation (tubule formation), cell morphology (nuclear pleomorphism) and proliferation (mitotic activity). Histological grade is highly correlated with the patients prognosis, being the worst prognosis attributed to the highest histological grade (poor differentiation) (Elston & Ellis 1991).

The histological progression from breast cancer initiation to metastasis results from the tumourigenic process. Several players are known to contribute to the malignant transformation of cells. In particular, over-expression and specific activation of Src-family kinases have been described in several human cancers, including mammary carcinomas (Irby & Yeatman 2000). More specifically, two distinct studies show that the vast majority of ER+ breast tumours present a gene expression signature associated with an increase in Src activity (Zhang et al. 2009; Bild et al. 2006). The outcomes of increased Src activity are associated to several of the so-called "Hallmarks of Cancer". So far, it has been established that Src is involved in cellular proliferation and epithelial-mesenchymal transition (EMT), and it also acts as a trigger of cancer cell migration and invasion. Additionally, it has been suggested that low or high levels of Src activity are differently associated with proliferation or invasiveness, respectively. This level-dependence of Src function overlaps quite well with the evolution of levels of c-Src expression/activity throughout colorectal cancer progression (Yeatman 2004; M S Talamonti et al. 1993). Although the association between Src and cancer has

been established, the mechanisms proposed to explain Src's role in tumourigenesis are still poorly understood.

Src activation can be triggered by several routes, through integrins, interleukin-6 receptor, amongst others, turning on crucial signalling pathways involved in malignant transformation, including mitogen-activated protein kinases (MAPK) or signal transducer and activator of transcription 3 (STAT3) pathways (Finn 2008). In addition, Src promotes tumour cell migration and motility at later stage of cancer progression through actin cytoskeleton regulation. Particularly, Src activation has a dramatic effect on the cells, manifested by complete loss of actin stress fibres and focal adhesions (Tarone et al. 1985; Winograd-Katz et al. 2011). Coupled to these changes occurs the formation of clusters of actin cytoskeletal proteins with adhesive properties and capable of degrading the extra-cellular matrix (ECM). These cancer cells structures, commonly called invadopodia, promote tumour metastasis (Finn 2008; Murphy & Courtneidge 2011). Despite decades of research on Src, the interaction between Src and specific actin cytoskeleton networks in early stages remains to be explored.

The actin cytoskeleton is an organelle built through the assembly of its monomers, the globular actin (G-actin), into filamentous actin (F-actin). The produced filaments are organized into distinct networks, in precise locations in the cytoplasm. Each of these F-actin-based structures is able to perform specific cellular functions. Actin filament polymerization, depolymerisation and organization into distinct ordered networks are tightly controlled by a myriad of proteins that directly interact with actin. These actin binding proteins (ABPs) can be grouped in six functional classes, based on their action on actin. Some 1) promote nucleation and polymerization of filaments (e.g., Arp2/3, Ena/Vasp). Others 2) inhibit polymerization or stabilize them (e.g., CapZ, Tropomyosin). In addition, some ABPs 3) depolymerize or sever F-actin (e.g., Destrin, Cofilin). The remaining 3 groups of ABP 4) promote the cross-linking or bundling of filaments with each other (e.g., Filamin), or 5) use actin as a trail (e.g., Myosin) or 6) play a

scaffolding role by promoting interactions between actin filaments and cytoplasmic targets (e.g., Cortactin) (Dos Remedios et al. 2003; Michelot & Drubin 2011).

For the first time, in 2013, our lab has demonstrated that in *Drosophila* epithelia, Src promotes apical F-actin accumulation. Moreover, overexpressing capping protein inhibits Src-induced apoptosis or tissue overgrowth through the control of F-actin. Based on the high level of functional conservation in genes between flies and human, these observations suggested that early during tumour progression, Src promotes tumour growth through F-actin regulation (Fernández et al. 2013).

To test this hypothesis, I describe in this chapter, my search for ABPs required for Src-induced proliferation. One possibility is that Src activation alters the expression levels of these ABPs. If so, I would expect that ABPs, whose expression is affected in proliferating pre-malignant breast lesions could be downstream Src targets involved in tumour growth. I therefore analysed gene expression profiles of breast tumour samples to identify ABPs misregulated in pre-malignant and malignant lesions and determined if these alterations correlated with increased Src expression. I then determined which of these ABPs were also dysregulated in the MCF10A human cell model with conditional Src induction and tested those for a role in Src-induced tissue overgrowth in the *in vivo* model *Drosophila melanogaster*.

2.3 MATERIAL AND METHODS

2.3.1 NORMALIZATION AND STATISTICAL ANALYSIS OF MICROARRAY DATA

The raw data (CEL files) from 16 publicly available microarray series were collected from Gene Expression Omnibus (GEO) database of National Center for Biotechnology Information (NCBI). Series Accession numbers, Affymetrix platforms, histological classification of samples and associated publications can be found in Table 2.1. Sample information was obtained from the correspondent Series Matrix File(s).

The Affymetrix HG-U133A Plus 2.0 Array is able to do a complete coverage of the U133 Set plus 6,500 additional genes for analysis of over 47,000 transcripts. Additionally, all probesets represented in Affymetrix HG-U133A Arrays are identically replicated on the GeneChip Human Genome U133 Plus 2.0 Arrays (GEO information platform).

The raw data selected for the microarrays analysis derived from the RNA hybridization in these two platforms. 4 of the 16 sample series were hybridized on HG-U133A Arrays, being the remaining 12 hybridized on HG-U133A Plus 2.0 Arrays. Both platforms cover an identical set of 150 genes encoding ABP. For other genes, only probesets present in both Affimetrix platforms were analysed.

The sample set used was mostly composed of Invasive Ductal Carcinoma tumours, being the majority of the samples ER+. There were only three series with samples of benign lesions compatible with stages of ER+ Breast Cancer progression available online: GSE2109 (DCIS - 1), GSE16873 (ADH – 12 and DCIS - 12) and GSE21422 (DCIS - 9).

Table 2.1: Number and histological classification of the samples used in the gene expression analysis, respective platforms and bibliographic references. N-Normal tissue; ADH – Atypical Ductal Hyperplasia; DCIS – Ductal Carcinoma In Situ; IDC – Invasive Ductal Carcinoma; ER - Oestrogen receptor. A - HG-U133A, B - HG-U133A PLUS 2.0

Series	Platform	Samples									Bibliography
					IDC						
		N	ADH	DCIS	Grade division (IDC,ER+)			Grade division (IDC,ER-)			
					I	II	III	I	II	III	
GSE15852	A	43	0	0	4	10	8	3	10	4	(Pau Ni et al. 2010)
GSE16873	A	12	12	12	n.a.	n.a.	n.a.	n.a.	n.a.	n.a.	(Emery et al. 2009)
GSE7390	A	0	0	0	21	54	27	0	13	43	(Desmedt et al. 2007)
GSE20194	A	0	0	0	7	64	44	0	13	80	(Popovici et al. 2010; Shi et al. 2010)
GSE10810	B	27	0	0	2	7	2	0	2	9	(Pedraza et al. 2010)
GSE21422	B	5	0	9	n.a.	n.a.	n.a.	n.a.	n.a.	n.a.	(Kretschmer et al. 2011)
GSE22544	B	4	0	0	n.a.	n.a.	n.a.	n.a.	n.a.	n.a.	(Hawthorn et al. 2010)
GSE23593	B	0	0	0	2	17	10	0	0	12	(Barry et al. 2010)
GSE5460	B	0	0	0	15	11	18	0	5	45	(Lin et al. 2010)
GSE5764	B	10	0	0	n.a.	n.a.	n.a.	n.a.	n.a.	n.a.	(Turashvili et al. 2007)
GSE10780	B	143	0	0	n.a.	n.a.	n.a.	n.a.	n.a.	n.a.	(Chen et al. 2010)
GSE2109	B	0	0	1	3	11	4	1	2	15	-
GSE3744	B	7	0	0	0	0	15	0	0	24	(Richardson et al. 2006; Alimonti et al. 2010)
GSE17907	B	4	0	0	1	4	8	0	3	17	(Sircoulomb et al. 2010)
GSE19615	B	0	0	0	13	11	21	0	6	36	(Li et al. 2010)
GSE23177	B	0	0	0	0	0	116	0	0	0	(Smeets et al. 2011)
Total		255	12	22	68	189	273	4	54	285	

2.3.2 ANALYSIS OF MICROARRAY DATA

R Programming Language for Statistical Computing 2.14.1 (22-12-2011) along with Bioconductor 2.10 packages were used to perform all the calculations (R Development Core Team 2011). The raw data was subjected to the frozen

Robust Multi-Array Average (fRMA) algorithm for background correction, adjustments for systematic errors and to removal of dye intensity effects (McCall et al. 2010). Followed by summarization based on multi-array model fitted using the Median Polish algorithm. Probesets were mapped using Entrez gene probeset definition to the HG-U133A platform. The expression values were transformed in log2 values. Then, ComBat algorithm was used to decrease the non-biological experimental variation or batch effect, of each gene independently (Johnson et al. 2007).

The genes differentially expressed in breast cancer progression were identified comparing data from the different histological stages to normal tissue. In each comparison, LIMMA (Linear Models for Microarray Data) algorithm, which uses a simple Bayesian model, was used to calculate de fold change (Log2R), B-statistics (lods), t-statistics and p-values. The list of genes differentially expressed was constituted by all the genes with lods value higher than 0, i. e., the probability of being differentially expressed was higher that 50%.(Smyth 2005) The differentially expressed genes selected were used for further analysis.

2.3.3 GENE ANNOTATION AND PATHWAY ANALYSIS

The Pathway-Express tool, part of the Onto-tools (http://vortex.cs.wayne.edu), was used to assess which biological processes and pathways were more affected during breast cancer progression. The list of differentially expressed (DE) genes was subjected to statistical analysis using the hypergeometric model, which calculates the probability of observing the actual number of genes just by chance, i.e., a p-value (Draghici et al. 2007). Additionally, the impact analysis considered the normalized fold change of the differentially expressed genes and the topology of the signalling pathway (Draghici et al. 2007).

2.3.4 CANDIDATE ABPS GENES

A list of all human Actin Binding Protein, and described function, was obtained from UNIPROT database, on January 2013, using as criteria: "actin-binding protein"; Organism:"9606"; Location: "cytoskeleton"; reviewed: "yes". The list was verified based on the presence of an actin-binding domain previously described. With this list it was possible to filter only the ABPs genes DE during breast cancer progression.

2.3.5 FUNCTIONAL CLASSIFICATION OF ABPS

The function of each ABP encoded by the genes present in the platform HG-U133A has been described in the literature and cited in the UNIPROT database. ABP genes were grouped in 6 different functional categories. Considering the protein function in the actin cytoskeleton dynamics, genes were group in the following classes: 1) Polymerization/ Branching filaments, 2) Inhibition of polymerization/ Stabilization, 3) Filament severing/ Depolymerization, 4) Cross-linking/ Formation of bundles, 5) Motor proteins and 6) Adapter/ Scaffold.

Percentage of ABPs genes up or down-regulated for each category was calculated over the total number of ABPs of each functional class, probed in the platform used as reference (HG-U133A).

2.3.6 FLY STRAINS AND GENETICS

Fly stocks used were *nub*-Gal4 (Calleja et al. 1996), *Src64B*^{UY1332} (Nicolaï et al. 2003); *UAS-p35* (Hay et al. 1994), UAS-*arp3-IR*^{KK108951}, UAS-*arpc5-IR*^{KK102012}, UAS-*Tm2-IR*^{KK107970}, UAS-*fhos-IR*^{GD19034} (VDRC), UAS-*ena-IR*^{JF01155}, UAS-*shot-IR*^{GL01286}, UAS-*GFP::arp3* (Hudson & Cooley 2002), UAS-*ena* (Ahern-Djamali et al. 1998; Gaspar et al. 2015); UAS-*shotL(A)-GFP* (Lee & Kolodziej 2002). *nub*-Gal4 or *nub*-Gal4, UAS-*mCD8::GFP* females were crosses to males carrying either one of

the UAS-*RNAi* line with or without UAS-*p35*. All crosses were maintained at 25ºC and progeny were dissected at the end of third instar larvae.

2.3.7 QUANTIFICATION OF WING DISC GROWTH

The NIH Image J program was used to perform measurements (Schneider et al. 2012). To quantify total wing disc area, each disc was outlined and measured using the *Area* function, which evaluates size in square pixels. To quantify the ratio of the *nub>GFP* domain over the total wing disc area, the ratio between the area of the GFP domain and the area of the whole disc domain, measured using the *Area* function for each disc, were performed. Statistical significance was calculated using a two-tailed *t*-test.

2.4 RESULTS

2.4.1 MORE THAN 60% OF THE TOTAL NUMBER OF ABPS IS DYSREGULATED THROUGHOUT BREAST CANCER PROGRESSION.

To identify ABPs involved in Src-mediated tumour growth, I first analysed gene expression profiles of pre-malignant and malignant breast lesions Raw data (CEL files) from publicly available microarrays of normal breast tissue and from tumours were collected (GEO database) and analysed. In total I compiled data from samples of 255 normal tissues, 12 ER+ ADH, 22 ER+ DCIS, 530 ER+ IDC and 343 ER- IDC. I then applied the fRMA and ComBat methods to eliminate the technical errors and batch-effects and used the LIMMA algorithm to sort out all genes differentially expressed between tumours at different stages of breast cancer progression and normal tissue. Genes were characterized as overexpressed when they presented a Log2R>0, and as under-expressed when they presented a Log2R<0. The quality assessment of the microarray analysis was performed using well-established breast cancer markers. As expected in ER+

luminal breast cancer, the genes encoding ER (ESR1), cytokeratins 8/18/19 (KRT8, KRT18 and KRT19) were overexpressed. As negative controls, three markers for basal-like breast cancers were used: KRT5, KRT14 and KRT17 (Malzahn et al. 1998; Weigelt et al. 2010; Colombo et al. 2011; Gudjonsson et al. 2005). As expected, these genes were under-expressed in all IDC grades relative to normal tissue (Table 2.2).

Table 2.2: Fold-change in gene expression of established breast cancer markers in ER+ breast tumour lesions. Microarray data of different lesions classified as Estrogen receptor positive (ER+) versus (vs) Normal tissue. As expected the gene encoding ER (ESR1) was overexpressed (darker gray), Genes encoding markers for ER+ luminal cancers (KRT 8, 18 and 19) were overexpressed (light gray). Markers for basal breast cancers were underexpressed (KRT 5, 14 and 17). Genes are considered as up-regulated or downregulated when Log2R>0 or Log2R<0, respectively. ADH - Atypical Ductal Hyperplasia; DCIS - Ductal Carcinoma In Situ; IDC1 - Invasive Ductal Carcinoma Grade 1; IDC2 - Invasive Ductal Carcinoma Grade 2; IDC3 - Invasive Ductal Carcinoma Grade 3 and N - Normal tissue.

	Fold Change (Log2R)				
	ER+ADH vs N	**ER+ DCIS vs N**	**ER+ IDC1 vs N**	**ER+ IDC2 vs N**	**ER+ IDC3 vs N**
ESR1			2.56	2.68	1.36
KRT8		1.62	2.14	2.26	2.24
KRT18		1.48	2.21	2.22	2.04
KRT19		2.18	2.978	2.83	2.346
KRT5			-2.53	-3.29	-3.33
KRT14			-2.40	-3.58	-3.95
KRT17			-1.86	-2.43	-2.43

Progression from ADH to IDC showed net increase of the number of genes differentially expressed when compared to normal breast tissue (Table 2.2). I identified a total of 7792 genes whose expression was affected in at least one type of lesion, when compared to normal breast tissue. Among those, 373 genes were differentially expressed in ADH; 1544 genes in DCIS; 4376 genes in IDC grade 1; 6307 genes in IDC grade 2 and 6956 genes in IDC grade 3. As expected, the number of genes differentially expressed increased between DCIS and all IDC grades with a more striking increase in high-grade IDC lesions (IDC1- 568 genes,

IDC2-749 genes and IDC3-1545 genes). While DCIS showed a net increase in the number of genes deregulated; when compared to ADH, this difference was not significant. This observation is consistent with the model by which ADH progresses to DCIS and indicates that in ADH, many genes already show a trend in gene expression alteration that is potentiated in DCIS. The majority of genes differentially expressed in ADH, relative to normal breast tissues were downregulated (53.89%). In contrast, DCIS, IDC1, IDC2 and IDC3 lesions showed a higher percentage of genes overexpressed, compared to normal tissue samples (57.97%, 53.43%, 54.37%, and 55.55%, respectively) (Figure 2.1). Interestingly, the percentage of genes whose expression is significantly altered from DCIS to IDC is smaller than 13% of the total number of genes differentially expressed in comparison to normal tissue (IDC 1 – 13%; IDC2 – 11.8%; IDC3 - 10.3%). These observations reinforce the importance of quantitative differences in gene expression for the evolution of breast cancer as a continuum. In addition, they also suggest the existence of two major transitions in gene expression: One that is qualitative associated with the transition from normal to hyperplasia and one quantitative transition from pre-invasive disease to invasive disease. Altogether, these observations strongly suggest the existence of two major transitions in tumourigenesis (normal ⟶ hyperplasia and DCIS ⟶ IDC).

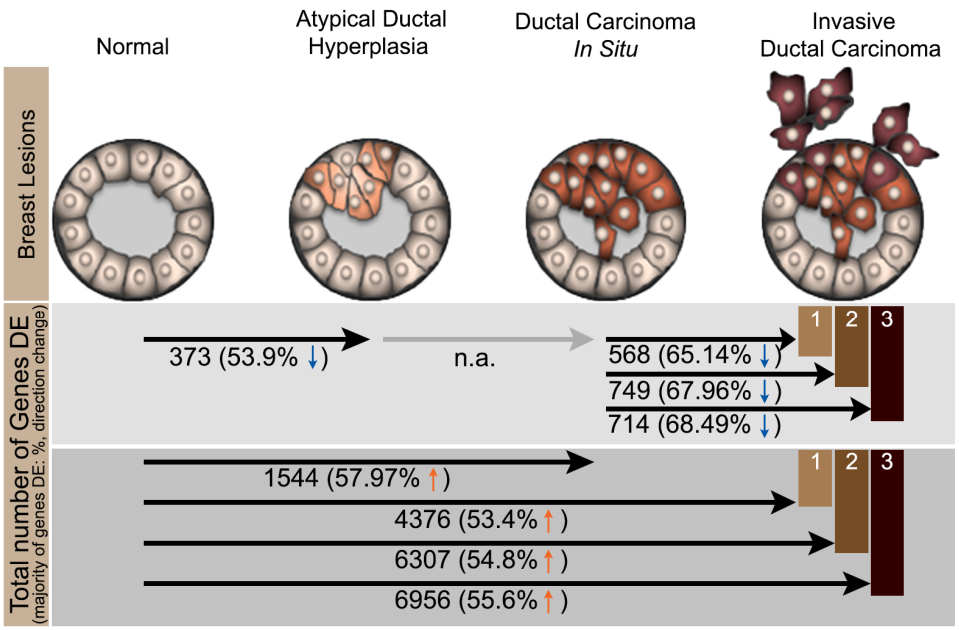

Figure 2.1: Gene expression analysis suggests two key transitions in tumour progression, from normal to ADH, and from DCIS to IDC. Total number of genes differentially expressed between each lesion and normal tissue, and between lesions. For each comparisson, information concerning the direction of change of the majority of genes differentially expressed is presented in parentheses. Blue arrow – underexpressed, orange arrow – overexpressed. none. – no genes were significantly altered between ADH and DCIS.

2.4.2 MISREGULATION OF ABP GENES IS PREDOMINANT IN NON-INVASIVE STAGES OF BREAST CANCER PROGRESSION

To identify a gene expression signature associated with the actin cytoskeleton, I restricted the list of genes of interest to those encoding direct modulators of the actin cytoskeleton. From the 274 entries for ABPs listed in UNIPROT, 150 ABPs genes were present in the microarray platforms used in these studies. Strikingly, among those, more than 60% were deregulated during breast cancer progression (Figure 2.2.A), with 47 (48.96%) under-expressed and 49 (51.06%) over-expressed (Figure 2.2.B). 4.6% of those ABPs were misregulated in ADH, 18% in DCIS (Figure 2.2.A). Thus, lesions that show higher percentage of ABP misregulated also show a significant increase of Src expression. These

lesions, IDC 2 and 3, are typically associated with highly aggressive phenotype and therefore with bad prognosis (Weigelt et al. 2010). However, when compared to the total number of genes deregulated, non-invasive tumours showed higher percentages of ABPs encoding genes deregulated than invasive tumours, with 1.88% and 1.75% in ADH and DCIS respectively, against 1.39%, 1.28% and 1.27% in IDC1, 2 and 3, respectively (Table 2.3). Additionally, the different enrichment of deregulated ABPs genes suggests different contributions of the actin cytoskeleton in the acquisition and maintenance of the hyperplastic phenotypes and posteriorly in the invasive ones. The enrichment of deregulated ABPs genes in non-invasive stages suggests an important role of the actin cytoskeleton at these stages.

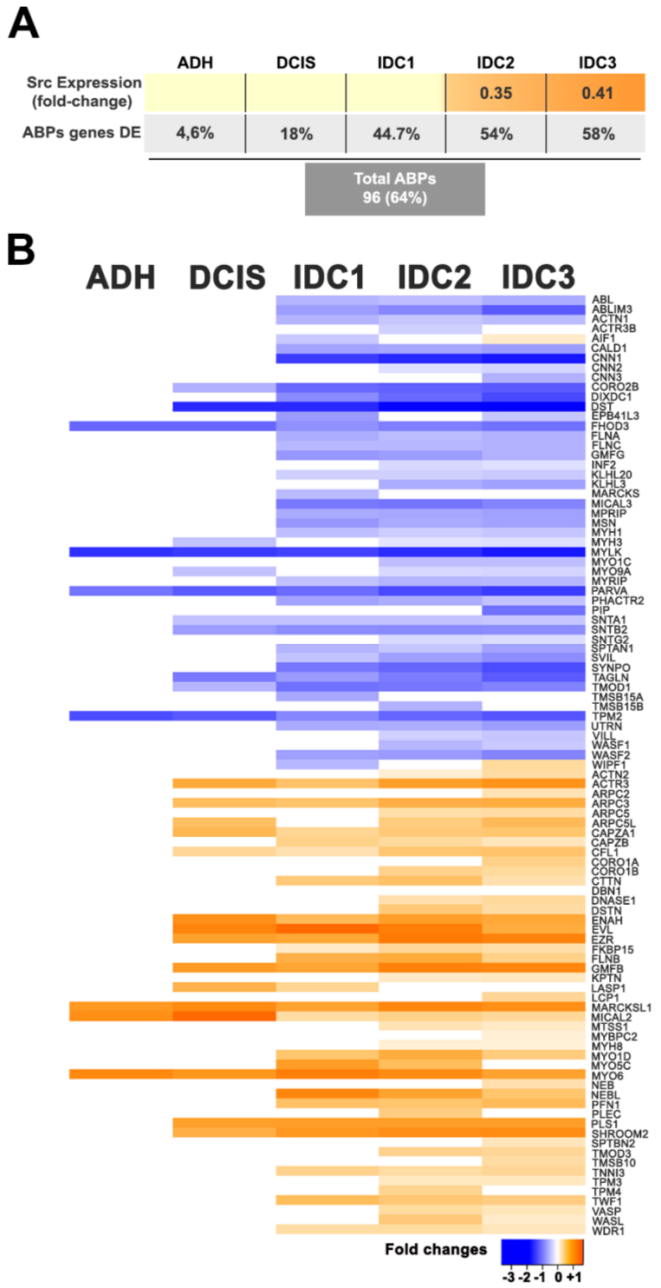

Figure 2.2: The majority of genes encoding ABPs are over-expressed, in at least one stage of tumour progression. (A) Table depicting the correlation between Src expression levels and the percentage of ABPs probed in the platform and that are dysregulated at different stages of ER+ breast lesions. **(B)** Heatmap of all ABPs differentially expressed at different stages of ER+ breast lesions. Fold-changes are in Log2R.

Table 2.3: Early stages of breast cancer progression show an enrichment of differentially expressed ABP's genes. Number of genes differentially expressed encoding ABPs and correspondent percentage over total number of DE genes in ADH, DCIS, IDC1, IDC2 and IDC3 lesions as compared to normal breast tissue. UP - Genes upregulated with Log2R>0; DOWN - Genes downregulated with Log2R<0. ADH - Atypical Ductal Hyperplasia; DCIS - Ductal Carcinoma In Situ; IDC1-3 - Invasive Ductal Carcinoma Grade 1-3.

	ABP/Total genes (%)	ABPs UP (%)	ABPs DOWN (%)
ADH	7 (1.88)	3 (42.86)	4 (57.14)
DCIS	27 (1.75)	15 (55.56)	12 (44.44)
IDC1	61 (1.39)	25 (40.98)	36 (59.01)
IDC2	81 (1.28)	42 (51.85)	39 (48.15)
IDC3	88 (1.27)	45 (51.14)	43 (48.86)

To identify signature of genes misregulated during breast cancer progression, I used the Pathway-Express tool, which takes into account the classical probabilistic component, the magnitude of each gene's expression range, their protein function and position on the given pathways and their interactions (Draghici et al. 2007).

As expected, ER+ breast tumour lesions affected several pathways, such as Wnt and MAPK signalling pathways, that have been previously associated with the development of other types of cancer, (Lamouille et al. 2014; Dhillon et al. 2007). Additionally, adherens junction (AJs), focal adhesion (FA) and tight junction pathways are also commonly affected during cancer progression (Parsons et al. 2010; Martin & Jiang 2008) (Figure 2.3). Interestingly, all these pathways were highly affected in at least one of the non-invasive stages. In particular, AJ and FA pathways were altered in the first transition, from normal tissue to ADH. Among these three adhesion pathways, only FA pathway has statistically significant number of differentially expressed genes at all stages and presents highly biological meaningful changes (higher Impact Factor) (Figure 2.3). Given that Src activity and actin are necessary for FA turnover and architecture (Frame et al. 2002), this observation suggests that the regulation of FA dynamics

might play an important role during breast cancer progression, possibly through coupling Src signalling activity and the actin cytoskeleton.

The get a broader perspective on the importance of the actin cytoskeleton in breast cancer progression, I focused my analysis on the Regulation of the Actin Cytoskeleton. Excitingly, the analysis showed that this pathway was highly affected in the first two stages of breast cancer progression, ADH and DCIS. When compared to normal tissue, it was one of the ten most affected in non-invasive lesions, ranking at position 8^{th} in ADH and DCIS, respectively. Surprisingly, Regulation of actin cytoskeleton did not appear as a category statistically altered in IDC1, and ranked at position 23 and 21 in IDC2 and IDC3 respectively (Figure 2.3). These results indicate that massive alterations of modulators of the actin cytoskeleton are associated with the development of non-invasive ER+ breast tumours. Thus, changes in the actin cytoskeleton and cell adhesion structures may be key steps for the development of pre-malignant lesions.

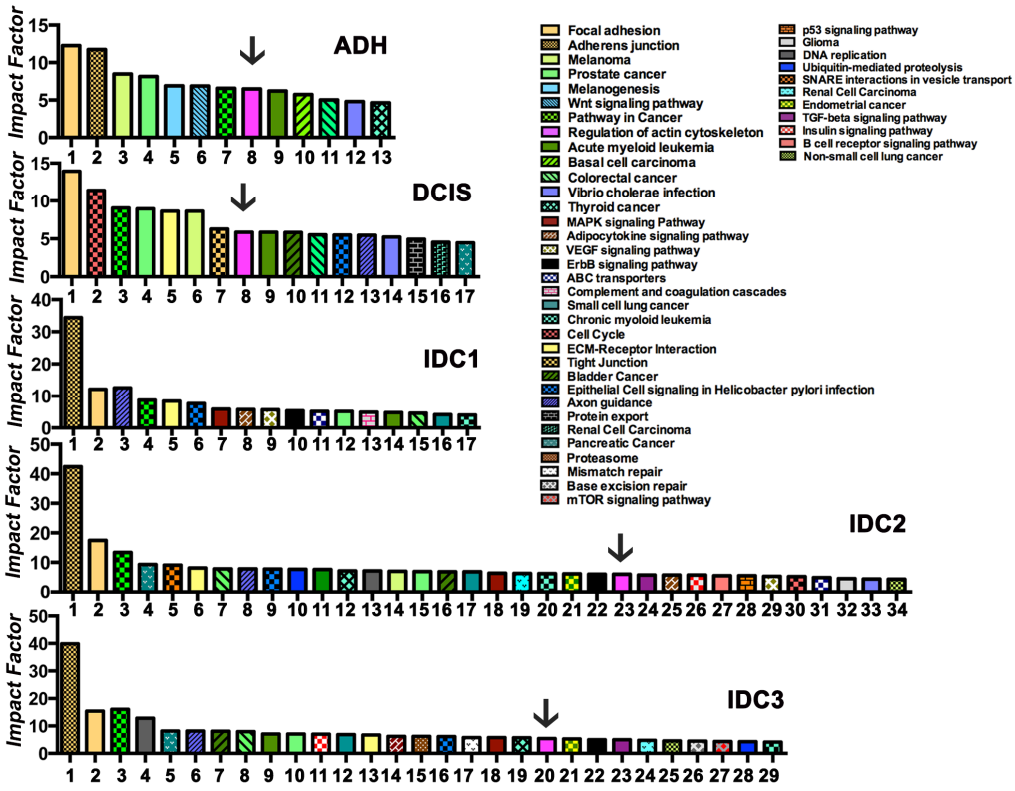

Figure 2.3: Pathway Impact Analysis for the sets of genes differentially expressed in ER$^+$ ADH, DCIS, IDC1, IDC2 and IDC3 when compared to normal breast tissue samples. All pathways significantly affected were plotted based on their impact factor for at each stage. N- Normal tissue; ADH – Atypical Ductal Hyperplasia; DCIS – Ductal Carcinoma In Situ; IDC – Invasive Ductal Carcinoma; ER - Oestrogen Receptor

2.4.3 NON-INVASIVE AND INVASIVE BREAST LESIONS HAVE DIFFERENT ABPS FUNCTIONAL PROFILES.

To get insight on whether non-invasive and invasive breast cancer showed distinct actin dynamics profiles, I explored whether breast cancer progression was associated to the enrichment of particular functional classes of ABPs. ABPs down and up-regulated in ER+ breast tumours were classified into 6 functional categories, based on their action on F-actin using the gene-ontology vocabulary. The 6 groups were defined as: 1) Polymerization, 2) Inhibition of

Polymerization/Stabilization, 3) Severing/Depolymerization, 4) Cross-linker/Bundler, 5) Motors and 6) Adaptors/Scaffold. Then, I calculated the percentage of ABPs up or down-regulated for each category over the total number of ABPs covered by the platform HG-U133A, used as reference. At this point, I was able to compare the F-actin remodelling profiles between non-invasive and invasive ER+ breast tumours.

The analysis of the functional categories showed that all lesions over-expressed ABP's involved in polymerization. On the contrary, inhibitors of polymerization showed a shift with a down-regulation of this category of ABPs in DCIS and their up-regulation in all IDCs (Figure 2.4). Thus, all IDCs upregulated similar number of polymerizing factors and inhibitors of polymerization, while non-invasive tumours up-regulated many F-actin-polymerizing factors but very few inhibitors of polymerization. These observations suggest that the actin machinery operating in pre-malignant and malignant lesions are distinct.

To determine if these F-actin remodelling profiles were associated with the stage of the disease and not with the ER-status, I also analysed the profile of ER- IDC tumours. Strikingly, almost 80% of the ABPs misregulated in ER+ IDCs, were also misregulated in the same direction in ER- IDC2 and 3 (Figure 2.2 and Supplementary Fig. S1). Thus, these shared ABPs may constitute a gene expression signature of metastasis behaviour. In addition, like ER+ IDCs, but in contrast to ER+ DCIS, ER- IDCs up-regulated both polymerizing factors and inhibitors of polymerization, indicating that an enrichment of these two functional classes of ABPs is likely a feature of invasive lesions. However, in contrast to ER+ IDCs, ER- IDCs were enriched in all classes of functional ABPs. This observation suggests that the F-actin turnover rate might be higher in ER- IDCs than in ER+ ones. Taken together, the ABPs functional profiling show that both non-invasive and invasive tumours over-express many F-actin polymerization factors, but non-invasive tumours express fewer inhibitors of polymerization.

These results show that malignant and non-malignant lesions are enriched for distinct functional classes of ABPs. Therefore, tumour progression may involve major differences in the F-actin networks built at different stages of breast cancer.

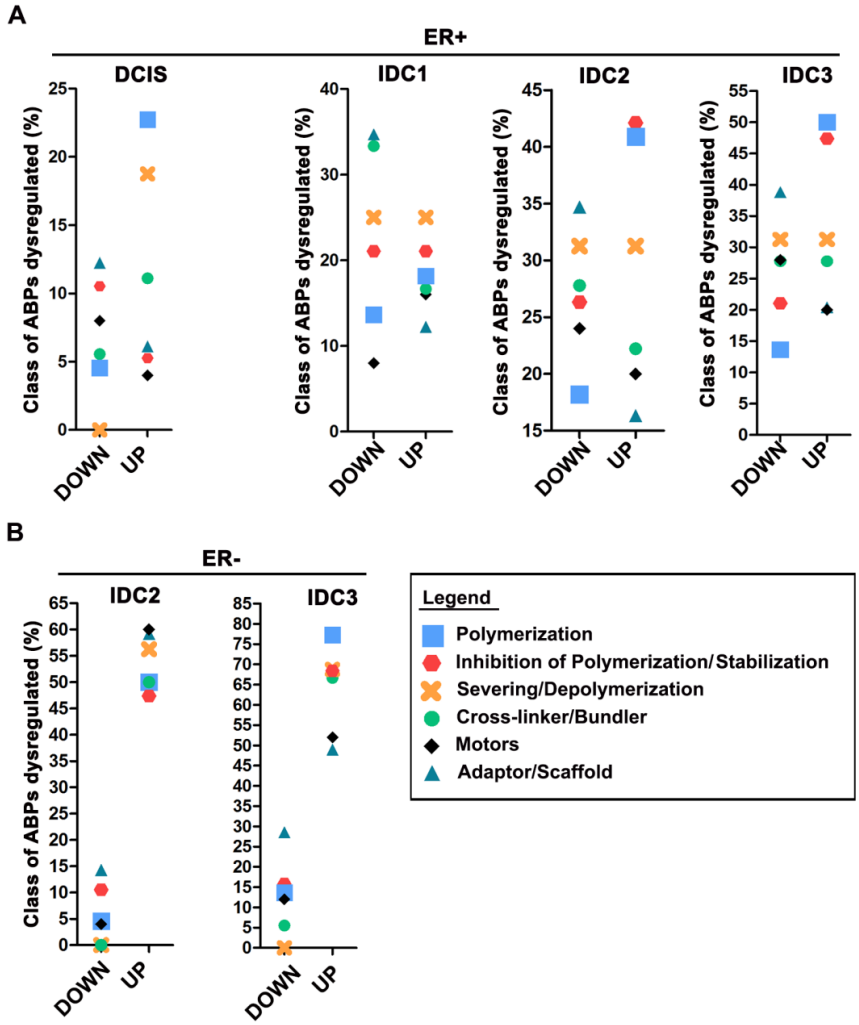

Figure 2.4: Functional classification of genes encoding ABP differentially expressed during ER+ breast cancer progression and ER- Invasive Ductal Carcinoma. The function of each ABP, encoded by the genes present in the list, was obtained in the literature. ABP genes were classified in 6 different functional categories, including Polymerization (Light Blue Square); Inhibition of polymerization/ Stabilization (Red Hexagon); Filament severing/ Depolymerization (Yellow Cross), Cross-linking/ Formation of bundles (Green Dot); Motor proteins/ Muscle contraction (Black Losangle) and Adapter/ Scaffold (Dark Blue Triangle), based on their function on actin.

2.4.4 6 COMMON ABPS ARE DIFFERENTIALLY EXPRESSED IN NON-INVASIVE TUMOURS AND IN MCF10A CELLS WITH CONDITIONAL SRC INDUCTION.

So far, my observations suggest a major role of actin cytoskeleton dynamics in the pre-malignant stages of ADH/DCIS. To explore the role of F-actin in tumour growth downstream of Src, I selected the ABPs deregulated in pre-malignant breast cancer lesions. Among those, the 7 ABPs genes dysregulated in ADH were still misregulated in DCIS. In addition, 20 ABPs started to be differentially expressed at this stage. Deregulation of these 27 ABPs were still observed in all the subsequent IDC grades (Figure 2.5.A), suggesting that these ABPs might be involved in tumour formation and growth, and later on in the development of malignant phenotypes. I next determined which of these ABPs were regulated by Src using available microarray data sets of the Src-inducible MCF10A-ER-Src (ER-Src) cell line. This cell line contains a fusion between the Src kinase oncoprotein (v-Src) and the ligand-binding domain of the Estrogen Receptor (ER-Src), which is inducible with tamoxifen (TAM) treatment (Hirsch et al., 2009; Iliopoulos et al., 2009). Conditional induction of Src activity in this non-transformed mammary epithelial cell line enables the study of tumourigenesis in cell culture. In 2D culture, the activation of Src triggers full phenotypic transformation, within 36 hours. In 2010, Hirsch and colleagues published a study in which using microarrays capable of assaying most protein-coding mRNAs, they identified the transcriptional profiling of TAM-induced ER-Src cells (eight time-points from 1-36h after TAM treatment. 1201 genes were identified as differentially expressed at any time point (Hirsch et al. 2010), including 35 ABPs genes (Figure 2.5.B). Among those, EVL, ARPC3, ARPC5L, DST, FHOD3 and TPM2, were deregulated in DCIS tumours. In addition four of these ABPS (CALD1, ABLIM3, LCP1 and FLNB) were deregulated only in IDCs. This observation suggests that the 6 ABPs deregulated in the same direction in DCIS

and in TAM-induced ER-Src cells might be required for Src-induced tumour growth.

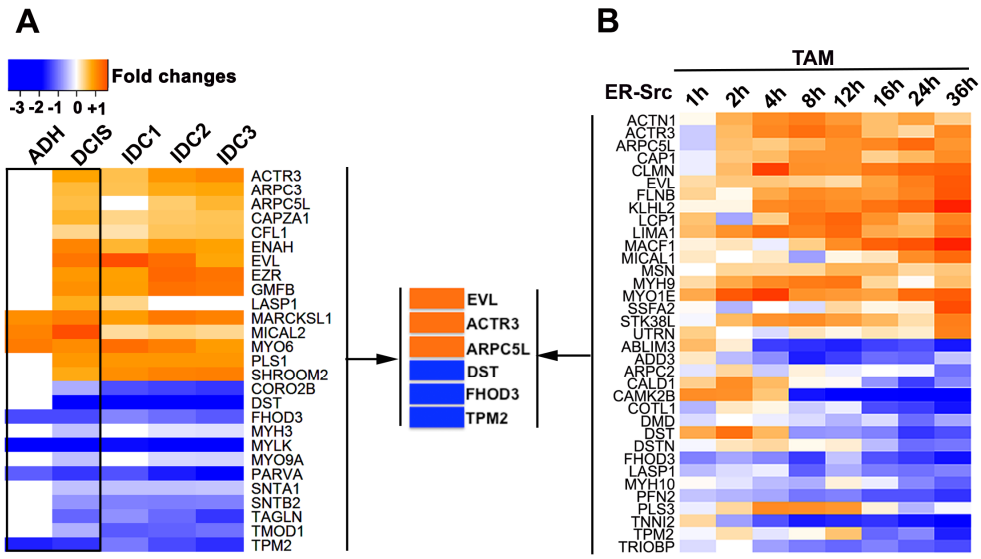

Figure 2.5: A set of 6 ABP are differentially expressed during ER+ breast cancer progression and in TAM-induced ER-Src cells. Heatmaps of ABP dysregulated in (left panel) ADH and/or DCIS and their expression in the three IDC grades or (right panel) ER-Src cells treated with TAM for 1, 2, 4, 8, 12, 16, 24 and 36 hours (Hirsch et al., 2010). Fold-changes are in Log2R. Common ABPs misregulated in the same direction in both ADH/DCIS and TAM-induced ER-Src cells (middle panel). Orange and blue indicate genes up- and down-regulated respectively.

2.4.5 ABPs DEREGULATED IN EARLY BREAST CANCER IMPACT THE GROWTH OF *DROSOPHILA* EPITHELIA.

To investigate if EVL, ARPC3, ARPC5L, DST, FHOD3 and TPM2 were relevant for Src-induced transformation, we first screened for those that affect the pro-growth function of Src in *Drosophila*, as this organism contains only one family member for each of these ABPs (Figure 2.6.A), reducing the risk of gene redundancy. To model Src-induced overgrowth, we overexpressed *Drosophila Src64B (*UAS-*Src64B)* together with GFP (UAS-*GFP*) using *nubbin*-Gal4 (*nub*-Gal4), which drives expression in the distal domain of the wing disc epithelium. We also expressed the Caspase inhibitor *p35* (UAS-*p35*), as high levels of *Src* overexpression triggers apoptosis (Vidal et al. 2007). As expected, the discs were significantly bigger compared to the control ones expressing only GFP (Figure 2.6.C-E) (Fernández et al. 2013).

We then investigated if altering the levels of each of the 6 ABPs could affect the overgrowth of *nub>Src,p35*-expressing tissue, ensuring that each genetic combination contained the same number of UAS transgenes. Strikingly, *nub>Src/p35*-expressing wing discs in which UAS-*GFP* was replaced by UAS constructs expressing double stand RNA (dsRNA) directed against *EVL/ena* (UAS-*ena-RNAi*) were not significantly bigger that *nub>GFP* control discs, indicating that EVL/ena is required for Src-induced tissue overgrowth (Figure 2.6.F-H). In contrast, knocking down *ACTR3*/*arp3* (UAS-*arp3-RNAi*), *ARPC5L/arpc5* (UAS-*arpc5-RNAi), DST/shot* (UAS-*shot-RNAi), FHOD3/fhos* (UAS-*fhos-RNAi)* or *TPM2/tm2* (UAS-*tm2-RNAi)* enhanced the overgrowth of *nub>Src/p35*-expressing wing discs (Figure 2.6.I-Z).

A

Human	*Drosophila*
EVL ENAH VASP	*ena*
ACTR3 ACTR3B	*Arp3*
ARPC5L ARPC5	*Arpc5*

Human	*Drosophila*
DST MACF1	shot
FHOD3 FHOD1	*fhos*
TPM2 TPM3 TPM4 TPM1	*tm2*

B

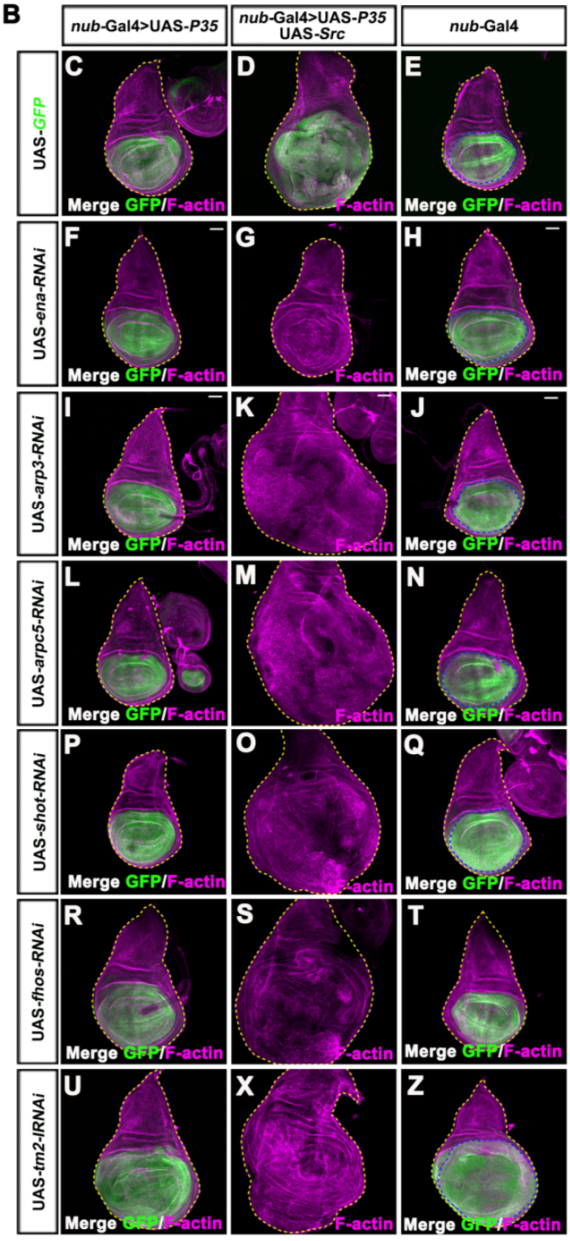

Figure 2.6: Knocking down the *Drosophila* orthologue of the 6 ABPs dysregulated in DCIS and in TAM-induced ER-Src cells affect the overgrowth of *nub>Src,p35*-expressing tissue. **(A)** Human ABPs dysregulated in TAM-induced ER-Src cells and in non-invasive ER+ breast lesions with their family members and their corresponding Drosophila counterpart. Orange and blue indicate genes up and down-regulated respectively. **(B)** Standard confocal sections of third instar wing imaginal discs with dorsal side up, stained with Phalloidin to mark F-actin (magenta). (C-Z) nub-*Gal4* driving (C,F,I,L,P,R,U) UAS-*p35* and UAS-*mCD8-GFP* (green) or (D,G,K,M,O,S,X) UAS-*p35* and *Src64B*^{UY1332} or (E,H,J,N,Q,T,Z) UAS-*mCD8-GFP* (green) and (F-H) UAS-*ena-RNAi* or (I-J) UAS-*arp3-RNAi* or (L-N) UAS-*arpc5-RNAi* or (P-Q) UAS-*shot-RNAi* or (R-T) UAS-*fhos-RNAi* or (U-Z) UAS-*tm2-RNAi.* The yellow dashed lines outline the whole wing disc area. The blue lines in E, H, J, N, Q, T and Z outline the nub>*GFP*-expressing domains. The scale bars represent 30 μm

In the converse experiments, we overexpressed these ABPs in *Src/p35*-overexpressing wing discs when transgenic flies were available. Consistent with our knocking down experiments, overexpressing *EVL/ena* strongly enhanced Src-induced tissue, while overexpressing *ACTR3/arp3* or *DST/shot* reduced the overgrowth of these tissues. Thus, *EVL/Ena* promotes *Src/p35*-induced tissue overgrowth, while *ACTR3/Arp3*, *ARPC5L/Arpc5*, *DST/Shot*, *FHOD3/Fhos* and *TPM2/Tm2* have the opposite effect (Figure 2.7).

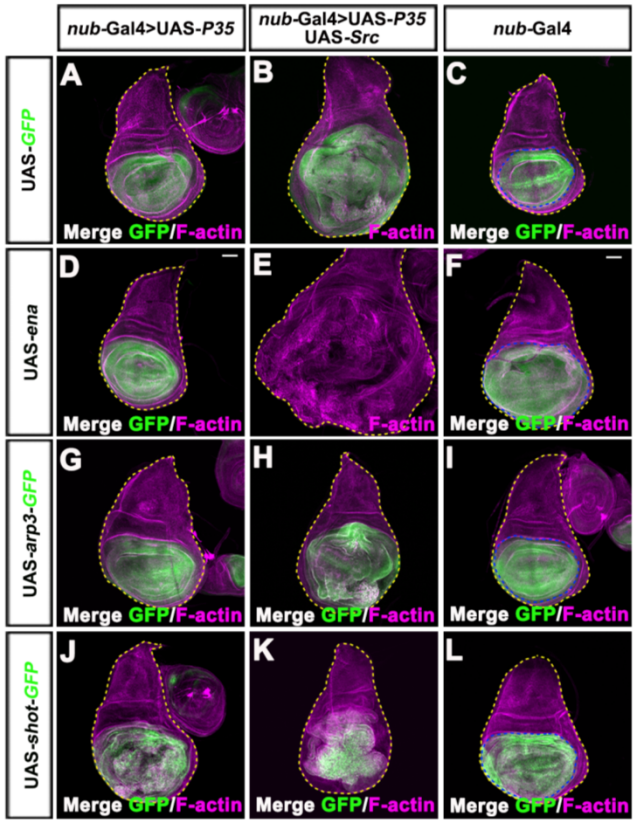

Figure 2.7: Overexpressing *ena*, *arp3* or *shot* affect the overgrowth of *nub>Src,p35*-expressing tissue. Standard confocal sections of third instar wing imaginal discs with dorsal side up, stained with Phalloidin to mark F-actin (magenta) (C-Z). nub-*Gal4* driving (A,D,G,J) UAS-*p35* and UAS-*mCD8-GFP* (green) or (B,E,H,K) UAS-*p35* and $Src64B^{UY1332}$ or (C,F,I,L) UAS-*mCD8-GFP* (green) and (D-F) UAS-*ena* or (G-I) UAS-arp3-*GFP* or (J-L) UAS-*shot-GFP*. The yellow dashed lines outline the whole wing disc area. The blue lines in C, F, I and L outline the nub>*GFP*-expressing domains. The scale bars represent 30 μm.

Knocking down or overexpressing these ABPs did not significantly affect the growth of control *p35*-overexpressing wing discs. To rule out that these ABPs are not sufficient to affect tissue growth, we expressed dsRNA directed against these ABPs and GFP using *nub*-Gal4 in wing discs that did not overexpressed *Src* and *p35*. Quantification of the ratio of the *nub>GFP*-expressing area over the total wing disc area showed that, knocking down *ACTR3/arp3*, or *ARPC5L/arpc5* or *FHOD3/fhos*, had no effect on tissue growth compared to *nub>GFP* control discs.

However, overexpressing *EVL/ena* or knocking down *DST/shot* or *TPM2/tm2* was sufficient to induce tissue overgrowth. In contrast, overexpressing *DST/shot* significantly reduced growth of control *nub>GFP* wing discs. Thus, *DST/Shot* and *TPM2/Tm2* are sufficient to limit tissue overgrowth, while *EVL/Ena* triggers tissue overgrowth (Figure 2.8).

		Tissue growth (fold changes)			
		Src+; p35+		*wt*	
GFP		1		1	
ena	*RNAi*	0.75	*p<0.0001*	1.03	
	Over.	1.20	*p<0.0001*	1.06	*p<0.0009*
Arp3	*RNAi*	1.47	*p<0.0001*	1	
	Over.	0.82	*p<0.0004*	1.03	
Arpc5	*RNAi*	1.40	*p<0.0001*	1.03	
shot	*RNAi*	1.12	*p<0.005*	1.06	*p<0.001*
	Over.	0.80	*p<0.0002*	0.96	*p<0.03*
fhos	*RNAi*	1.08	*p<0.03*	0.99	
tm2	*RNAi*	1.18	*p<0.0001*	1.41	*p<0.0009*

Figure 2.8: Effect of knocking down (RNAi) or overexpressing (Over.) *ena, Arp3, Arpc5, shot, fhos* and *tm2* on growth of wing imaginal discs overexpressing *Src64B*^{UY1332} (contains UAS P-element insertion located upstream of the Src64B transcriptional start site) and UAS-p35 under nub-Gal4 control or wild type (wt) for Src and p35 but expressing UAS-*mCD8::GFP* under nub-*Gal4* control. Values represent fold changes relative to (first column) nub>*GFP*, *Src64B*^{UY1332}, *P35* (first lane) or to (second column) nub>*GFP* (first lane). Blue and yellow indicate a significant suppression or enhancement, respectively, relative to control.

From the 3 ABPs upregulated upon Src induction (Figure 2.5.B and Hirsch et al. 2010), EVL/Ena is the only one acting as an oncogene in fly tissue, therefore we tested if Src also affects EVL/Ena levels in *Drosophila*. Indeed, the posterior compartment of wing discs overexpressing *Src* together with *p35* and *GFP*, but not *p35* and *GFP* only, accumulated high EVL/Ena protein levels. We conclude that *in vivo*, EVL/Ena is upregulated upon Src activation and is necessary and sufficient to promote Src-induced tissue overgrowth (Figure 2.9).

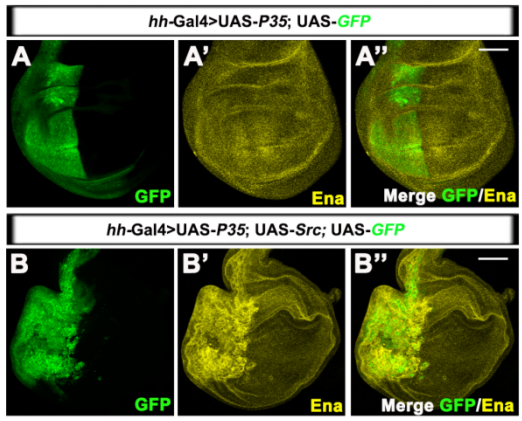

Figure 2.9: *Ena*, the *Drosophila* orthologue of human EVL, accumulates upon Src overexpression. Standard confocal sections of third instar wing imaginal discs stained with anti-Ena (yellow), in which hh-Gal4 drives UAS-*P35*, *Src64B*^{UY1332} and UAS-*mCD8-GFP* (green). Dorsal is side up and posterior is to the left.

2.5 DISCUSSION

ER+ and ER- tumours share a set of ABPs deregulated associated with the invasive phenotype.

Several studies have correlated the metastatic abilities of tumoural cells with changes in expression of particular ABPs (Gross 2013). In agreement with these reports, my study, allowed me to identify several of these ABPs that were upregulated in the three grades of ER+ IDCs, including Cofilin (CFL1), Cortactin (CTTN), Ezrin (EZR), Capping Protein (CAPZA1 and CAPZB) and the Arp3 subunit of the Arp2/3 complex (ARPC3). I also found the two subunits that encode for Arpc5 (ARPC5 and ARPC5L), VASP and Tropomyosin 3 (TPM3) that were upregulated in IDC2 and 3 and the subunit Arp2 (ARPC2) upregulated in IDC3 (Figure 2.2.B). Interestingly, these ABPs were also upregulated in ER- IDCs, and amongst them, CFL1, CAPZA1, CAPZB, ARPC3 and ARPC5 have been previously associated with an "Invasion signature" (Patsialou et al. 2012; Wang et

al. 2004). Therefore, these 5 ABPs may constitute a minimal actin cytoskeleton signature of invasion in all IDC lesions.

Although ER+ and ER- invasive tumours show similar changes of expression of these ABPs, these lesions also show distinct actin cytoskeletal features. For instance, up-regulation of EVL is specifically associated with ER+ IDC. On the contrary, Moesin (MSN) and Beta-2-syntrophin (SNTB2) are downregulated in ER+ IDC and up-regulated in ER- IDCs. Consistent with my observations, it has been previously observed that Moesin up-regulation was associated with the invasiveness or metastatic potential characteristic of the ER- breast cancer phenotype (Carmeci et al. 1998). MSN and SNTB2 were both previously included in the above-mentioned, "Invasion signature" defined from the triple negative MDA-MD-231 cell line (Patsialou et al. 2012; Wang et al. 2004). These observations reinforce the association between the high expression levels of these two ABPs and invasiveness. Additionally, ER^- IDCs highly up-regulate all functional classes of ABPs, suggesting that global increase in ABP expression may determine the high metastatic abilities of ER^- IDCs and the poor prognosis for these patients (Knight et al. 1977; Sigurdsson et al. 1990).

Major alterations in the expression of Focal Adhesion components and ABPs are predominantly found in benign breast lesions.

My analysis of the pathways significantly affected in ER+ breast cancer progression identified Focal Adhesion as the first and second most affected pathway in benign and malignant tumours respectively (Figure 2.3). Focal adhesions are signalling platforms associated with actin stress fibres that anchor cells to the extracellular matrix (Petit & Thiery 2000; Oakes et al. 2012). A major component of focal adhesions, the Focal Adhesion kinase (FAK) has been associated with growth factor signalling and tumour formation. In fact, a FAK knock-out transgenic model of human breast cancer ($FAK^{flox/flox}$) shows impaired cell proliferation, correlated with a decreased tumour mass and volume (Provenzano & Keely 2009). Furthermore FAK has been shown to support Ras-

and PI3K-dependent mammary tumour initiation, maintenance, and progression to metastasis (Pylayeva et al. 2009). Thus, my study is in agreement with these observations, arguing for major remodelling of Focal Adhesions structures associated with distinct stage-specific transformed features, including proliferation, survival, migration and invasion during breast cancer progression.

Importantly, Focal adhesion assembly maturation and disassembly relies on actin stress fibre dynamics. In turn, actin stress fibres assembly is directly linked to the formation and turnover of Focal Adhesions (Petit & Thiery 2000; Oakes et al. 2012). I also found that among all genes deregulated during breast cancer progression, ABP's genes are substantially enrichment in ADH and DCIS (Table 2.3). Moreover, regulation of the actin cytoskeleton is one of the most affected pathways at these stages (Table 2.3 and Figure 2.3). This could be a general feature of pre-malignant lesions, as similar observations were reported for colorectal dysplasia (Kanaan et al. 2010). Because of the close interplay between focal adhesions and associated stress fibres, their remodelling might be key steps for the development of pre-malignant lesions. Thus, my observations argue that deregulation of the actin-cytoskeleton pathway play an important role not just in invasion/metastasis but also in dysplasia.

Src deregulation has been associated with highly invasive tumours (Elsberger et al. 2010; Kanomata et al. 2011). In agreement, our expression profiles show an increase of Src expression IDC grades 2 and 3, which might suggest an increase in Src levels. Src activation triggers massive alterations in the expression of ABPs in the MCF10A cell model (Figure 2.5). I found that 6 of these ABPs are also misregulated in the same direction in pre-malignant ADH and/or DCIS (Figure 2.5). Therefore, a stepwise increase in Src activity levels may be one of the mechanism by which these pre-malignant breast lesions deregulate the expression of focal adhesion actin cytoskeleton components.

Alteration in F-actin may regulate the morphologic and phenotypic events of pre-malignant cells.

Several observations argue that changes in F-actin regulate the morphologic and phenotypic events of pre-malignant cells by modulating the signalling activities of oncogenes and tumour suppressor pathways. A decreased expression of high molecular weight Tropomyosin (Tms) in primary breast tumours, hepatocellular carcinoma and neuroblastoma is associated with oncogenic transformation, changes in cell morphology, tumour growth, and tumour metastasis. The Tm1 isoform is the high molecular weight variant of the TPM2 gene. The importance of Tm1 as a tumour suppressor is further evidenced by its ability to revert the malignant phenotypes of the breast cancer cell line MCF-7 and of fibroblasts transformed with the Src or Ras oncogenes (Braverman et al. 1996; Mahadev et al. 2002; Pawlak et al. 2004; Prasad et al. 1993; Prasad et al. 1999; Raval et al. 2003; Yager et al. 2003). In agreement with these observations, TPM2 is downregulated in pre-malignant breast tumour lesions and in TAM-induced ER-Src cells (Figure 2.5) and Drosophila TMP2/Tm2 limits Src-induced tissue overgrowth (Figure 2.6). The Arp2/3 regulator N-WASP has also been found downregulated in breast cancer tissues and its overexpression reduces growth of the breast cancer cell line MDA-MD-231 (Martin et al. 2008). Two members of the Ena/VASP family protein, VASP and Mena, have also been associated with the carcinogenic process. In particular, Mena is overexpressed in a subset of human benign breast lesions, its inhibition prevents metastatic dissemination but cannot prevent progression to malignancy (Roussos et al. 2010; Di Modugno et al. 2006; Di Modugno et al. 2007).

Pre-malignant ER+ breast cancer lesions may accumulate long actin filaments.

Strikingly, I show that while malignant breast lesion are characterized by an enrichment of ABPs that promote both F-actin polymerization and F-actin depolymerization, pre-malignant lesions upregulate ABPs the promote polymerization but downregulate F-actin depolymerisation factors (Figure 2.4).

For long time, it has been known that the formation of branched F-actin structures requires the presence of both promoters and inhibitors of polymerization (Blanchoin et al. 2014). The presence of inhibitors of polymerization, like capping proteins, is essential to block the filaments growth at their barbed ends. The absence of capping proteins results in the limitless elongation of the branches, leading to growing parallel bundles (Blanchoin et al. 2014). In early lesions, exclusively, the set of up-regulated inhibitors of polymerization is outnumbered by the set of up-regulated polymerizing ABPs (Figure 2.4). For instance, although capping protein (CAPZ) is up-regulated in non-invasive stages; also members from the Ena/VASP (ENAH and EVL) family are upregulated. Ena/VASP proteins compete with capping proteins for the barbed ends, and uncap them, leading to the barbed ends elongation enhancement (Blanchoin et al. 2014). Besides competing with capping proteins, Ena/VASP proteins also compete with Arp2/3, exerting anti-branching activity (Bear & Gertler 2009). Altogether, my observations suggest that the assembly of long filaments is favoured in non-invasive stages, to the detriment of short ones. When malignancy traits are acquired there is an increase in the number of over-expressed inhibitors of polymerization, indicating that there is a requirement for short, branched filaments. Thus, tumour growth may involve an accumulation of long fibres, while the development of malignant features may require short-branched filaments. In agreement with this model, it is known that lamellipodia and invadopodia, both playing key roles in cellular migration, result from the accumulation of short branched filaments at the leading edge of cells (Gross 2013).

The set of ABPs commonly misregulated in Breast tissue and ER-Src cells is involved in Src-induced tissue overgrowth in *Drosophila melanogaster*.

To further explore the role of F-actin dynamics in tumour development, I identified which of the 6 ABPs deregulated in DCIS and in transformation of ER-Src cells would impact in overgrowth of Src-overexpressing issue, in *Drosophila*.

To evaluate these ABPs pro-growth role, downstream of Src activation, *Drosophila melanogaster* was used as *in vivo* model. These experiments strongly suggested that EVL/Ena behaves as an oncogene, while ACTR3/Arp3 and ARPC5L/Arpc5 restrict Src-induced overgrowth of *Drosophil*a epithelia. These are really exciting results, as they confirm that the regulation of expression of these ABPs might be used to differentially control the promotion or suppression of tumourigenesis. Previously our lab has described that loss of capping proteins and Src overexpression induce the same phenotypic outcomes in wing imaginal disc (Fernández et al. 2013). Taking in to consideration that Ena/Vasp proteins not only act as elongation factors but also present anti-capping activity (Blanchoin et al. 2014), our recent results suggest that Src induce increased levels of Ena, that compete with capping protein for the barbed ends. Due to the increased levels of Ena, fewer filaments are capped, long filaments are formed which ultimately results in tissue overgrowth. In contrast, when cells overexpress ACTR3/Arp3 and ARPC5L/Arpc5 might cooperate with capping protein to form branched filaments to restrict tumour growth. In DCIS, the overexpression of ACTR3 and ARPC5L, that would increase the possibility of formation of branched filaments, might be a mechanism to counteract transformation. Cells would overcome this tumour suppressor mechanism overexpressing EVL and inducing the formation of long filaments. If this is the case, these observations not only suggest that different networks promote different phenotypes, but also that branched networks can protect from cell transformation in early stages but later on promote acquisition of malignant traits.

My study shows for the first time the genetic interaction between Src and the fly orthologue for each of the 6 ABPs identified in human tumourigenesis

(Figure 2.5). Throughout evolution, these proteins were conserved and play a role in the developmental programme. It is quite exciting to observe that these 6 ABPs orthologues are part of tightly controlled machinery used to regulate tissue growth and the disruption of these mechanisms lead to tumour development (Figure 2.6-Figure 2.8).

2.6 CONCLUSIONS

Collectively my data argue for a model by which early during breast tumoral progression, low levels of Src activity would affect the expression of specific sets of ABP, which would promote the accumulation of un-branched actin filaments. In turn, the change in F-actin would increase proliferation, and ultimately trigger tumour growth. Later during breast cancer progression, higher levels of activated Src resulting from Src overexpression would upregulate the expression of many other ABPs, including polymerization factors and inhibitors of polymerization. This would result in a reduction in F-actin levels with the assembly of, branched-filaments, essential for migration and invasion of malignant cells (Figure 2.10).

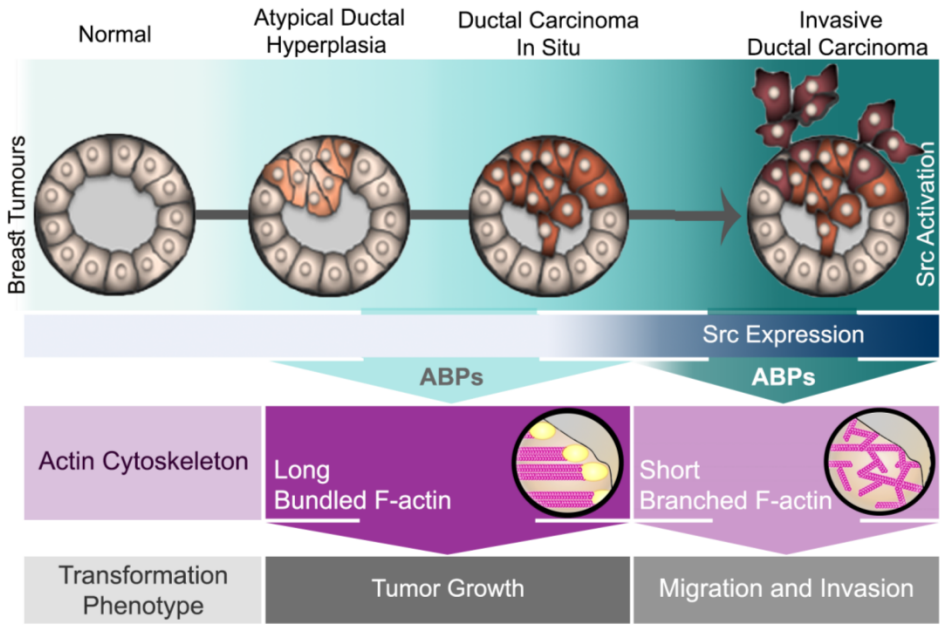

Figure 2.10: Model by which different levels of Src activity promotes distinct transformation phenotypes through regulation of the actin cytoskeleton. In benign lesions, the misregulation of ABPs would lead to the accumulation of un-branched actin filaments, resulting in tumour growth. In malignant stages, high levels of activated Src would affect the expression of many other ABPs involved in the assembly of short, branched-filaments, essential for migration and invasion of fully transformed cells.

2.7 ACKNOWLEDGEMENTS

I would like to acknowledge Florence Janody who performed the *Drosophila* genetics experiments and Joana Vaz Cardoso for her help and supervision throughout the development of this bioinformatics study.

2.8 SUPPLEMENTARY DATA

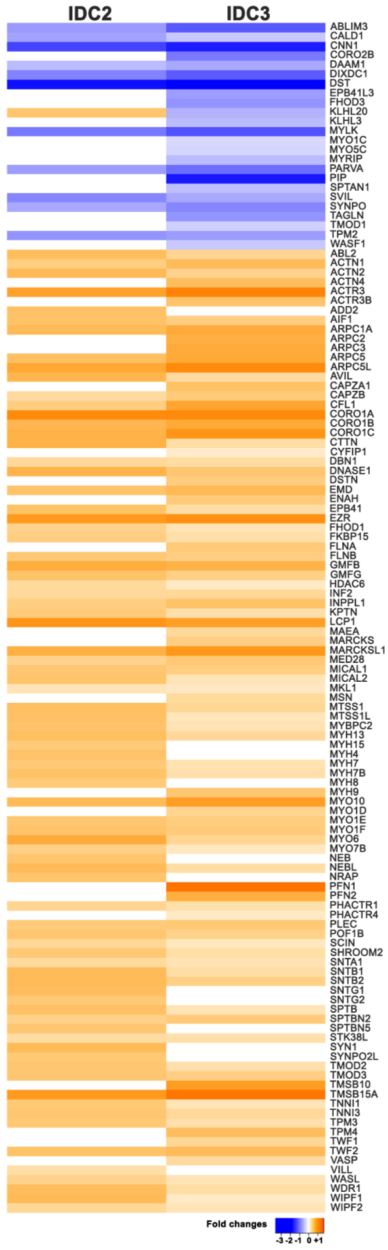

Supplementary Fig. S1: About 85% of ABPs are dysregulated in high grade IDC, in ER- Breast Cancer. Heatmap of ABP dysregulated in IDC 2 and 3 in ER- tumour samples. Fold-changes are in Log2R. Orange and blue indicate genes up- and down-regulated respectively.

Chapter 3

The oncogenic transformation of MCF10A-ER-Src cells involves a pre-malignant and malignant phases associated with striking F-actin-dependent alteration in cell stiffening.

"A curiosidade, instinto de complexidade infinita, leva por um lado a escutar às portas e por outro a descobrir a América; - mas estes dois impulsos, tão diferentes em dignidade e resultados, brotam ambos de um fundo intrinsecamente precioso, a actividade do espírito."

Eça de Queirós, Notas Contemporâneas

For this chapter, Catarina Brás Pereira performed the immunoblotting for Cyclin B1, E-cadherin, P-cadherin and β-catenin, and João Lagarto contributed to the wound healing experiments analysis. Anna Tautenberger helped in AFM measurements of cells in 2D culture, and performed measurements in 3D ER-Src structures. I performed all the remaining described in this chapter.

3.1 SUMMARY

In the previous chapter, I have proposed a model by which early during tumour progression, low levels of Src activity would lead to the differential expression of specific sets of ABP that would promote the accumulation of long actin fibres, resulting in tumour growth. At later stages, higher levels of activated Src would induce changes in the expression of many more ABPs. These ABPs would promote the assembly of short, branched-filaments networks, essential for the development of the malignant phenotypes. In this chapter, I use a human cell line with conditional Src induction to validate this model.

Using the Src inducible mammary epithelial cell line MCF10A-ER-Src, which recapitulates the natural history of Src-induced breast cancer, I show that cellular transformation can be divided into two distinct phases. The first phase, which takes place during the first 12 hours of Src activation, displays pre-malignant breast cancer features characterized by the acquisition of self-sufficiency in growth properties with no sign of phenotypical transformation and migratory behaviour. During the second phase, cells gain malignant properties, characterized by the upregulation of mesenchymal markers, the acquisition of mesenchymal-like cell morphology, stemness properties, anchorage-independent growth features in the absence of the epidermal growth factor (EGF) and invasive properties in three-dimensional (3D) matrigel culture.

Strikingly, these two phases are associated with distinct behaviours in term of actin cytoskeleton organization and mechanical properties. The pre-malignant phase involves the transient polymerization of polarized actin stress fibres decorated by phospho-Myosin light chain and Filamin B and a transient increase in cellular stiffness. In contrast, the malignant phase is characterized by the disassembly of the longitudinal actin fibres and a reduction of cell stiffness.

In conclusion, different levels of Src activation may promote the assembly of distinct actin networks, which, in turn, could mediate the pre-malignant and malignant phenotypes associated with each phase of cellular transformation.

3.2 INTRODUCTION

Tumour progression can be defined by the evolution of normal cells into cells with increasingly neoplastic phenotypes. In a temporally-ordered manner, cells have to successfully overcome different barriers to reach a fully transformed phenotype. Early stages of epithelial tumorigenesis are characterized by decreased apoptosis and increased growth signalling. Lesions with cells presenting exclusively this set of altered features are considered benign. When these cells acquire the ability to degrade the extracellular matrix, migrate and invade distant tissues, a fully transformed phenotype is established. At these late stages, cells have turned into cancer cells (Pinder & Ellis 2003; Damonte et al. 2008).

The c-Src non-receptor tyrosine kinase is one of the oldest and most investigated proto-oncogenes implicated in the development, growth, progression, and metastasis of a number of human cancers including those of the breast (Zhang & Yu 2012). Src protein levels and, to a greater extent, Src protein kinase activity are frequently elevated in breast cancer specimens when compared to adjacent normal tissues and correlate with reduced survival of breast cancer patients (Elsberger et al. 2010; Elsberger et al. 2009; Kanomata et al. 2011).

Several observations argue that basal Src activity that occurs early during tumour progression, promotes cell proliferation and survival via its interaction with transmembrane receptor tyrosine kinases (RTKs) at the cell membrane, which directly transduces survival signals to downstream effectors. During later stages of tumour progression further Src activation may facilitate other malignancy-associated properties, such as cell migration, adhesion and invasion (Zhang & Yu 2012). These later processes mostly depend on the regulation of the actin cytoskeleton by Src (Frame 2004). Many reports have demonstrated that Src activation induces the disassembly of actin stress fibres and the formation of dot-like contact sites, called invadopodia. Found mainly in motile cells, invadopodia control the activity of matrix metalloproteases and are thought to contribute to

tissue invasion and matrix remodelling (Winograd-Katz et al. 2011). However, earlier during tumour progression, no role for the actin cytoskeleton downstream of Src had been reported.

The semi-flexible polymers of filamentous actin (F-actin), which is assembled from monomeric actin (G- actin) subunits, exert or resist against forces to drive a large number of cellular processes, including changes in cell shape, cell mobility, cytokinesis, intracellular transport, or cell contraction. In addition, actin filaments transmit external forces into biochemical signalling events that guide cellular responses. These distinct functions are dictated by the way actin filaments organize into distinct architectures through the control of a plethora of actin binding proteins (ABPs) strongly conserved between species (Blanchoin et al. 2014; Lee & Dominguez 2010). Our lab has previously reported that in *Drosophila* epithelia, the pro-growth function of various oncogenes, including Src, c-Jun N-terminal kinase (c-JNK) and Yorkie (YAP/TAZ in mammals) is controlled by the actin cytoskeleton (Fernández et al. 2011; Fernández et al. 2013; Gaspar et al. 2015; Jezowska et al. 2011). In particular, the Capping Protein αβ heterodimer, which inhibits F-actin accumulation, counteracts the effect of Src on F-actin, restricting Src-mediated apoptosis or proliferation (Fernández et al. 2011). The extensive phenotypic similarities of the effects of Src activation between *Drosophila* and mammalian cells in culture (Fernández et al. 2013; Vidal et al. 2006; Vidal et al. 2007), suggest that Src activation may also promote tumour growth via F-actin regulation. Consistent with this hypothesis, I have identified 6 ABPs deregulated by Src activation and in pre-malignant breast lesions that could be involved in Src-induced tumour growth (Chapter 2).

To demonstrate this hypothesis, I took advantage of the inducible MCF10A-ER-Src cell line. MCF10A cells derived from human fibrocystic mammary tissue. The isolation and establishment of this cell line had occurred spontaneously, without treatments with pro-carcinogen (Soule et al. 1990). MCF10A cells are considered to be a normal-like breast epithelial cell line because they show (a) a lack of tumorigenicity in nude mice; (b) grow in polarized three-

dimensionally acini in collagen and (c) require growth factors to proliferate. Their karyotype is near-diploid with minimal rearrangement. Because these cells fail to express the three most common hormonal receptors, including the estrogen receptor (Soule et al. 1990; Kao et al. 2009), MCF10A stable cell lines carrying oncogenes fused to the oestrogen binding domain can be conditionally induced through treatment with the oestrogen analogue Tamoxifen (TAM). The MCF10A-ER-Src cell line were stably transfected with a construct encoding a fusion protein between the Schmidt Rupin A form of v-Src and the hormone binding domain of the human estrogen receptor (Figure 3.1). This fusion protein is maintained inactivated in the absence of ligand-binding to the ER-binding domain. However, in the presence of TAM, TAM binds to the ER-binding domain and triggers an active conformational change of the ER-Src fusion protein and its activation. TAM treatment for 36 hours is able to trigger full phenotypic transformation, with cells forming multiple colonies in soft agar, mammospheres in non-adherent conditions and tumours upon injection into nude mice (Iliopoulos et al. 2009; Hirsch et al. 2010; Hirsch et al. 2009). Thus, this *in vitro* model with conditional Src activation gives the rare opportunity to follow and study the timely ordered events that lead to full malignant transformation (Iliopoulos et al. 2009).

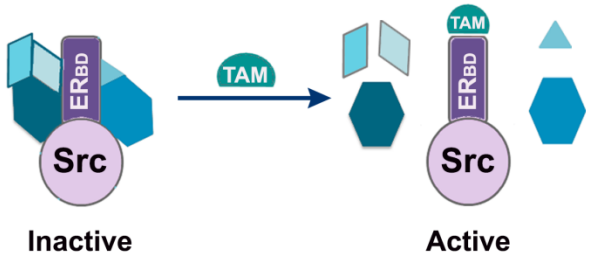

Figure 3.1: Schematics of activation of ER-Src fusion protein by TAM.

In this chapter, I aimed to determine if the proliferative advantage given by src activation is associated with alteration in F-actin. To do so, I investigated the transformation features acquired during the multistep development of Src-

induced cellular transformation and the dynamic changes in the actin cytoskeleton.

3.3 MATERIAL AND METHODS

3.3.1 CELL LINES, CULTURE CONDITIONS AND 4OH-TAM TREATMENT

The MCF10A-ER-Src (ER-Src) and MCF10A-PBabe (PBabe) cell lines cultured in monolayer (2D) were grown, as described in (Hirsch et al., 2009). To treat cells with 4OH-TAM or EtOH, 50% confluent cells were plated and allowed to adhere for at least 12 hours before treatment with 1 μM 4OH-TAM (Sigma H7904) or with identical volume of EtOH for the time periods indicated in the text. Cell culture media containing EtOH alone or 4OH-TAM diluted in EtOH was replaced every 12h.

3.3.2 3D MATRIGEL™ CULTURES

Lab-Tek II plates (Lab-Tek II, #155409) were coated with 20 μl Matrigel™ (BD Biosciences; 356231). 1000 cells were suspended in 100 μl Matrigel™ and overlaid in wells. After polymerization at 37°C, 500 μl of cell culture media were added and replaced every 3 days. Cells were grown for 14 days and treated with cell culture media containing EtOH or 4OH-TAM.

3.3.3 PCR GENOTYPING

The presence or absence of the v-Src:ER construct in ER-Src and PBabe cells, respectively, was confirmed by PCR reactions. The set of primers used are listed in Table 3.1. The PCR reaction products were electrophoresed in 1 % agarose gel.

Table 3.1: Primers used to genotype MCF10A cells.

Primer Name	Sequence
5'-Src-ER Beginning	GGGAGCAGCAAGAGCAAGCCTAAG
3'-Src-ER Beginning	CGGGGGTTTTCGGGGTTGAGC
5'-Src-ER Fusion	GTGGCTGGCTCATTCCCTCACTACA
3'-Src-ER Fusion	GCACCCTCTTCGCCCAGTTGA
5'-Src-ER End	AGAGGGTGCCAGGCTTTGTG
3'-Src-ER End	GGGCGTCCAGCATCTCCAG

3.3.4 IMMUNOBLOTTING ANALYSIS

Cells were scraped in TRIS lysis buffer (containing protease and phosphatase inhibitors), and lysed for 20 minutes on ice. Lysates were then cleared by centrifugation at 14,000 rpm at 4°C for 30 minutes. 20 ug of protein were resolved by SDS-PAGE electrophoresis and transferred to PVDF membranes (Amersham Pharmacia). Membranes were blocked with 5% milk in TBS 0.1% Tween 20 and incubated with: anti-activated Src (1:1000, 44-660G, Invitrogen), anti-GAPDH (1:2000, 2D4A7, Santa Cruz); anti-Actin (1:500, A2066, Rabbit), anti-P-cadherin (1:500, 610228, BD Biosciences), anti-E-cadherin (1:1000, 24E10, Cell Signalling), anti-Cyclin B1 (1:1000, sc-245, Santa Cruz), anti-β-catenin (1:500, c19220, BD Transduction Laboratories) and anti-FLNB (1:250, sc-376241, Santa Cruz Biotechnology). Detection was performed by using HRP-conjugated antisera (1:5000, Amersham Pharmacia) and Enhanced Chemi-Luminescence (ECL) detection. Western blots quantification were performed using the Image Studio Lite program.

3.3.5 CD24/CD44 PROFILING

Flow cytometry was performed on single cell suspensions from ER-Src cells treated with EtOH or TAM for 36h. Cells at a density of 10^6 cells/100 μL were stained with CD44 antibody (1:12.5, PE-conjugated, 555479, BD Biosciences) and with CD24 antibody (1:12.5, FITC-conjugated, 555427, BD Biosciences). Cells were incubated with the fluorescent antibodies for 30 min at 4°C, protected from

light. CD44 and CD24 staining profiles were obtained using FACS Calibur. Three independent experiments were performed.

3.3.6 BrdU incorporation profile

Sub-confluent cells were incubated in culture media containing EtOH or 4OH-TAM for 4, 12, 24 and 36 hours. Cell culture media containing EtOH alone or 4OH-TAM diluted in EtOH was replaced every 12h. On the last hour of treatment, 10 μM Bromodeoxyuridine (BrdU) (10280879001, Roche) was added to each well. Cells were then trypsinized, fixed with 70% EtOH and incubated in 2M HCl for 30 min, at room temperature. HCL was then removed, before incubation with an anti-BrdU antibody (1:50, 347580, Becton-Dickinson) for 20 min, at room temperature in the dark. Staining with FITC-conjugated secondary antibody and Propidium Iodide (PI) (10 μg/mL, P4170, Sigma) to mark DNA content was performed at room temperature in the dark for 20 min. BrdU and PI staining profiles were obtained using FACS Calibur. The Flow Logic software was used for quantification of the % of BrdU positive cells. Three independent experiments were performed.

3.3.7 Time lapse imaging

For time lapse imaging, samples were maintained at 37°C in a controlled unit with 95% relative humidity, 5% CO_2. Transmitted light DIC images were acquired on a Yokogawa CSU-X Spinning Disk confocal each 30 or 15 minute interval for a period of 60 hours for 3D Matrigel culture or 2D, respectively. Images were acquired using the MicroManager 1.4.15 acquisition software. Processing and compression were performed using Fiji (ImageJ package distribution).

3.3.8 Wound Healing Motility Assay and quantification

Wound Healing Motility Assays were performed as described in (Iliopoulos et al. 2009). ER-Src cells were seeded in 6 well-plates or in 8-well

chamber slide (Lab-Tek II, #155409) for live-imaging. A single scratch wound was performed using a p200 or p10 micropipette tips to confluent cells. Cells were washed three times with PBS to remove cell debris, and incubated in assay medium (MCF10A growth medium containing 2% serum and no EGF) supplemented with EtOH or TAM, for 36 hours. Time-lapse images were captured by phase-contrast microscopy using a 10x objective every hour for 25 hours. The ImageJ software was used to quantify cell movement. Images were reduced in quality and treated using the "Find Edge" function to define the wound edge and reduce artefacts. Images were then reconverted to their original size and a threshold was applied to measure the distance in pixels line by line, from the wound edges to the image edges, used as reference. Distances were then compared between images acquired every 60 min. Each time point was then averaged, to quantify the speed, the position of cells and the total movement of the wound edge.

3.3.9 SOFT AGAR COLONY ASSAY

$5x10^3$ cells in cell culture media containing no EGF were mixed with 0.36% gelling agarose (A9045 - Sigma) and plated on top of a solidified layer of 0.7% agarose in cell culture media with no EGF. Cells were fed every 6 to 7 days with cell culture media with no EGF. Number of colonies was counted 15-21 days later. Experiment was performed in triplicates and repeated three times. Statistical significance was calculated using a Student's t test.

3.3.10 CELL CYCLE PROFILE

Sub-confluent cells were cultured overnight in media without EGF. Cells were then incubated in culture media containing or depleted of EGF and with EtOH or 4OH-TAM for 12 hours. Cells were then fixed with 70% EtOH and stained with Propidium Iodide (10 µg/mL, P4170, Sigma). Cell cycle profiles were obtained using FACS Calibur. The Flow Logic software was used for

quantification of the % of S-phase cells. Three independent experiments were performed.

3.3.11 PROLIFERATION RATE

The proliferation rate was calculated based on the number of cells, at different time-points in each condition. Measurements were performed using the Scepter™ 2.0 Handheld Automated Cell Counter. The proliferation rate of cells cultured in medium containing EGF and treated with EtOH was used as normalizing condition. Three independent experiments were performed.

3.3.12 IMMUNOFLUORESCENCE ANALYSIS

ER-Src or PBabe cells were plated in poly-L-lysine-coated coverslips (Sigma P-8920) and fixed in 4% paraformaldehyde in phosphate buffer solution (PBS) at pH7, for 10 min. Cells were then permeabilized with TBS-T (Tris-buffered saline - 0.1 % Triton X-100) at RT and blocked in TBS-T supplemented with 10 % BSA, 1h at RT. Primary antibodies were incubated overnight at 4ºC in blocking solution. Coverslips were then washed three times with TBS and incubated with secondary antibodies (in blocking solution) and with Rhodamine-conjugated Phalloidin (Sigma) at 1:200, for 1h at RT. After three washes in TBS, cells were stained with 2 μg/mL DAPI (D9542, Sigma) for 5 min in TBS, washed again with TBS and mounted in Vectashield. Primary antibodies used were: anti-activated Src (1:100, 44-660G, Invitrogen), anti-phospho-Myosin Light Chain 2 (Thr18/Ser19) (1:200, 3674, Cell Signaling) and anti-FLNB (1:50, sc-376241, Santa Cruz Biotechnology). Secondary antibodies were from Jackson Immunoresearch (1:200). Fluorescence images were obtained on a Leica SP5 confocal coupled to a Leica DMI6000, using the 63x 1.4 NA Oil immersion objective.

3.3.13 QUANTIFICATION OF STRESS FIBRES ANISOTROPY

Anisotropy was measured using the Fibril Tool plugin for NIH Image J program, as described in (Boudaoud et al. 2014).

3.3.14 G/F ACTIN ASSAY

The G-actin/ F-actin In vivo Assay Kit (Cytoskeleton, Denver, CO, USA) was used to quantify the F- and G-actin pools, according to manufacturer instructions, except that cell lysates were centrifuged at 90,000*g*, for 90 min at room temperature. G and F-actin fraction were analysed by immunoblotting analysis and quantified using the Image Studio Lite program, as the ratio between F- and G-actin levels for each experimental condition.

3.3.15 ATOMIC FORCE MICROSCOPY (AFM)

For the AFM indentation experiments a nanowizard I (JPK Instruments, Berlin) equipped with Cellhesion Module was used. Arrow-T1 cantilevers (Nanoworld, Neuchatel) with a polystyrene bead of 5µm diameter (microparticles GmbH, Berlin) were calibrated using the thermal noise method. To assess the stiffness of the cells, the cantilever was lowered with a speed of 5 µm/s onto the cells surface until a relative set point of 2.5 nN was reached. The resulting force distance curves were analysed using the JPK image processing software (JPK instruments). Force distance data were corrected for the tip sample separation and fitted with a Hertz model fit for a spherical indenter. A Poisson ratio of 0.5 was assumed. Experiments were carried out at 37◦C in CO_2 independent medium (life technologies, Darmstadt) during a 1.5h time-window.

3.4 RESULTS

3.4.1 TAM-TREATMENT INDUCES HIGH LEVELS OF SRC ACTIVATION IN THE MCF10A-ER-SRC CELL LINE.

The human cell line MCF10A is a commonly used experimental model to study non-transformed cell features, in the mammary context (Imbalzano et al. 2009). A derivative of the MCF10A cell line carrying a PBabepuro plasmid, expressing a fusion protein comprising the Src kinase oncoprotein (v-Src) and the hormone-binding domain of the human Estrogen Receptor (ER-Src) (Figure 3.2.A) is particularly useful to study overtime how Src induces oncogenic transformation. Upon Tamoxifen (TAM), but not Ethanol (EtOH) treatments, the ER-Src cell line undergoes full phenotypical transformation, with cells forming multiple foci, colonies in soft agar, mammospheres in suspension and tumour induction in nude mice (Iliopoulos et al. 2009). To control for unspecific effects resulting from EtOH or TAM treatment, I have also used an MCF10A cell line carrying an empty PBabepuro plasmid (hereafter defined as PBabe). To confirm the absence or the presence of ER-Src in the PBabe and ER-Src cells, respectively, I used sets of specific primers that would amplify by PCR the sequence encoding for the N-terminal v-Src domain (Figure 3.2.B, upper panel), or for the junctional domain between the C-terminal v-Src kinase domain and the N-terminal of the Estrogen-binding domain (ER_{BD}) (Figure 3.2.B, middle panel), or for the ER_{BD} (Figure 3.2.B, lower panel). Using this approach, I could confirm that ER-Src cells, but not PBabe cells, carried the ER-Src coding sequence (Figure 3.2.B, left panel). Consistent with these observations, Western blot analysis on extracts from TAM- or EtOH-induced ER-Src or PBabe cell, revealed that at all time-points analysed, the phosphorylated activated form of ER-Src (ER-pSrc) accumulated at high levels in TAM-induced ER-Src cells (Figure 3.2.C), but not in TAM-induced pBabe cells (Figure 3.2.D). EtOH-treated ER-Src cells also accumulated weak levels of ER-pSrc activation (Figure 3.2.C), indicating some degree of leakiness in the activation of the ER-Src fusion protein in the absence of TAM treatment. In addition,

treatment of ER-Src cells with TAM triggered the phosphorylation of endogenously expressed Src (pSrc) (Figure 3.2.C), arguing for a positive feedback involving Src. Thus, as expected the transformation of TAM-induced ER-Src cells is associated with high Src activity levels.

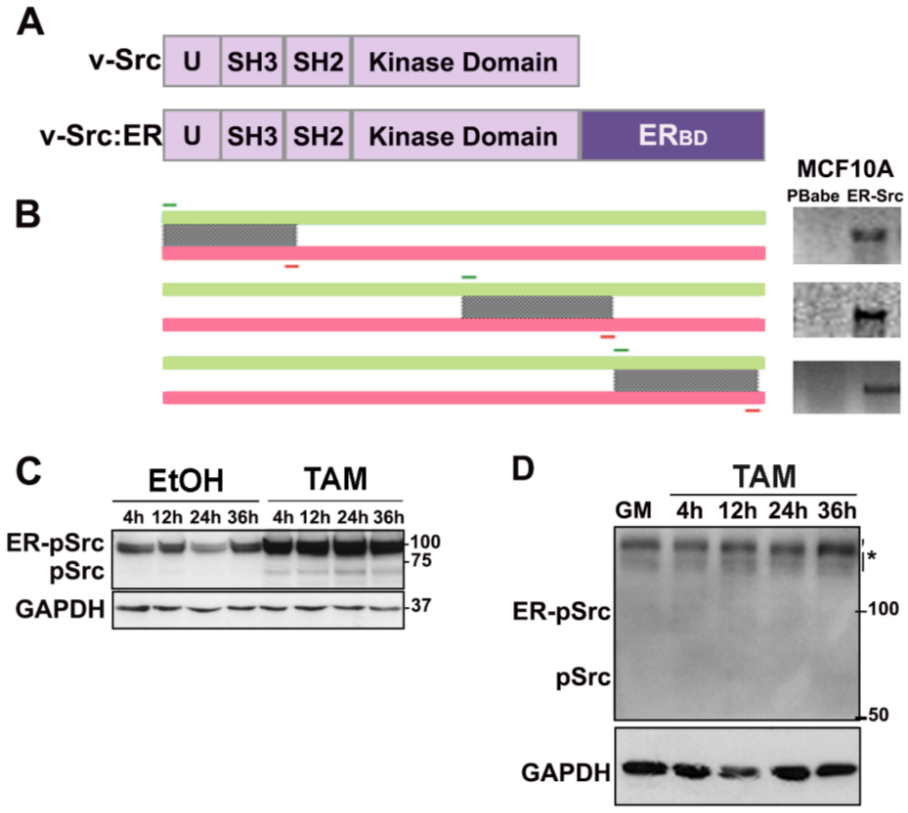

Figure 3.2: Only TAM-induced ER-Src cells contain high Src activity levels. (A) Schematics of the v-Src domains fused to the hormone binding-domain of the human estrogen receptor (ERBD). **(B)** Regions of the construct amplified by three different pairs of primers (gray area)- Primers are represented by small lines in dark green and dark red (left panel). On the right are presented the correspondent PCR reactions products amplified from PBabe and ER-Src cell extracts (right panel). **(C)** Western blot on protein extracts from ER-Src cells treated with EtOH for 4 (lane 1), 12 (lane 2), 24 (lane 3) or 36 (lane 4) hours or with TAM for 4 (lane 5), 12 (lane 6), 24 (lane 7) or 36 (lane 8) hours, blotted with (upper panel) anti-pSrc, which reveals v-Src fused to the oestrogen-binding domain (ER-pSrc; upper band) and endogenous Src levels (pSrc; lower band) or (middle panel) anti-GAPDH used as control or (lower panel). **(D)** Western blot on protein extracts from untreated PBabe cells (lane 1) or PBabe cells treated with TAM for 4 (lane 2), 12 (lane 3), 24 (lane 4) or 36 (lane 5) hours, blotted with (upper panel) anti-pSrc or (lower panel) anti-GAPDH used as control. The asterisk indicates non-specific bands revealed by the anti-pSrc antibody.

3.4.2 ER-SRC SHOW MALIGNANT MORPHOLOGICAL FEATURES 36H AFTER TAM TREATMENT

I then investigated the morphological alterations associated with Src activation. In monolayer cell culture, untreated PBabe and ER-Src cells grown as clusters, with cells at the edge of colonies frequently forming lamellipodia-liked structures. In confluent culture, cells presented a cobblestone appearance, a typical feature of epithelial cells (data not shown). 12 hours after TAM treatment, ER-Src cells started to lose their cobblestone morphology, acquired a spindle-like shape and acquired ability to grow on top of each other (Figure 3.3.A,B). This new morphology may indicate a transition from epithelial to mesenchymal phenotypes. Accordingly, 36 hours after Src activation, many cells rounded up, disaggregated from the substrate and clustered together (Figure 3.3.B). These morphological alterations have been previously associated with a full transformation phenotype (Iliopoulos et al. 2009). In contrast, EtOH-treated ER-Src (Figure 3.3.A, B) or EtOH- or TAM-treated PBabe cells (Figure 3.3.C) maintained a cobblestone appearance, indicating that the morphological alterations of TAM-induced ER-Src cells is the consequence of Src overactivation.

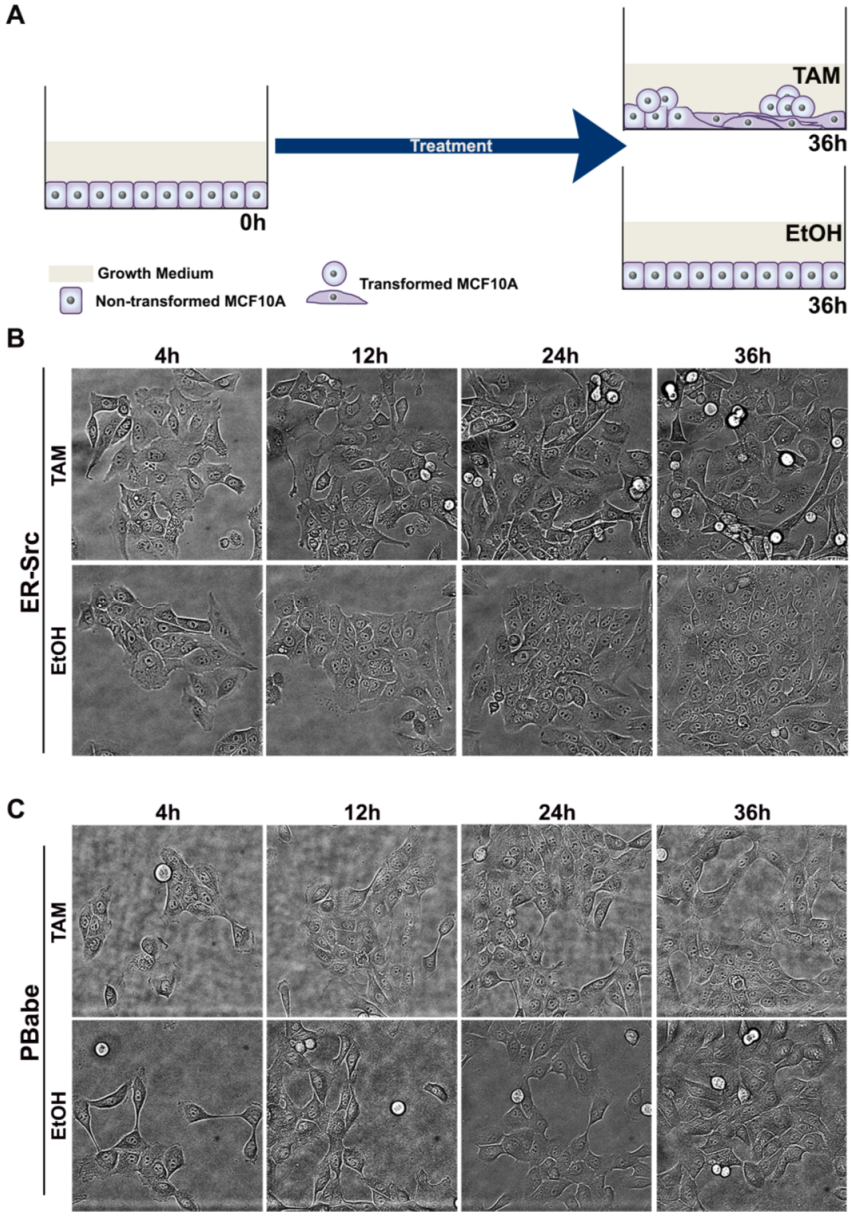

Figure 3.3: Only TAM-induced ER-Src cells undergo morphological alterations associated with a full transformation phenotype 36 hours after treatment. (A) Experimental design to follow the Src-dependent cellular morphological alterations overtime. Cells were treated for 36h with growth medium supplemented with TAM or EtOH. Time-lapse images were acquired every 15 minutes. **(B)** Images by phase contrast microscopy of ER-Src cells, 4, 12, 24 or 36 hours after EtOH or TAM treatments. **(C)** Images by phase contrast microscopy of PBabe cells, 4, 12, 24 or 36 hours after EtOH or TAM treatments.

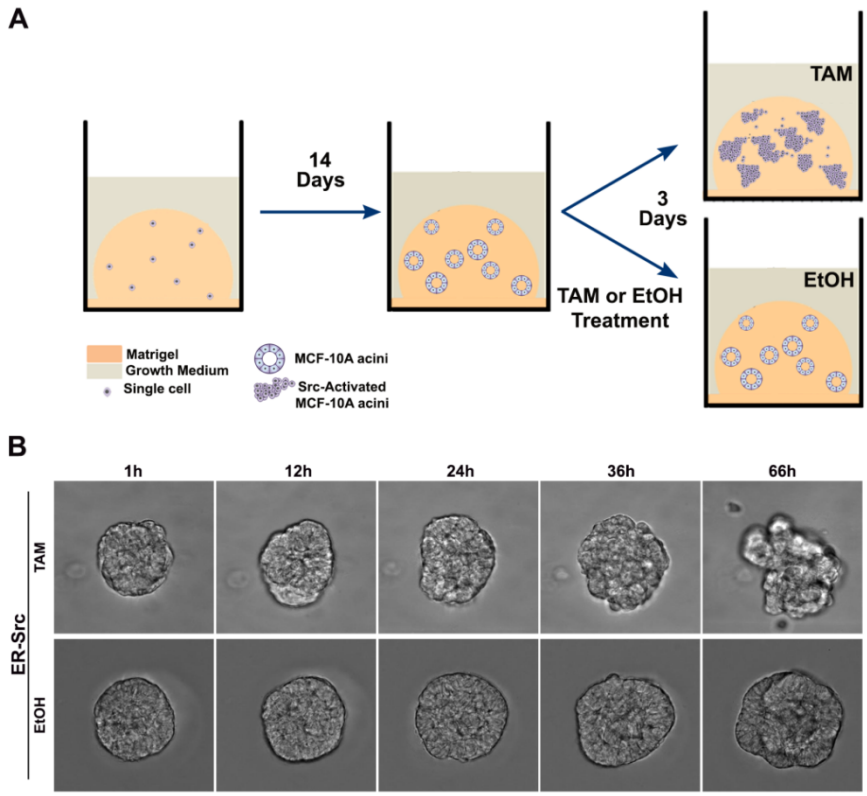

Figure 3.4: TAM-treated acini progressively loss their epithelial organization and invade the Matrigel after 24 hours of treatment. (A) Experimental design to evaluate the Src-dependent morphological changes of cells grown in reconstituted basement membrane. Single cells were plated in matrigel. On the 14th day of acini development, cells were treated with EtOH or TAM 1μM. Time-lapse images were acquired every 30 minutes, for 66 hours. **(B)** Images by phase contrast microscopy of ER-Src acini, 1, 12, 24, 36 or 66 hours after EtOH or TAM treatments.

In three-dimensional (3D) cultures of reconstituted basement membrane (Matrigel), un-treated ER-Src cells grown for 14 days formed polarized acini-like spheroids that recapitulate several aspects of the glandular architecture of breast tissues (Figure 3.4.A) (Debnath et al. 2003). During the first 24 hours of EtOH or TAM treatments, all ER-Src acini maintained a spherical organization with smooth outer edges (Figure 3.4.B; 1h). 24 hours after treatment onwards, TAM-treated ER-Src acini started to display striking morphological differences compared to those exposed to EtOH (Figure 3.4.B and Movie 1, 2). Acini progressively lost their smooth edges and compactness, possibly resulting from

the loss of cell-cell adhesion. Finally, 60 hours after TAM treatment, some ER-Src cells extruded from the spherical acinar-like structure, and invaded the Matrigel (Figure 3.4.B and Movie 1). These morphological alterations resemble hallmarks of highly invasive cells, which result from massive alterations in cell polarity, in cell attachment to neighbour cells and in extracellular matrix composition (Hanahan & Weinberg 2011). I conclude that Src induction induces a progressive loss in the organization of the polarized epithelial structure, likely as a result of the loss of cell-cell adhesion, and invading abilities.

3.4.3 ER-Src cells upregulate mesenchymal markers 24h after TAM treatment

The E-cadherin-β-Catenin complex is a key element required for cell-cell adhesion. In particular, E-cadherin loss with concomitant upregulation of the mesenchymal marker N-cadherin, termed cadherin switch is the hallmark of the epithelium-mesenchymal transition (EMT) process, associated with invasion and metastasis phenotypes (Hanahan & Weinberg 2011). Therefore, I analysed if the acquisition of malignant morphological features associated with Src activation involved the alterations in E-cadherin and β-catenin protein levels by Western Blot during the first 36 hours of treatments. Surprisingly, although TAM-induced ER-Src cells appeared to show a progressive reduction in E-cadherin and β-catenin levels overtime, compared to EtOH-treated cells (Figure 3.5.A), quantifications showed that in TAM-induced ER-Src cells, the E-cadherin levels, normalized to EtOH-treated ER-Src cells were not significantly affected 24 and 36 hours after treatments (Figure 3.5.B). These observations suggest that TAM-induced ER-Src cells do not undergo a classical cadherin switch to loss cell-cell adhesion, cell polarity and acquire migratory and invasive properties.

Other highly invasive tumours, like basal-like breast carcinomas, do not loss E-cadherin expression nor overexpress N-cadherin (Paredes et al. 2005). Instead, these tumours usually overexpress other classical cadherin, including P-

cadherin, which appears to identify an intermediate EMT state (Ribeiro & Paredes 2014). I therefore analysed if the acquisition of malignant morphological features associated with Src activation involved an increased in P-cadherin protein levels. By Western blot, P-cadherin levels were not significantly different between TAM and EtOH-treated ER-Src cells, 4 and 12 hours after treatment. However, TAM-treated ER-Src cells significantly accumulated P-cadherin 24 hours after treatment (Figure 3.5.C and D). Thus, Src activation may induce a intermediate EMT state, characterized by the maintenance of E-cadherin levels and the upregulation of P-cadherin that is concomitant with the acquisition of malignant morphological features.

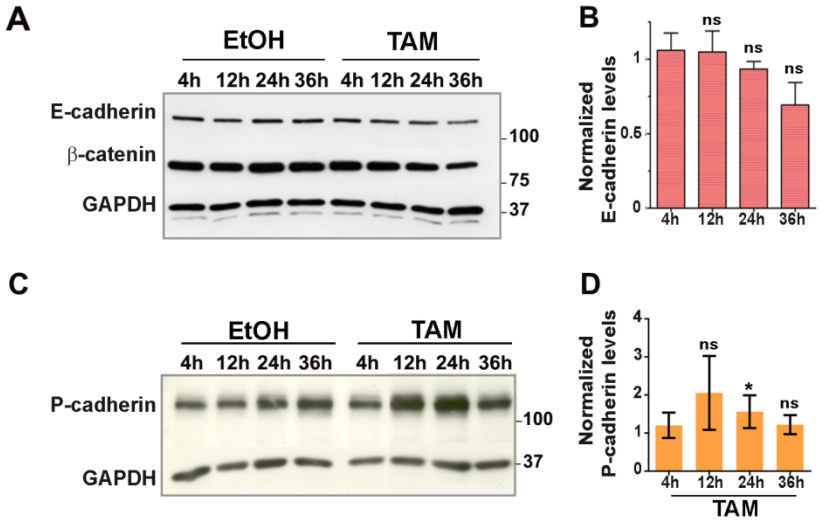

Figure 3.5: ER-Src cells maintain E-cadherin and β-catenin levels and upregulate P-cadherin 24h after TAM treatment (A) Western blot on protein extracts from ER-Src cells treated with EtOH for 4 (lane 1), 12 (lane 2), 24 (lane 3) or 36 (lane 4) hours or with TAM for 4 (lane 5), 12 (lane 6), 24 (lane 7) or 36 (lane 8) hours, blotted with anti-E-Cadherin and β-Catenin (upper band) and anti-GAPDH (lower band) used as control. **(B)** Quantification of E-Cadherin levels in ER-Src cells treated with TAM for 4 (lane 1), 12 (lane 2), 24 (lane 3) or 36 (lane 4) hours, normalized to EtOH-treated ER-Src cells for the same time points. Error bars indicate SD. ns indicate non-significant. **(C)** Western blot on protein extracts from ER-Src cells treated with EtOH for 4 (lane 1), 12 (lane 2), 24 (lane 3) or 36 (lane 4) hours or with TAM for 4 (lane 5), 12 (lane 6), 24 (lane 7) or 36 (lane 8) hours, blotted with anti-P-cadherin (upper band) and anti-GAPDH (lower band) used as control. **(D)** Quantification of P-cadherin levels in ER-Src cells treated with TAM for 4 (lane 1), 12 (lane 2), 24 (lane 3) or 36 (lane 4) hours, normalized to EtOH-treated ER-Src cells for the same time points. GAPDH was used as loading control. Error bars indicate SD. ns indicate non-significant. * indicate P<0.05.

3.4.4 ER-Src cells do not show higher ability to migrate in wound healing assay during the 36h of TAM treatment

As reviewed by Ribeiro and Paredes, P-cadherin identifies an intermediate EMT state associated with a metastable phenotype (Ribeiro & Paredes 2014). Therefore, I directly assessed the ability of TAM-induced ER-Src cells to migrate. In wound-healing response assay, TAM-induced ER-Src cells did not show better abilities to close the wound than TAM-treated PBabe ones, 25 hours after treatments (Figure 3.6.A and B). In both experimental conditions, the wound closure is most likely a consequence of cells that proliferate, filling in the free space (doubling time of cells is ~12 hours). To confirm these observations, I followed wound closure using time-lapse microscopy during the 36h of EtOH or TAM treatments and measured the distance travelled by ER-Src cells front overtime. During the first 24h of EtOH or TAM treatment, the cells-free area decreased at the same rate in both experimental conditions (Figure 3.6.C), indicating no difference in the migratory potential of EtOH- or TAM-treated ER-Src cells. Surprisingly, between 24 and 36 hours of treatments, cells exposed to TAM seemed to travel less than the EtOH-treated ones (Figure 3.6.C).

The wound healing assay does not take into consideration single cell locomotion parameters, such as speed, directional movement, and persistence duration (Decaestecker et al. 2007). Moreover, transformed single cells not always coordinate their cell movement in 2D (Wu et al. 2014). Furthermore, monolayer TAM-induced ER-Src cells were found to accumulate on the top of each other (Figure 3.3.B) Therefore, the failure to detect higher migrating abilities of TAM-treated ER-Src cells in wound healing assay does not discard the possibility that these cells acquire migratory potential. Alternatively, these cells may display higher migrating potential after 36 hours. In agreement with this possibility, I found that in 3D culture, ER-Src cells extruded from the spherical acinar-like structure, and invaded the Matrigel 60 hours after TAM treatment (Figure 3.4.B and Movie 1).

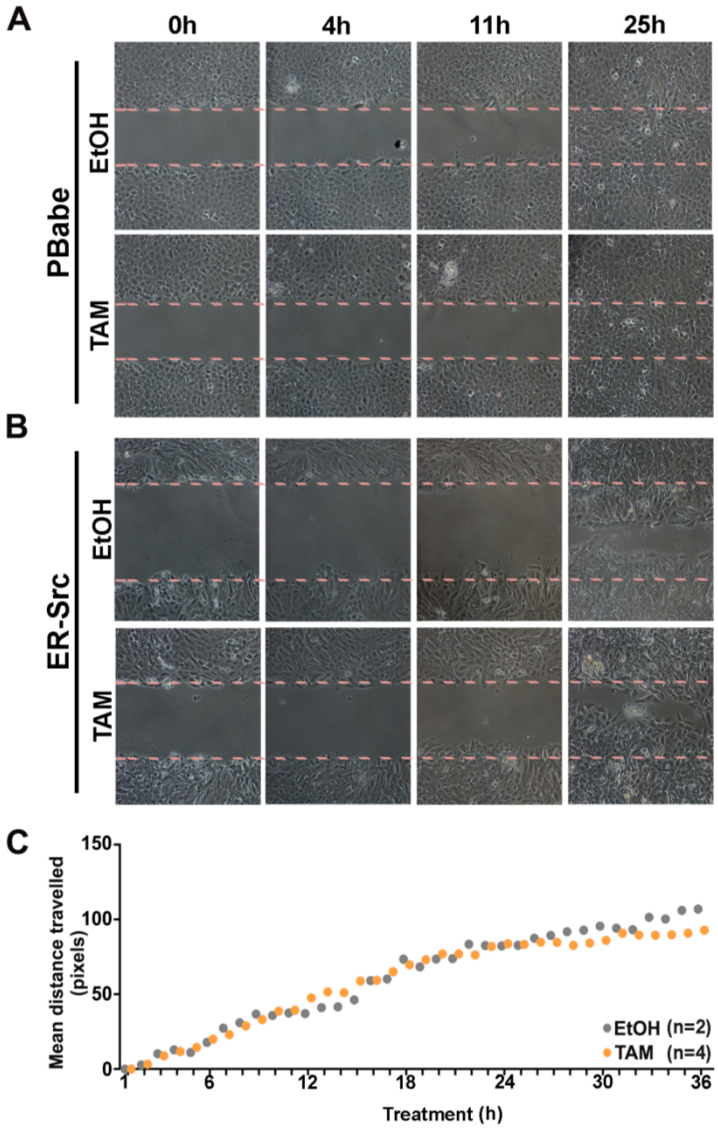

Figure 3.6: Wound healing assays does not allow detecting higher migratory abilities of ER-Src cells during the 36 hours of TAM treatment. (A) And (B) Phase-contrast microscopy images of wound-healing response assays of PBabe and ER-Src cells treated with EtOH or TAM, respectively, for 25 hours. Images were acquired at 0, 4, 11 and 25h of treatment. (C) Quantification of distance travelled, observed by time-lapse imaging, by ER-Src cells during 36 hours of treatment with EtOH or TAM.

3.4.5 TAM-induced ER-Src cells differentiate a pool of cells with Cancer Stem Cell features

As the 2D migration assays were not conclusive regarding when TAM-induced ER-Src cells develop full transformed features, I analysed the ability of TAM-induced ER-Src cells to aquire additional features of malignant transformation. P-cadherin as been directly associated with the expression of some stem markers, including CD44 (Vieira et al. 2014). High expression of the CD44 marker ($CD44^{high}$), combined with low CD24 expression ($CD24^{low}$) are features of a mesenchymal-like state, in which cancer cells would exhibit breast stem cells features and enhanced invasive properties (Sheridan et al. 2006; Liu et al. 2014). Using flow cytometry, I assessed the changes in expression of these two cell-surface glycoproteins in ER-Src cells after treatments with EtOH or TAM. Interestingly, 36 hours after treatments, while around 25% of EtOH-treated ER-Src were $CD44^{high}/CD24^{low}$, this population represented 70% of the TAM-induced ER-Src cells (Figure 3.7.A and B), suggesting that the majority of TAM-induced ER-Src cells acquires stemness properties. These observations reinforce the hypothesis by which TAM-induced ER-Src cells already display malignant features 24 hours after Src activation, in particular the enrichment of a Cancer Stem Cell (CSC)-like population, expressing $CD44^{high}/CD24^{low}$, associated with higher P-cadherin levels.

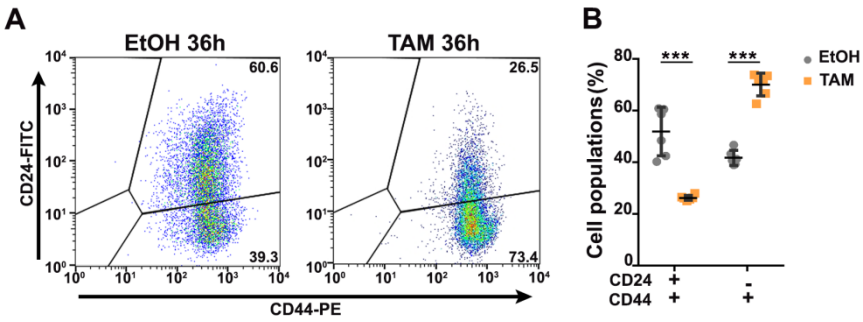

Figure 3.7: A pool of ER-Src cells express CSCs markers 36 hours after TAM treatment. (A) Populations of cells CD44^{high}/CD24^{low} and CD44^{high}/CD24^{high} 36 hours after treatment with EtOH or TAM. (B) Quantification in percentages of CD44h^{high}/CD24^{low} or CD44^{high}/CD24^{high} cells 36 hours after treatment with EtOH or TAM. Error bars indicate SD. *** indicate P<0.0001.

Breast CSCs expressing the cell surface marker profile CD44^{high}/CD24^{low} present lower levels of the proliferation marker Ki67 staining, indicative of a quiescent state (Liu et al. 2014). I therefore assessed the proliferation rate of TAM-induced ER-Src cells during transformation usinf BrdU incorporation assays, which reveals actively proliferating cells undergoing DNA synthesis. Excitingly, while EtOH- and TAM-treated ER-Src cells showed similar number of BrdU-positive cells 4 and 12 after treatments, at 24 hours, the percentage of BrdU-positive TAM-treated ER-Src cells was significantly smaller (~25%) than the one of control cells (~33%) (Figure 3.8.A). Cells cycle profiles of ER-Src cells 24 hours after EtOH or TAM treatments showed that the majority of TAM-induced cells that had incorporated BrdU displayed a reduction in DNA content compared to those treated with EtOH (Figure 3.8.B). In agreement with a previous report demonstrating that the acquisition of stemness markers take place 16 hours after TAM induction in this cell line (Iliopoulos et al. 2011), my observations argue that a quiescent CSC population had arised in ER-Src cells 24 hours after Src activation.

Surprisingly, while 36 hours after TAM treatment, 70% of ER-Src cells expressed CSC markers (Figure 3.7), the number of BrdU-positive cells were not significantly different between EtOH- and TAM-treated cells at this time point (Figure 3.8.A). To make sense of this discrepancy, I used an alternative approach

to evaluate the proliferative abilities of TAM-induced ER-Src cells. Cell cycle regulation is tightly controlled by key regulatory factors, whose levels can be used as read-out of cell proliferation (Uzman et al. 2000). Particularly, I monitored during transformation of TAM-induced ER-Src cells changes in Cyclin B1 levels, which is indispensable for the transition from G2 to M phase (Androic et al. 2008). Consistent with the enrichment of a quiescent CSC population, with mesenchymal-like features, TAM treated ER-Src showed decreased levels of Cyclin B1 24 and 36 hours after TAM treatment, compared to EtOH-treated ER-Src cells (Figure 3.8.C and D).

At 36h, the BrdU incorporation results suggest an increase in DNA synthesis. This might indicate a transition to a different state of CSCs in which cells would express additional markers, e.g. CD49f or aldehyde dehydrogenase (ALDH), among others and exhibit a different proliferative profile (Kotiyal & Bhattacharya 2014).

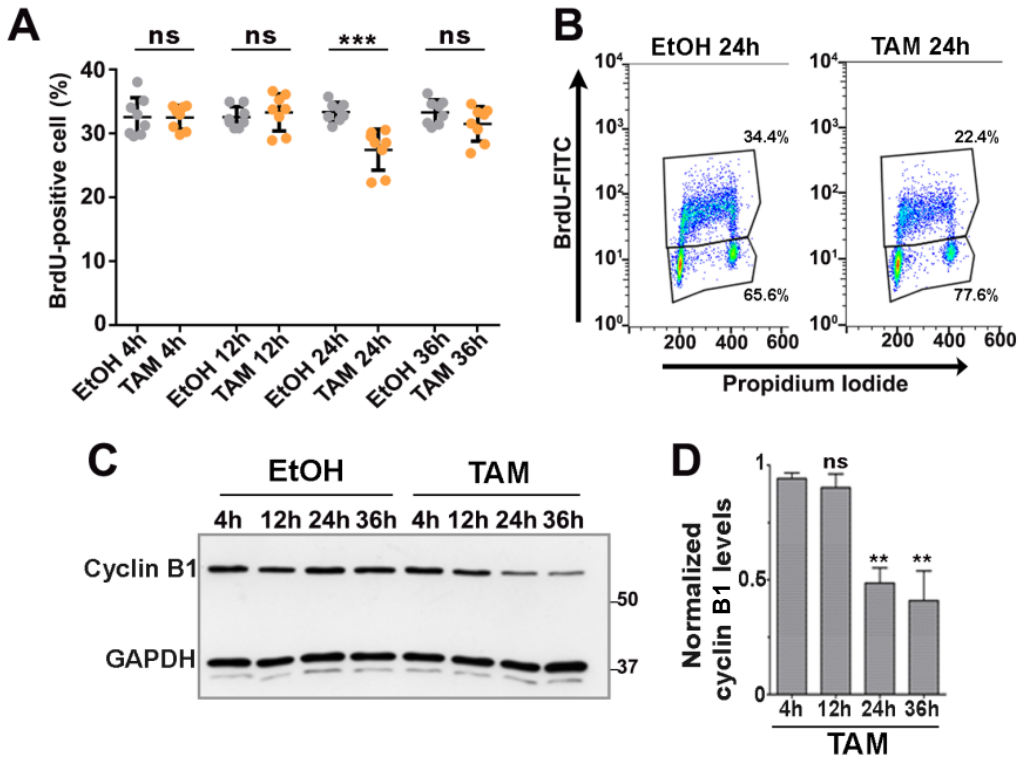

Figure 3.8: Proliferation is decreased at 24 hours of activation of Src. (A) Relative number of ER-Src cells treated with TAM or EtOH for 4, 12, 24 or 36 hours, that show BrdU incorporation. (B) Cell cycle analysis by FACS of cells treated with TAM or EtOH for 24 hours. (C)Western blot on protein extracts from ER-Src cells treated with EtOH for 4 (lane 1), 12 (lane 2), 24 (lane 3) or 36 (lane 4) hours or with TAM for 4 (lane 5), 12 (lane 6), 24 (lane 7) or 36 (lane 8) hours, blotted with anti-Cyclin B1 (upper band) and anti-GAPDH (lower band) used as control. (D) Quantification of Cyclin B1 levels in ER-Src cells treated with TAM for 4 (lane 1), 12 (lane 2), 24 (lane 3) or 36 (lane 4) hours, normalized to EtOH-treated ER-Src cells for the same time points. GAPDH was used as loading control. Error bars indicate SD. ns indicate non-significant. ** indicate P<0.001. *** indicate P<0.0001.

3.4.6 ER-SRC CELLS ACQUIRE SELF-SUFFICIENCY IN GROWTH PROPERTIES 12H AFTER SRC ACTIVATION.

It has been recently shown that cells with stemness features and self-renewal capacity have abilities to survive and form anchorage-independent colonies in soft agar (Liu et al. 2014). I therefore tested the abilities of EtOH and TAM-treated ER-Src cells to form colonies in this assay. Although monolayer ER-Src cells treated with TAM for 36 hours and left to grow in soft agar for 21 days (Figure 3.9.A) formed a higher number of colonies in anchorage independent-conditions compared to EtOH-treated ones, this difference was not significant (Figure 3.9.B and D). This lack of striking difference could be explained by the leakiness of the ER-Src construct I observed by western blot in EtOH-treated cells (Figure 3.2.B) and consequently the presence of $CD44^{high}/CD24^{low}$ stem/progenitor cell population (Figure 3.7). To reveal the tumorigenicity of TAM-treated ER-Src cells, I challenged cells in conditions of growth factor deprivation as only transformed cells would be able to survive and proliferate in this assay. Excitingly, only ER-Src cells treated with TAM were able to form colonies in soft agar in the absence of Epidermal Growth Factor (EGF) (Figure 3.9.B and C). Moreover, TAM-treated ER-Src cells formed as many colonies in soft agar with or without EGF (Figure 3.9.B and C). These observations indicate that in soft agar assays, only TAM-induced ER-Src cells acquire self-sufficiency in growth properties.

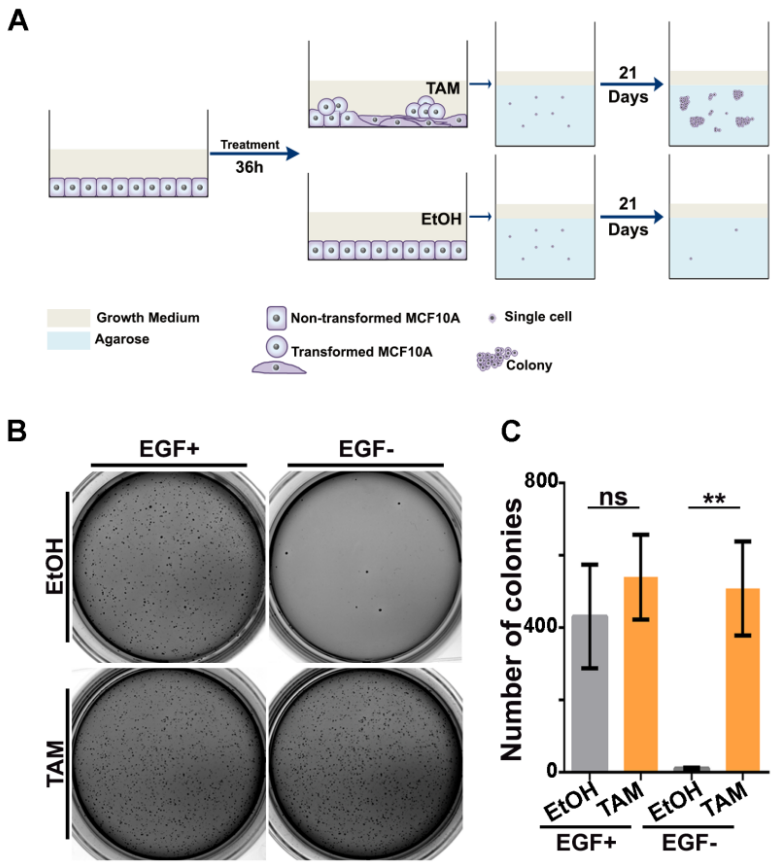

Figure 3.9: TAM-induced Er-src cells grow colonies in soft agar in the absence of EGF. (A) Experimental design used to evaluate Src-dependent acquisition of self-sufficiency in growth. Induction of transformation was performed in monolayer culture. 36h after induction, cells were plated in agarose. Cells were incubated for 21 days in the same culture medium conditions in which they were transformed. **(B)** Soft Agar colony assays of cells grown in the presence or absence of EGF and treated with EtOH or TAM for 36 hours. **(C)** Quantification of the number of EtOH- or TAM-treated ER-Src colonies grown in the presence or absence of EGF. Error bars indicate SD. ns indicate non-significant. ** indicates $P<0.001$.

To confirm that TAM-treated ER-Src cells sustain growth signalling in the absence of EGF in other culture conditions, I tested the effect of EGF restriction on the growth of EtOH- and TAM-treated acini. As expected, in 3D cell culture, ER-Src cells treated with EtOH gave rise to polarized, acini-like spheroids exclusively in the presence of EGF. In the absence of EGF, these cells could still be observed after 14th day of 3D-culture as single cells that were unable

to proliferate. In contrast, TAM-treated ER-Src cells were able to proliferate in Matrigel in the absence of EGF. Moreover, similar to TAM-treated ER-Src acini grown in the presence of EGF, these acini formed highly disorganized structures, with spike-like figures and individual cells extruding and invading the reconstituted basement membrane (Figure 3.10.B). Thus, these observations confirm that only TAM-induced ER-Src cells acquire self-sufficiency in growth ability.

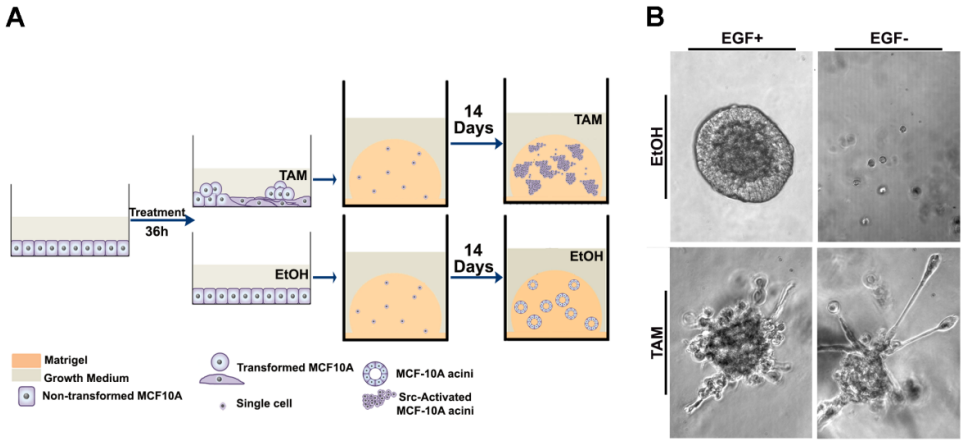

Figure 3.10: TAM-induced ER-Src cells form malignant-like acini, in the absence of EGF. **(A)** Experimental design to evaluate the ability of EtOH- or TAM-treated ER-Src cells to form acini in the presence or absence of EGF. Induction of transformation was performed in 2D culture. 36h after induction, cells were plated in matrigel. Cells were incubated for 14 days in the same culture medium conditions in which they were transformed. **(B)** Phase-contrast images of EtOH- or TAM-treated ER-Src cells grown in the presence or absence of EGF.

As I aim to demonstrate a role of the actin cytoskeleton in Src-induced tumour growth, I used two complementary approaches to estimate the time required for TAM-treated ER-Src cells to acquire the ability to self-sustain growth. As a first approach, I quantified the number of cells in S-phase of the cell cycle in ER-Src cells, grown in the presence and absence of EGF during the first 36 hours of EtOH or TAM treatments. As a second approach, I used an assay inspired from bacterial proliferation rate assessment, which evaluate growth rate through quantification of the total number of ER-Src cells, grown in the presence and absence of EGF during the first 36 hours of EtOH or TAM treatments.

Although these two strategies are less accurate than BrdU incorporation assay, both reduce the number of processing steps. In EGF-containing growth culture conditions, both strategies showed that EtOH and TAM-treated ER-Src cells maintained their ability to proliferate overtime with no significant difference between both treatments (Figure 3.11.A and C). However, when growth medium was depleted of EGF, significant differences appeared between 4 and 12 hours of treatment (Figure 3.11.B and D). 4 hours after EtOH or TAM treatments, ER-Src cells showed no difference in the number of S-phase cells. In contrast, 12 hours onward after treatments, EtOH-treated ER-Src cells showed a progressive reduction in S-phase figures overtime, while TAM-induced ER-Src cells maintained their number of S-phase to levels significantly higher than EtOH-treated cells (Figure 3.11.B). Consistent with ER-Src cells acquiring self-sufficiency in growth properties between 4 and 12 hours after TAM treatment, the proliferation rate of ER-Src cells grown in the absence of EGF was significantly higher than the one of cells treated with EtOH between 4 and 12 hours after TAM treatment. Between 12 hours and 24 hours after treatments, EtOH and TAM-treated ER-Src cells did not show any significant difference of their proliferation rate, possibly due to the decreased proliferation of TAM-induced ER-Src cells I previously observed at this time point (Figure 3.8). However, between 24 and 36 hours after treatment, the ability of TAM-induced ER-Src cells to proliferate at higher rate compared to EtOH-treated ones was restored (Figure 3.11.D).

Taken together, this set of experiments clearly demonstrates that the acquisition of self-sustained growth signalling occurs during the first 12 hours of Src-induced cellular transformation.

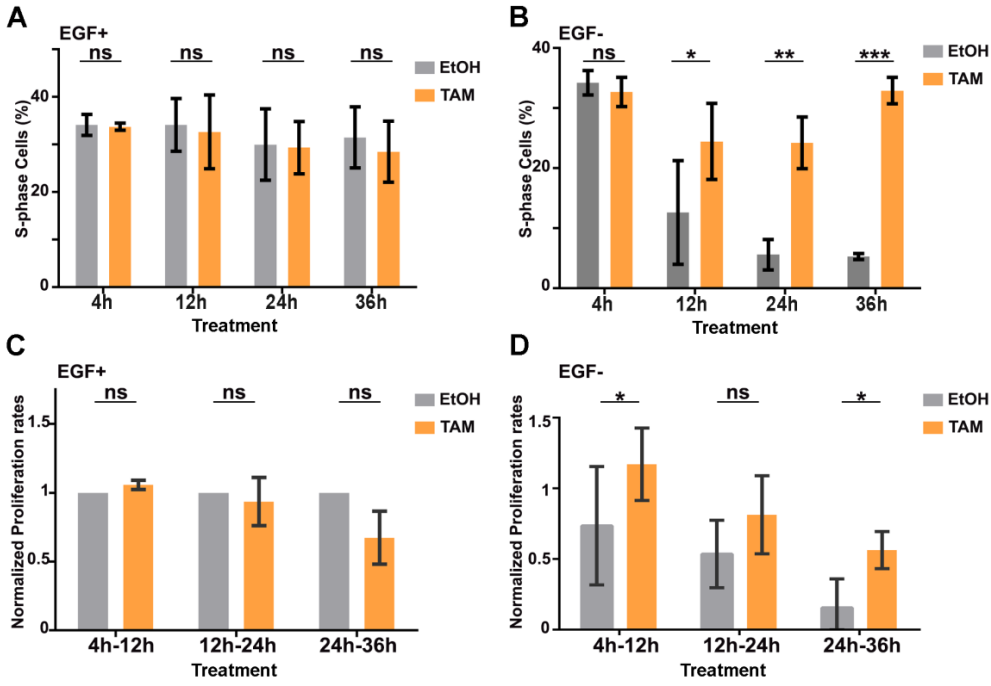

Figure 3.11: The ability of TAM-treated Er-Src cells to grow in the absence of EGF is acquired during the first 12h of Src activation. (A and B) Relative number of cells in S-phase in EtOH or TAM-treated ER-Src cells grown in the presence (A) or absence (B) of EGF. (C and D) Proliferation rates of EtOH- or TAM-treated ER-Src cells, grown in the presence (C) or absence (D) of EGF. Proliferation rates were normalized to the proliferation rate of EtOH-treated ER-Src cells grown in the presence of EGF. Error bars indicate SD. ns indicate non-significant. * indicate P<0.05. ** indicate P<0.001. *** indicate P<0.0001.

3.4.7 PARALLEL SRC-DEPENDENT STRESS FIBRES ARE TRANSIENTLY ASSEMBLED IN THE FIRST 12H OF MALIGNANT TRANSFORMATION.

To investigate if the acquisition of self-sufficiency in growth properties by Src activation is associated with alterations in the actin cytoskeleton, I first analysed the changes in F-actin in TAM-induced ER-Src cells. Strikingly, the transformation of TAM-induced ER-Src cells was associated with the accumulation of basal actin fibres 12 hours after Src induction in cells that contained high Src activated levels. These actin structures then disappeared between 12 and 24 hours after Src induction. In contrast, EtOH-treated ER-Src cells or did not show major alterations in F-actin during the 36 hours of treatment

(Figure 3.12.A). Interestingly, these transient actin fibres appeared highly polarized (anisotropy). To compare the organization of the transient Src-dependent actin fibres to those of actin fibres present in EtOH-treated control cells, I quantify their anisotropy using the Image J plug-in, Fibril tool. As expected, actin fibres from TAM-treated ER-Src cells displayed a highly significant increase in anisotropy, when compared to fibres in control conditions (Figure 3.12.B). The accumulation of actin fibres is not an artefact of TAM treatment, as PBabe cells subjected to EtOH or TAM treatments for 12 hours did not show major alterations in the actin cytoskeleton (Figure 3.12.C). These observations demonstrate that activated Src triggers the formation of transient polarized actin filaments.

To get insight on the identity of these actin filaments, I used an antibody specific to the phosphorylated form of phospho-Myosin light chain (pMLC) at threonine 18 and serine 19. The latest phosphorylation events has been reported to be involved in the assembly of stress fibres (Totsukawa et al. 2000). As shown in Figure 3.13.A, pMLC was recruited to the Src-dependent polarized actin fibres 12 hours after TAM treatment, arguing that these transient actin structures are actin stress fibres. If so, I would expect that these actin structures are decorated by additional ABPs that give actin stress fibres their identity. In agreement with this hypothesis, Filamin B (FLNB), which localizes to stress fibres (Takafuta et al. 2003), was also upregulated in TAM-induced ER-Src cells (Hirsch et al. 2010) and, accumulated by Western Blot in ER-Src cell extracts 4 hours after TAM induction (Figure 3.13.C). Moreover, FLNB was recruited to the transient Src-dependent parallel actin fibres 12 hours after TAM treatment (Figure 3.13.B).

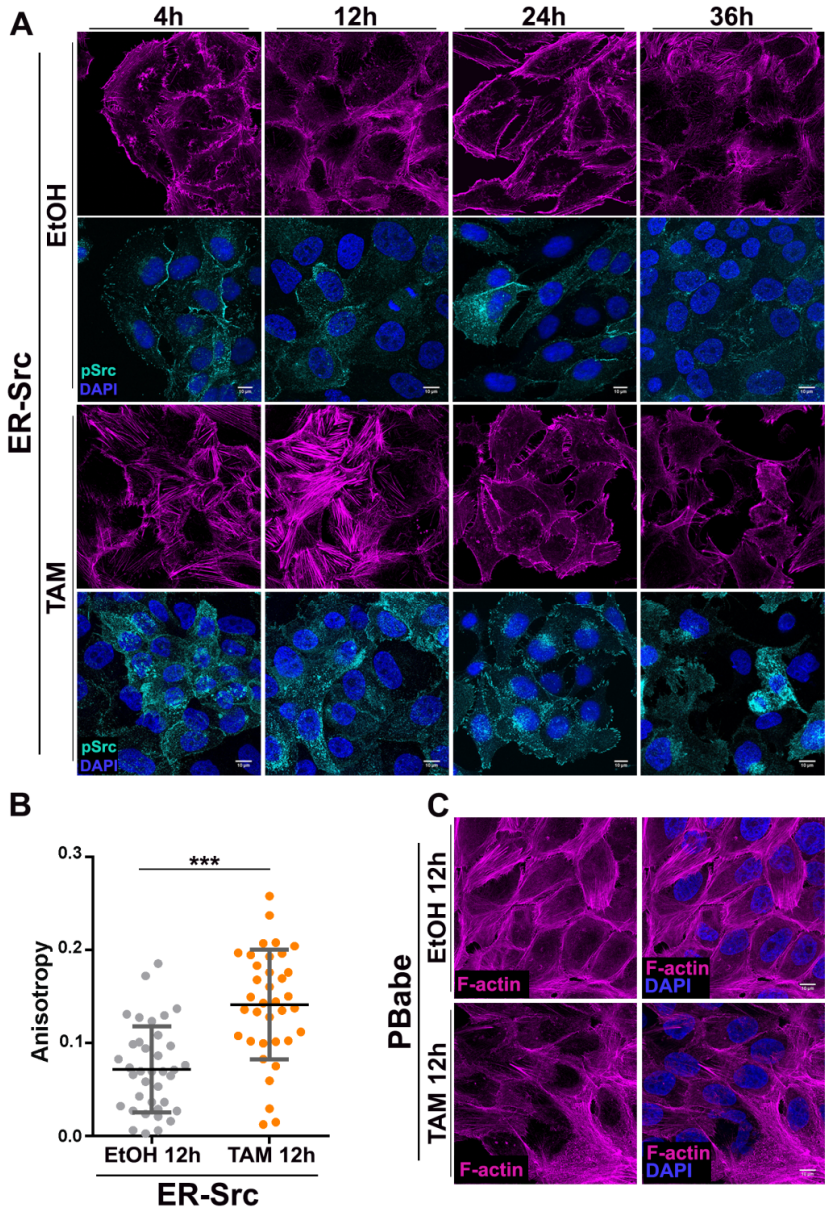

Figure 3.12: Src activation induces the formation of transient, parallel actin fibres. (A) Standard confocal sections of ER-Src cells treated with TAM or EtOH for 4, 12, 24 or 36 hours, stained with Phalloidin (magenta) to mark F-actin, anti-p-Src (cyan) and DAPI (Blue) to mark nuclei. Scale bars represent 10 μm. **(B)** Quantification of the anisotropy of actin fibres in ER-Src cells treated with EtOH- or TAM-for 12 hours. Error bars indicate SD. *** indicates P<0.0001. **(C)** Confocal images of PBabe cells 12 hours after EtOH or TAM treatments, stained with Phalloidin (magenta), which marks F-actin and DAPI (blue), which marks the nucleus. Scale bars represent 10 μm.

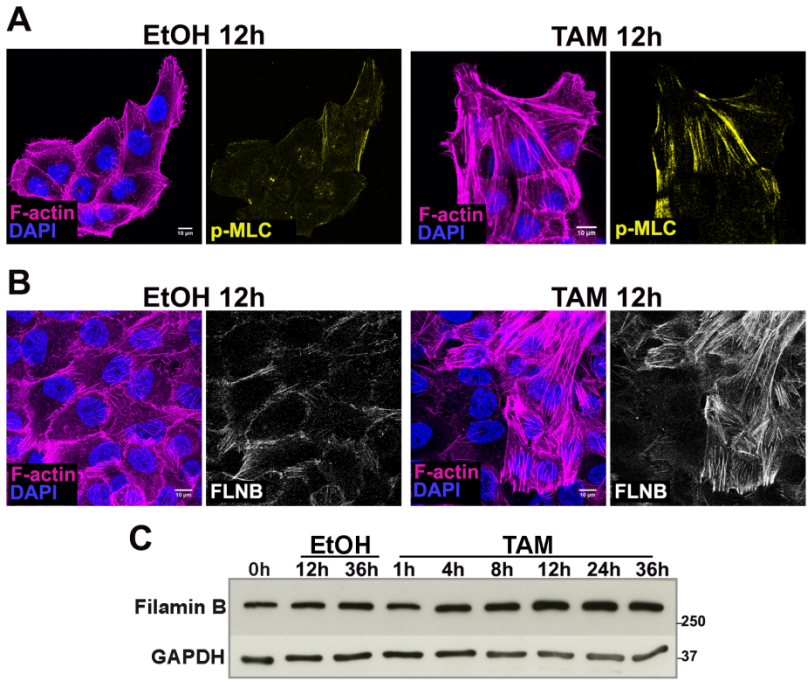

Figure 3.13: Actin fibres are enriched in pMLC and FLNB, at 12hours of Src activation. Standard confocal sections of ER-Src cells, treated with EtOH or TAM for 12 hours, stained with Phalloidin (magenta) to mark F-actin, DAPI (blue) to mark nuclei and anti-pMLC (yellow) (A) or FLNB (B). Scale bars correspond to 10 µm. (C) Western blot on protein extracts from ER-Src cells untreated (lane 1), treated with EtOH for 12 (lane 2), 36 (lane 3) hours or with TAM for 1 (lane 4), 4 (lane 5), 8 (lane 6), 12 (lane 7), 24 (lane 8) or 36 (lane 9) hours, blotted with anti-FLNB (upper band) and anti-GAPDH (lower band) used as control.

Because these drastic changes in the actin cytoskeleton correlate with the acquisition of self-sufficiency in growth ability, these observations suggest that the transient accumulation of polarized actin stress fibres induced 12 hours after Src activation may be involved in the acquisition of early tumorigenic traits.

3.4.8 SRC PROMOTES THE TRANSIENT POLYMERIZATION OF ACTIN FIBRES

The accumulation of the Src-dependent longitudinal stress fibres could result from an increase in actin expression. These excessed actin monomers (G-actin) could be incorporated into filaments (F-actin) to maintain the balance between the pools of G- and F-actin. Alternatively, this accumulation could result from an increase in actin polymerization at filament-barbed ends, consequently reducing the pool of G-actin. In turn, a reduction in the pool of G-actin can trigger the nuclear translocation of co-transcription factors tether by G-actin in the cytoplasm, including the MAL co-transcription factor, which activate gene expression via its interaction with Serum Response Factor (SRF) (Miralles et al. 2003).

To determine if by inducing the transient formation of stress fibres, Src activation affects the balance between the pools of G- and F-actin, I analysed if Src-induced cellular transformation is associated with alterations in the total pool of G-actin and in the ratio between G and F-actin. As shown in Figure 3.14.A, Western Blot on protein extracts from EtOH- and TAM-treated ER-Src cells did not show difference in total actin levels during the 36 hours of treatments. In contrast, Western Blot in which the G-actin pool was separated from the F-actin ones showed that ER-Src cells contained higher levels of F-actin 12 hours after TAM-treatment compared to EtOH-treated cells at the same time point (Figure 3.14.B). Since total actin levels remained constant during the transformation process (Figure 3.14.A), these transient changes in F-actin fibres would be due to an increase in actin polymerization. Thus, the Src-dependent increase in stress fibre polymerization may alter signal transduction pathways that respond to G-actin levels.

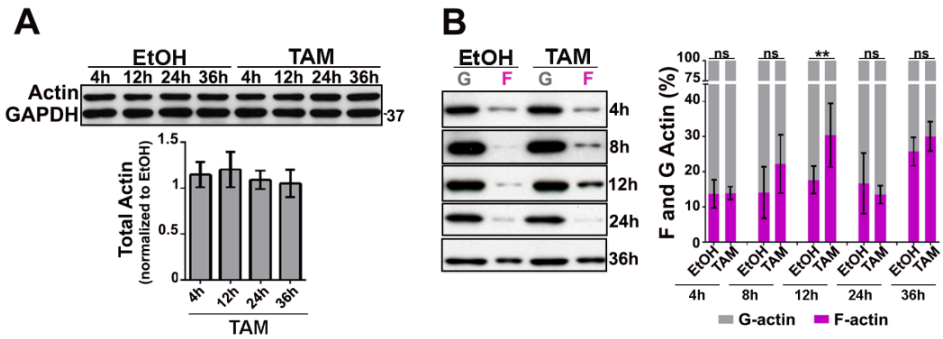

Figure 3.14: Src activation induces transient actin filament polymerization in the first 12 hours of transformation. (A) Western blot on protein extracts from ER-Src cells treated with EtOH for 4 (lane 1), 12 (lane 2), 24 (lane 3) or 36 (lane 4) hours or with TAM for 4 (lane 5), 12 (lane 6), 24 (lane 7) or 36 (lane 8) hours, blotted with anti-actin (upper band) and anti-GAPDH (lower band) used as control (lower panel). Quantification of total actin levels in ER-Src cells treated with TAM for 4 (lane 1), 12 (lane 2), 24 (lane 3) or 36 (lane 4) hours, normalized to EtOH-treated ER-Src cells for the same time points. GAPDH was used as loading control. **(B)** Western blot on protein extracts from ER-Src cells treated with EtOH (lane 1 and 2) or TAM (lane 3 and 4) for 4, 8, 12, 24 or 36 hours, blotted with anti-actin to visualize the G- (lane 1 and 3) and F-actin (lane 2 and 4) pools (left panel). Quantification of the percentage of G- (grey) and F-actin (magenta) ratio between EtOH and TAM-induced ER-Src cells for the different time point indicated (right panel). Error bars indicate SD. ** indicate P<0.001.

3.4.9 Increased F-actin accumulation in the first 12 hours of Src activation is associated with increased cell stiffness

Higher absolute amount of F-actin or stress fibres formation have been associated with increased cell stiffness, whereas a reduction in F-actin or stress fibre disassembly correlates with lower cell stiffness (Bhadriraju & Hansen 2002; Doornaert 2003). I therefore investigated if the dynamic alterations in F-actin levels associated to Src-mediated transformation correlate with changes in cell stiffness. Atomic Force Microscopy (AFM) based indentation measurements revealed that monolayer ER-Src cells presented a significantly higher Young's Modulus 12 hours after TAM treatment compared to EtOH-treated ones (Figure 3.15.B), indicating an increase in cell stiffness. In contrast, at 36 hours, when TAM-induced ER-Src cells have disassembled the Src-dependent stress fibres and acquired stem cell properties, cells were more deformable than control cells

(Figure 3.15.A). To control for unspecific effects resulting from TAM treatment, similar measurements were performed in PBabe cells treated with EtOH or TAM for 12 hours. In contrast to ER-Src cells, PBabe cells showed no changes in cell stiffness between EtOH and TAM treated cells, arguing that the transient increase in cell stiffness of TAM-induced ER-Src cells results from Src activation.

Cells mechanical properties are affected by a myriad of factors, including their physical environment (Gupta et al. 2015). AFM measurements of monolayer cell in culture were performed on glass-bottom dishes (2-4 GPa) that by no mean, resemble the physical properties in which breast cells are embedded physiologically (800 Pa) (Butcher et al. 2009). Therefore, it was crucial to perform equivalent AFM measurements of cells cultured in Matrigel, whose physical properties are more like the ones of breast tissue extracellular matrix (450 Pa) (Soofi et al. 2009). Nevertheless, even in more physiological conditions, ER-Src cells isolated from TAM-treated acini cultured in Matrigel showed a transient increase in cell stiffness at 12 hours compared to ER-Src acini treated with EtOH for identical time (Figure 3.15.C). In addition, like cells cultured in monolayer, the increase in cell stiffness of TAM-treated ER-Src cells was only transient, as 36 hours after treatments, the young´s modulus were not significantly different between TAM and EtOH-treated ER-Src cells. In contrast to 2D cultures, however, TAM-treated ER-Src cells were not more deformable than EtOH-treated ones at this time point (Figure 3.15.D). This may be due to the fact that phenotypic transformation took longer in 3D cultures, with cells starting to extrude from the spherical acinar-like structure 60 hours after TAM treatment (Figure 3.4.B). Altogether these observations demonstrate that Src activation triggers the polymerization of polarized stress fibres, associated with an increase in cell stiffness and the acquisition of self-sufficiency in growth properties.

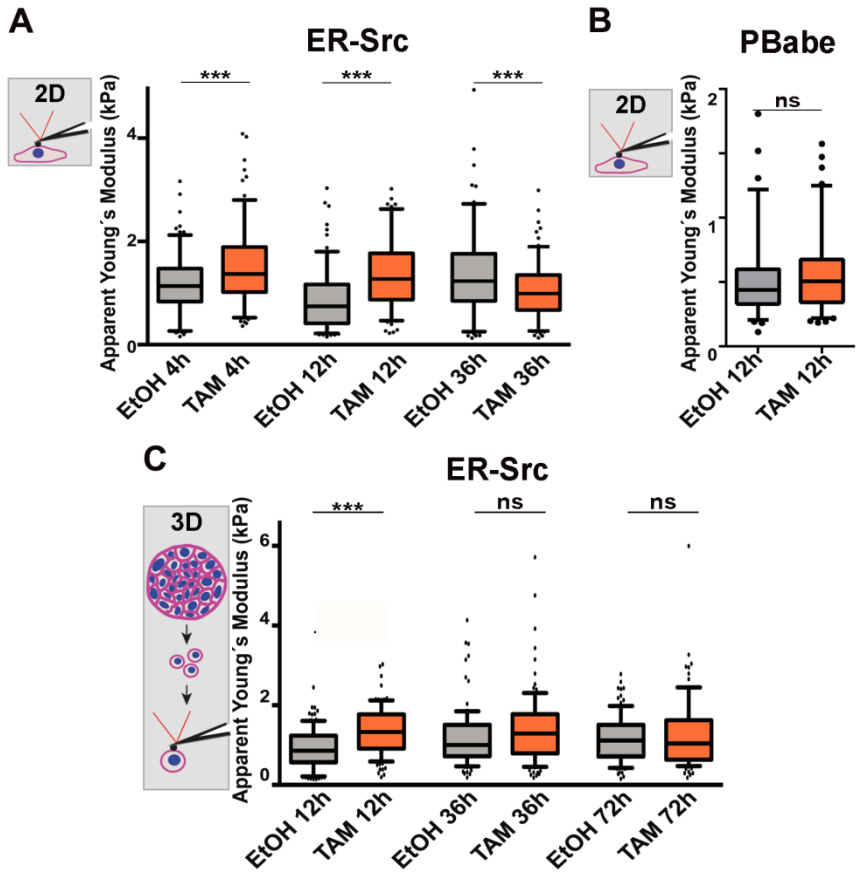

Figure 3.15: Cells undergoing Src-dependent transformation become transiently stiffer before exhibiting softer properties. (A) Apparent Young' moduli of ER-Src cells induced with EtOH or TAM for 4, 12 or 36 hours. (B) Apparent Young´s modulus of PBabe cells 12 hours after EtOH or TAM treatments. (C) Apparent Young's modulus of ER-Src cells isolated from 3D (Matrigel) cultures for 7 days and induced with EtOH or TAM for 12, 36 or 72 hours. All the data points are represented as dots with horizontal line indicating median values. ns indicates non-significant. ** indicate P<0.001. *** indicates P<0.0001.

3.5 DISCUSSION

In this chapter, I took advantage of the inducible ER-Src cell line, which permits to follow the multistep development of Src-induced cellular transformation to demonstrate that transformation involves 2 distinct phases: a pre-malignant and a malignant phases, associated to drastic changes in the actin cytoskeleton.

Acto-myosin-dependent cell stiffening: a feature of the pre-malignant phase of transformation.

I found that transformation of this cell line can be divided into two main phases. The first phase occurs during the first 12 hours of cellular transformation and precedes all morphological features associated to phenotypic transformation. This phase is characterized by the increase polymerization of longitudinal actin fibres (Figure 3.12; 3.14). In agreement with these observations, the activation of Src in chick embryonic fibroblasts also triggers the assembly of actin-containing parallel microfilament bundles during the first 24 hours (Wang & Goldberg 1976). These actin-based structures are contractile stress fibres, enriched for activated pMLC and FLNB that are associated to Focal Adhesions (FAs) (Figure 3.13). Accordingly, this transient accumulation of acto-myosin stress fibres is associated with an increase in cell stiffness (Figure 3.15) and coincides with a boost in the production of the Interleukin 6 (IL6) cytokine, which activates the STAT3 oncogene (Iliopoulos et al. 2009) and with the acquisition of self-sufficiency in growth properties (Figure 3.11), one of the early hallmarks of cancer cells.

The second phase of transformation involves the acquisition of stemness features and a reduction in acto-myosin-dependent stiffening.

In the second phase of Src-induced cellular transformation, cells acquire morphological features, including spindle like-cell shape in monolayer cell culture (Figure 3.3) or spike-like projections with cells extruding from the spherical acinar-like structure and invading the basement-membrane in 3D

culture (Figure 3.4) that are both reminiscent to mesenchymal-like behaviour, another hallmark of cancer cells. Accordingly, ER-Src cells upregulate the EMT marker P-cadherin 24 hours after TAM-treatment (Figure 3.5). In contrast, E-cadherin and β-catenin levels are not affected during the 36 hours of Src-induced cellular transformation (Figure 3.5). In contrast, to tumours that show a cadherin switch (downregulation of E-cadherin associated to the concomitant upregulation of N-cadherin), tumours that overexpress P-cadherin, maintain E-cadherin levels. Moreover, the invasive phenotype mediated by P-cadherin has been shown to be dependent on the concomitant expression of wild- type E-cadherin (Ribeiro & Paredes 2014). Thus, the maintenance of E-cadherin levels in TAM-induced ER-Src cells might also be required for the ability of P-cadherin to induce a metastatic phenotype. Indeed, TAM-induced ER-Src cells cultured in 3D acquire invasive ability (Figure 3.4). Surprisingly, in 2D culture, TAM-induced ER-Src cells do not show better ability to migrate than EtOH-treated control cells, even 36 hours after TAM treatment (Figure 3.6). These cells might take longer to acquire higher invasive ability in these conditions of experiment. Several reports propose that EMT drives the acquisition of CSC properties (Liu et al. 2014; May et al. 2011). P-cadherin expression has also been directly associated with breast CSC features (Vieira et al. 2014). Accordingly, a large pool of TAM-induced ER-Src cells express breast CSC markers, characterized by high levels of CD44 and low levels of CD24 (Figure 3.7). Moreover, like $CD44^{high}$/ $CD24^{low}$ mesenchymal-like breast CSCs that have been described as being quiescent (Liu et al. 2014), ER-Src cells show a reduction in their ability to incorporate BrdU and a decrease in Cyclin B1 levels, 24 and 36 hours after TAM treatment (Figure 3.8)., Furthermore, TAM-induced ER-Src cells have been previously shown to have mammospheres-forming abilities (Iliopoulos et al. 2011). Finally TAM-induced ER-Src cells acquired the ability to survive and form anchorage-independent colonies in soft agar in the absence of EGF (Figure 3.10), a feature of cells with stemness features and self-renewal capacity (Liu et al. 2014). Therefore, between 12 to 24 hours after TAM treatment, many TAM-induced ER-Src are likely to acquire bona fide CSCs

properties. This second phase of cellular transformation is associated with the depolymerization of the polarized actin fibres (Figure 3.12) and cell softening (Figure 3.14). These observations were expected, since decreased cell stiffness had been associated with malignancy, in particular with the metastatic potential ovarian cancer cells (Xu et al. 2012). Moreover, Guck's laboratory has demonstrated that invasive cancer cells show significantly different mechanical behaviour, with a higher mean deformability compared to their healthy counterparts (Guck et al. 2001). Furthermore, invasive cancer cells display a significantly reduction in the absolute amount of F-actin (Remmerbach et al., 2009) Finally, undifferentiated stem cells are softer than differentiated ones (Keefer & Desai 2011; Hammerick et al. 2011).

Distinct Src-dependent actin structures mediate the acquisition of different transformation features.

Altogether, these observations are consistent with a model by which the control of F-actin by Src activation not only facilitate malignancy-associated properties, including cell invasion (Zhang & Yu 2012) but is also required for Src-induced tumour growth earlier during tumour progression. To perform these different functions, Src appears to build distinct F-actin-based structures depending on the cellular context. Src-mediated cell invasion is linked to its ability to trigger organized F-actin ring structures containing dynamic sites of matrix attachment known as podosomes or invadopodia (Eckert & Yang 2011; Murphy & Courtneidge 2011). However, I show that earlier during cellular transformation, Src induction induces the transient polymerization of polarized stress fibres (Figure 3.12, 3.13, 3.14) that correlate with an increase in cell stiffness (Figure 3.15). The orientation of fibres plays a key role in the overall mechanical properties of cells, being the transition from isotropic to nematic associated with low and high elastic modulus (Gupta et al. 2015).

3.6 CONCLUSIONS

My observations are consistent with a model by which, low Src activity induced during the first phase of Src-induced cellular transformation, triggers the polymerization of parallel actin stress fibres, which may induce an increase in cell stiffness. In turn, cell stiffening could sustain self-sufficiency in growth properties (Figure 3.16). In agreement with a role of cell stiffening in providing a proliferative advantage, cell stiffening has been shown to enhance the activity of mitogen factors. For instance, YAP/TAZ are activated in response to mechanical forces through cytoskeleton changes (Aragona et al., 2013). Nuclear targeting of ERK/MAPK (extracellular-signal regulated kinase/mitogen-activated protein kinase) has also been linked to F-actin re-organization upon integrin engagement at focal adhesion (Aplin and Juliano, 2001; Aplin et al., 2001). Src-dependent cell stiffening may further enhance Src activation to trigger the second phase in malignant transformation, as Src is also activated in response to F-actin-mediated mechanical stretches in mammals (Sniadecki 2010). Moreover Src translocation and activation to focal adhesion is acto-myosin stress fibre-dependent (Fincham et al., 2000; Fincham et al., 1996). Accordingly, I found that activation of ER-Src cells induces the phosphorylation of endogenously expressed Src (Figure 3.2). Higher Src activation would promote a reduction in F-actin-dependent cellular stiffness, which, in turn, may trigger EMT and/or CSC identity, leading to the dissemination of tumour cells away from their primary site of growth (Gross 2013; Machesky 2008; Barry et al. 2010; Vignjevic & Montagnac 2008).

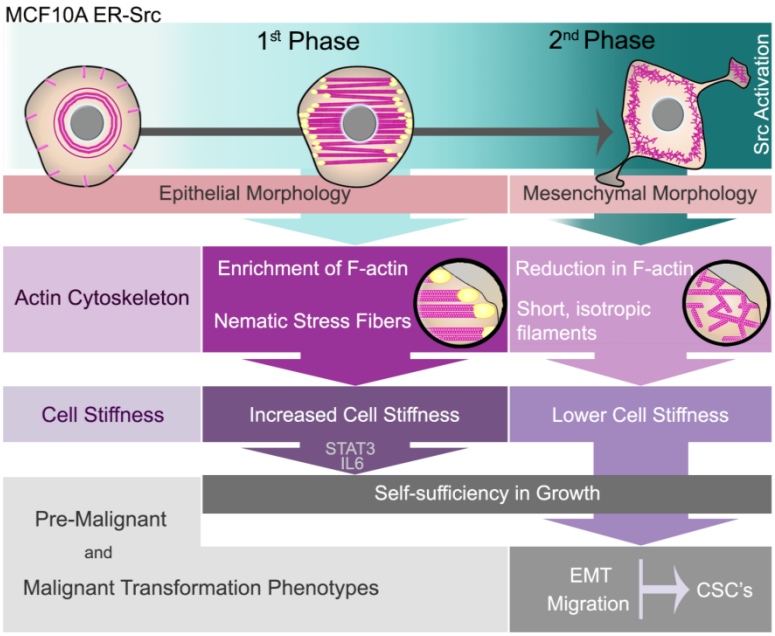

Figure 3.16: Model by which Src promotes self-sufficiency in growth signals, during the first phase of breast tumour progression, and the acquisition of malignant traits in the second phase. In the first phase of cell transformation, low Src activity levels promote the polymerization of parallel stress fibres, an increase in cell stiffness and self-sufficiency in growth. In contrast, in the second phase, further Src activation, depolymerizes the parallel stress fibres, reduces cell stiffness, promotes the acquisition of EMT features, CSC properties and migratory potential.

3.7 ACKNOWLEDGEMENTS

I would like to acknowledge peoples who have contributed to the work described in this chapter, including Catarina Brás Pereira, who performed the immunoblotting for Cyclin B1, E-cadherin, P-cadherin and β-catenin, and João Lagarto for his contribution to the wound healing experiments analysis. Finally, I would like to acknowledge Anna Tautenberger for her help in AFM measurements of cells in 2D culture, and for her measurements in 3D ER-Src structures.

Chapter 4

EVL-mediated orientation of stress fibres promoted malignant transformation of cells.

"O que ainda tornava a vida tolerável era de vez em quando uma boa risada. Ora na Europa o homem requintado já não ri, – sorri regeladamente, lividamente. Só nós aqui, neste canto do mundo bárbaro, conservamos ainda esse dom supremo, essa coisa bendita e consoladora – a barrigada do riso!"

Eça de Queirós, Os Maias

For this chapter, I performed the majority of the experiments described. Anna Taubenberger contributed with stiffness measurements in EVL KD cells. Nuno Pimpão Martins helped in live-imaging and quantification of cells migration and André Vieira and António Polónia analysed EVL levels in human tumour samples.

4.1 SUMMARY

Previously, I have proposed a model in which early and low levels of Src activity would lead to the differential expression of specific sets of ABP, in different stages of breast cancer progression. In early stages, the misregulation of ABPs would lead to the formation and accumulation of long stress fibres, resulting in tumour growth. Then, using a human cell line I validated this model. I have described that Src-mediated transformation in MCF10A cells can be divided in two main phases, corresponding the non-invasive phase to the first 12 hours of Src induction. In the first phase, Src activity induction promotes the transient polymerization of polarized stress fibres and a transition from low and high elastic modulus, associated with pre-malignant traits acquisition. After 36 hours of TAM treatment, there is a full phenotypic transformation, with cells forming multiple colonies in soft agar, and tumours upon injection into nude mice.

In this chapter, I used one of the ABPs identified in the second chapter, to get insight on the role of stress fibres in promoting early events in cell transformation. Using the same inducible ER-Src cell line, I have identified EVL, a member of the Ena/VASP family of protein, as a key mediator of Src-induced cellular transformation. In particular, I have shown that EVL accumulates upon Src activation and that Src-induced transformation is dependent on EVL. My findings argue that during the first phase of Src-induced cellular transformation, EVL promotes the orientation of transient longitudinal actin fibres. In turn, these actin fibres increase cellular stiffness, which consequently sustains cell growth. Accordingly, I show that high levels of EVL are associated with non-invasive stages of breast cancer progression. Finally, I show that EVL increased levels are correlated with Luminal A non-invasive lesion and with invasive ones.

In conclusion, in this chapter I propose a model in which the multistep development of breast tumours requires the polarization of stress fibres in early stages.

4.2 INTRODUCTION

Breast cancer is the most common carcinoma worldwide and the second most frequent cancer-related cause of death. Several models of progression have been proposed to describe the progression of the majority of all Invasive Ductal Carcinomas (IDCs) (Ellis et al. 2003). It is believed that these lesions follow a classical mode of progression, in which the normal breast tissue develops atypical ductal hyperplasia (ADH). This type of lesion is associated with an increased risk of Ductal Carcinoma In Situ (DCIS) development. DCIS tumours have an inherent potential to acquire malignant features and evolve to Invasive Ductal Carcinoma (IDC) through the invasion of the surrounding stroma (Lopez-Garcia et al. 2010; Bombonati & Sgroi 2011; Ellis et al. 2003). Precursor lesions and a range of invasive lesions may be histologically classified as innocuous (I), intermediate (II) or aggressive (III) (Lopez-Garcia et al. 2010). Histological grade is highly correlated with the patients prognosis, being the worst prognosis attributed to the highest histological grade (Elston & Ellis 1991).

Histological progression of breast lesions is the reflection of the evolution of normal cells into cells with increasingly neoplastic phenotypes. Early stages of epithelial tumorigenesis are characterized by decreased apoptosis and increased growth signalling. Cells presenting exclusively this set of altered features are considered benign and constitute the ADH and DCIS lesions. When epithelial cells acquire the ability to degrade the extracellular membrane, migrate and invade distant tissues, a fully transformed phenotype is established. At these late stages, cells have turned into cancer cells (Pinder & Ellis 2003; Damonte et al. 2008) and the tumours are classified as IDC.

The c-Src non-receptor tyrosine kinase is one of most investigated proto-oncogenes implicated in the development, growth, progression, and metastasis in several human cancers (Zhang & Yu 2012). Src protein levels and, to a greater extent, Src protein kinase activity are frequently elevated in breast cancer specimens when compared to adjacent normal tissues and correlate with reduced

survival of breast cancer patients (Elsberger et al. 2010; Elsberger et al. 2009; Kanomata et al. 2011).

Several observations argue that basal Src activity that occurs early during tumour progression, promotes cell proliferation and survival. Interestingly, during later stages of tumour progression further Src activation may facilitate other malignancy-associated properties, such as cell migration, adhesion and invasion (Zhang & Yu 2012). These later processes mostly depend on the regulation of the actin cytoskeleton by Src (Frame 2004).

The semi-flexible filaments of actin (F-actin), which are assembled from monomeric actin (G-actin), sense and respond to forces driving a large number of cellular processes, including changes in cell shape, cell mobility, or cell contraction. In addition, actin filaments translate external forces into biochemical signalling events that guide cellular responses through changes in filaments. These changes are dictated by the way they organize into distinct architectures through the action specific subsets of actin binding proteins (ABPs) (Dos Remedios et al. 2003; Michelot & Drubin 2011). Previously, in Drosophila epithelia, it has been reported that the pro-growth function of various oncogenes, including Src, c-Jun N-terminal kinase (c-JNK) and Yorkie (YAP/TAZ in mammals) is controlled by the actin cytoskeleton (Fernández et al. 2011; Fernández et al. 2013; Gaspar et al. 2015; Jezowska et al. 2011). Particularly, Capping Protein inhibit F-actin accumulation, which counteracts the effect of Src on F-actin, restricting Src-mediated apoptosis or proliferation in Drosophila epithelia (Fernández et al. 2011).

The action of Capping protein on F-actin filaments is antagonized by the Ena/VASP (enabled/vasodilator stimulated phosphoprotein) family proteins comprising Mena, VASP and Ena/VASP -like (EVL) (Barzik et al. 2005). *In vitro* experiments have shown that enrichment of Ena/VASP protein results in long and unbranched filaments, because they protect barbed ends from capping proteins. In contrast, the depletion of Ena/VASP protein from their normal

locations promoted formation of dense actin networks with short, highly branched filaments (Bear et al. 2002; Lebrand et al. 2004).

In human breast cancer, EVL expression has been shown to be up-regulated in IDC (Hu et al. 2008). In another study performed at the protein level, in IDC lesions, EVL is inversely correlated with high invasiveness and poor prognosis (Mouneimne et al. 2012). Although, it has been suggested that EVL-mediated actin bundling suppressed the invasive abilities of breast cancer cells (Mouneimne et al. 2012), so far nothing is known regarding the role of EVL in benign lesions.

To get insight on the role of stress fibres in promoting early events in cell transformation, I took advantage of the inducible MCF10A-ER-Src cell line. Malignant transformation of ER-Src cells comprises two main phases, the non-invasive phase that corresponds to the first 12 hours of Src induction and the second one that takes place from 12 hours of Src-induction onwards. In the first phase, Src activity induction promotes the transient polymerization of polarized stress fibres and a transition from low and high elastic modulus, associated with pre-malignant traits acquisition (Chapter 3). After 36 hours of TAM treatment, there is a full phenotypic transformation, with cells forming multiple colonies in soft agar (Figure 3.9), and tumours upon injection into nude mice (Iliopoulos et al. 2009; Hirsch et al. 2010; Hirsch et al. 2009).

In this chapter, my aim was to understand the role of the actin cytoskeleton structures in the early events of Src-mediated malignant transformation. To accomplish my goal I used EVL, one of the previously identified ABPs (Chapter 2), to assess the importance of stress fibres in cells mechanical properties and in cancer phenotypes, particularly the ones developed in first phase of transformation (Chapter 3). Finally, I wanted to validate my *in vitro* observations in the pathological context, therefore I searched for a possible association between EVL levels and breast cancer stages and molecular subtypes.

4.3 MATERIAL AND METHODS

4.3.1 CELL LINES, CULTURE CONDITIONS AND 4OH-TAM TREATMENT

The MCF10A-ER-Src (ER-Src) and MCF10A-PBabe (PBabe) cell lines cultured in monolayer (2D) were grown, as described in (Hirsch et al., 2009). To treat cells with 4OH-TAM or EtOH, 50% confluent cells were plated and allowed to adhere for at least 12 hours before treatment with 1 μM 4OH-TAM (Sigma H7904) or with identical volume of EtOH for the time periods indicated in the text. Cell culture media containing EtOH alone or 4OH-TAM diluted in EtOH was replaced every 12h.

4.3.2 3D MATRIGEL™ (3D) CULTURES

Lab-Tek II plates (Lab-Tek II, #155409) were coated with 20 μl Matrigel™ (BD Biosciences; 356231). 1000 cells were suspended in 100 μl Matrigel™ and overlaid in wells. After polymerization at 37°C, 500 μl of cell culture media were added and replaced every 3 days. Cells were grown for 14 days and treated with cell culture media containing EtOH or 4OH-TAM.

4.3.3 IMMUNOBLOTTING ANALYSIS

Cells were scraped in TRIS lysis buffer (containing protease and phosphatase inhibitors), and lysed for 20 minutes on ice. Lysates were then cleared by centrifugation at 14,000 rpm at 4°C for 30 minutes. 20 ug of protein were resolved by SDS-PAGE electrophoresis and transferred to PVDF membranes (Amersham Pharmacia). Membranes were blocked with 5% milk in TBS 0.1% Tween 20 and incubated with: anti-EVL (1:250, HPA018849, Sigma) and anti-GAPDH (1:2000, 2D4A7, Santa Cruz). Detection was performed by using HRP-conjugated antisera (Amersham Pharmacia) and Enhanced Chemi-Luminescence (ECL) detection. Western blots quantification were performed using the Image Studio Lite program.

4.3.4 shRNA ADENOVIRUS INFECTION AND NUMBER OF CELLS

ER-Src cells were plated in 6-well plates to reach 30% confluence by the time of infection. EVL short-hairpin RNA (shEVL) or Scrambled short-hairpin RNA (shScr) virus-containing media were added at a MOI of 10^3 PFU per cell, reaching 100% of efficiency of gene delivery. Media were changed after 24h. Treatments with cell culture media containing EtOH or 4OH-TAM were performed 72h after infection.

The number of cells in each condition was measured after 36 hours of treatment, by the Scepter™ 2.0 Handheld Automated Cell Counter. Three independent experiments were performed.

EVL shRNA#1:

GCCAAATGGAAGATCCTAGTACTCGAGTACTAGGATCTTCCATTTGGC;

EVL shRNA#2:

ACGATGACACCAGTAAGAAATCTCGAGATTTCTTACTGGTGTCATCG;

ShScr:

GACACGCGACTTGTACCACTTCAAGAGAGTGGTACAAGTCGCGTGTCTTTTTTACGCGT

4.3.5 REAL-TIME PCR ANALYSIS

1 µg of purified RNA samples from untreated or EtOH- or TAM-induced ER-Src cells expressing shScr or shEVL, were reverse-transcribed using intron-exon-specific primers. Real-time qPCR were performed using PerfeCTa® SYBR® Green FastMix (Quanta Biosciences) in 384 well plates in the Bio-Rad, #1725125**.** The relative amount of EVL mRNA was calculated after normalization to the *GAPDH* transcript. Three independent experiments were performed in triplicate. Data are presented as mean ± SD. Statistical significance was calculated using a *t-test.* Primers used for EVL were GAAGAGTCCAACGGCCAGAA and ACTGGGAGGCTGCTTTTCTC. Primers used for GAPDH were CTCTGCTCCTCCTGTTCGAC and ACCAAATCCGTTGACTCCGAC

4.3.6 MIGRATION TRACKING

Untreated or EtOH- or TAM-induced ER-Src cells expressing shScrambled or shEVL were seeded in 8-well chamber slide (Lab-Tek II, #155409) for live-imaging. Time-lapse images were captured by phase-contrast microscopy using a 10x objective every hour for 25 hours.

4.3.7 SOFT AGAR COLONY ASSAY

$5x10^3$ cells in cell culture media containing no EGF were mixed with 0.36% gelling agarose (A9045 - Sigma) and plated on top of a solidified layer of 0.7% agarose in cell culture media with no EGF. Cells were fed every 6 to 7 days with cell culture media with no EGF. Number of colonies was counted 15-21 days later. Experiment was performed in triplicates and repeated three times. Statistical significance was calculated using a Student's t test.

4.3.8 CELL CYCLE PROFILE

Sub-confluent cells were cultured overnight in media without EGF. Cells were then incubated in culture media containing or depleted of EGF and with EtOH or 4OH-TAM for 12 hours. Cells were then fixed with 70% EtOH and stained with Propidium Iodide (10 µg/mL, P4170, Sigma). Cell cycle profiles were obtained using FACS Calibur. The Flow Logic software was used for quantification of the % of S-phase cells. Three independent experiments were performed.

4.3.9 IMMUNOFLUORESCENCE ANALYSIS

ER-Src or PBabe cells were plated in poly-L-lysine-coated coverslips (Sigma P-8920) and fixed in 4% paraformaldehyde in phosphate buffer solution (PBS) at pH7, for 10 min. Cells were then permeabilized with TBS-T (TBS - 0.1 % Triton X-100) at RT and blocked in TBS-T supplemented with 10 % BSA, 1h at RT. Primary antibodies were incubated overnight at 4ºC in blocking solution.

Coverslips were then washed three times with TBS and incubated with secondary antibodies (in blocking solution) and with Rhodamine-conjugated Phalloidin (Sigma) at 1:200, for 1h at RT. After three washes in TBS, cells were stained with 2 μg/mL DAPI (D9542, Sigma) for 5 min in TBS, washed again with TBS and mounted in Vectashield. Primary antibodies used were:, anti-EVL (1:50, HPA018849, Sigma), anti-phospho-Myosin Light Chain 2 (Thr18/Ser19) (1:200, 3674, Cell Signaling) and anti-Paxillin (1:200, 610051, BD Pharmingen). Secondary antibodies were from Jackson Immunoresearch (1:200). Fluorescence images were obtained on a Leica SP5 confocal coupled to a Leica DMI6000, using the 63x 1.4 NA Oil immersion objective.

4.3.10 Quantification of stress fibres anisotropy

Anisotropy was measured using the Fibril Tool plugin for NIH Image J program, as described in (Boudaoud et al. 2014).

4.3.11 G/F actin assay

The G-actin/ F-actin In vivo Assay Kit (Cytoskeleton, Denver, CO, USA) was used to quantify the F- and G-actin pools, according to manufacturer instructions, except that cell lysates were centrifuged at 90,000*g*, for 90 min at room temperature. G and F-actin fraction were analysed by immunoblotting analysis and quantified using the Image Studio Lite program, as the ratio between F- and G-actin levels for each experimental condition.

4.3.12 Atomic Force Microscopy (AFM)

For the AFM indentation experiments a nanowizard I (JPK Instruments, Berlin) equipped with Cellhesion Module was used. Arrow-T1 cantilevers (Nanoworld, Neuchatel) with a polystyrene bead of 5μm diameter (microparticles GmbH, Berlin) were calibrated using the thermal noise method. To assess the stiffness of the cells, the cantilever was lowered with a speed of 5 μm/s onto the cells surface until a relative set point of 2.5 nN was reached. The resulting force

distance curves were analysed using the JPK image processing software (JPK instruments). Force distance data were corrected for the tip sample separation and fitted with a Hertz model fit for a spherical indenter. A Poisson ratio of 0.5 was assumed. Experiments were carried out at 37◦C in CO_2 independent medium (life technologies, Darmstadt) during a 1.5h time-window.

4.3.13 BREAST CARCINOMA SERIES

Our archive comprises formalin-fixed and paraffin-embedded breast tumor samples, including 150 invasive breast carcinomas and 91 in situ carcinomas, from which areas of in situ and invasive carcinoma can be found in the same block for 71 patients. All breast tumor cases were previously characterized regarding ER, progesterone receptor (PR), epidermal growth factor receptor (EGFR), epidermal growth factor receptor 2 (HER2), cytokeratin 5 (CK5), P-cadherin (P-cad), and the antigen Ki-67, in addition to patient's age and clinicopathological features, such as grade, tumor infiltrating lymphocytes (inflammation) and lymph nodes status. Breast tumor components were classified into luminal A and B, HER2 overexpressing, and basal-like carcinomas, according to the immunoprofile (Martins et al., 2011). 24 cases of normal breast samples derived from reduction mammoplasties or adjacent to tumor tissue were included in this study. All morphological and immunohistochemical assessments were conducted by a pathologist. The study was conducted under the national regulative law for the handling of biological specimens from tumor banks, the samples being exclusively available for research purposes in retrospective studies.

4.3.14 IMMUNOHISTOCHEMISTRY (IHC) AND QUANTIFICATION

IHC was performed using the Ultravision Detection System Anti-polyvalent HRP (Lab Vision Corporation) for EVL. Antigen unmasking was performed using a dilution of 1:100 from a commercially available solution of citrate buffer, pH = 6.0 (Vector Laboratories) at 98 °C for 30 minutes. After the antigen retrieval procedure, slides were washed in PBS and submitted to blockage

of the endogenous peroxidase activity by incubation in methanol (Sigma-Aldrich) containing 3% hydrogen peroxide (Panreac). Slides were further incubated with the primary antibody for EVL (1:100, HPA018849, Sigma). The IHC reaction was revealed with diaminobenzidine (DAB) chromogen (DakoCytomation). The positive control was a tonsil sample, which was included in each run, in order to guarantee the reliability of the assays. Non-neoplastic breast tissues, as well as normal breast surrounding the neoplastic cells, were considered internal controls. Normal breast tissues and each component of breast carcinoma were semi-quantitatively scored regarding the intensity (I) of stain as negative (0, no staining), weak (1, diffuse weak) or strong (3, defined as strong staining) and the extent (E) of stained cells was evaluated as a percentage. For each case, a staining score was obtained by multiplying E x I (range 0-300). Cases that presented the staining score = or < 100 were considered negative and the cases with score >100 were classified as positive. Statistical analyses were conducted using IBM SPSS Statistics (Version 22.0. Armonk, NY: IBM Corp). The associations between categorical variables were tested for statistical significance using the chi-square test. A two-tailed significance level of 5% was considered as statistically significant ($P < 0.05$).

4.4 RESULTS

4.4.1 SRC ACTIVATION INDUCES EVL UP-REGULATION AND LOCALIZATION AT THE STRESS FIBRES.

We have previously identified 6 ABPs that are deregulated in the same direction in tumours and inducible ER-src cell line, and affect the ability of Src to promote tissue overgrowth in *Drosophila* epithelia (Figure 2.5). Among those, the EVL orthologue in fly, Ena, which promotes the elongation of actin filaments bundles, accumulates upon Src activation (Figure 2.9). Strikingly, Ena act as an oncogene downstream of Src (Figure 2.6-Figure 2.9). To confirm that EVL plays a role in transformation, we started by assessing EVL's protein levels in different time-points of malignant transformation. Then, we evaluated localization of EVL in the first phase of malignant transformation, at 12h (Figure 4.1).

Consistent with a role of EVL in transformation, EVL expression levels increased in TAM-inducible ER-Src cells. Quantification of the ratio of EVL levels between TAM- and EtOH-treated ER-Src cells showed significant increased levels of EVL at 12 and 24 hours, compared to 4 hours after Src induction (Figure 4.1.A). However, this increase was only transient, as 36 hours after TAM treatment, EVL levels were not significantly higher than after 4 hours of treatment. The transient increase of EVL protein levels suggests an association with the acquisition of non-invasive features by Src-induced cells.

In the previous chapter, I have described the formation parallel actin stress fibres, inducing an increase in cell stiffness and the development of self-sufficiency in growth properties, in the first phase of Src-induced cellular transformation. One of the steps of the stress fibres formation is the barbed end elongation, which involves proteins like EVL (Mouneimne et al. 2012; Blanchoin et al. 2014). In accordance with its role on the stress fibres formation, 12 hours after TAM-treatment, EVL strongly accumulated at tips of actin fibres in ER-Src cells (Figure 4.1.B). Altogether, these results suggest that EVL is associated with

the acquisition of non-invasive features by Src-induced cells, through its action on the assembly of stress fibres upon Src activation.

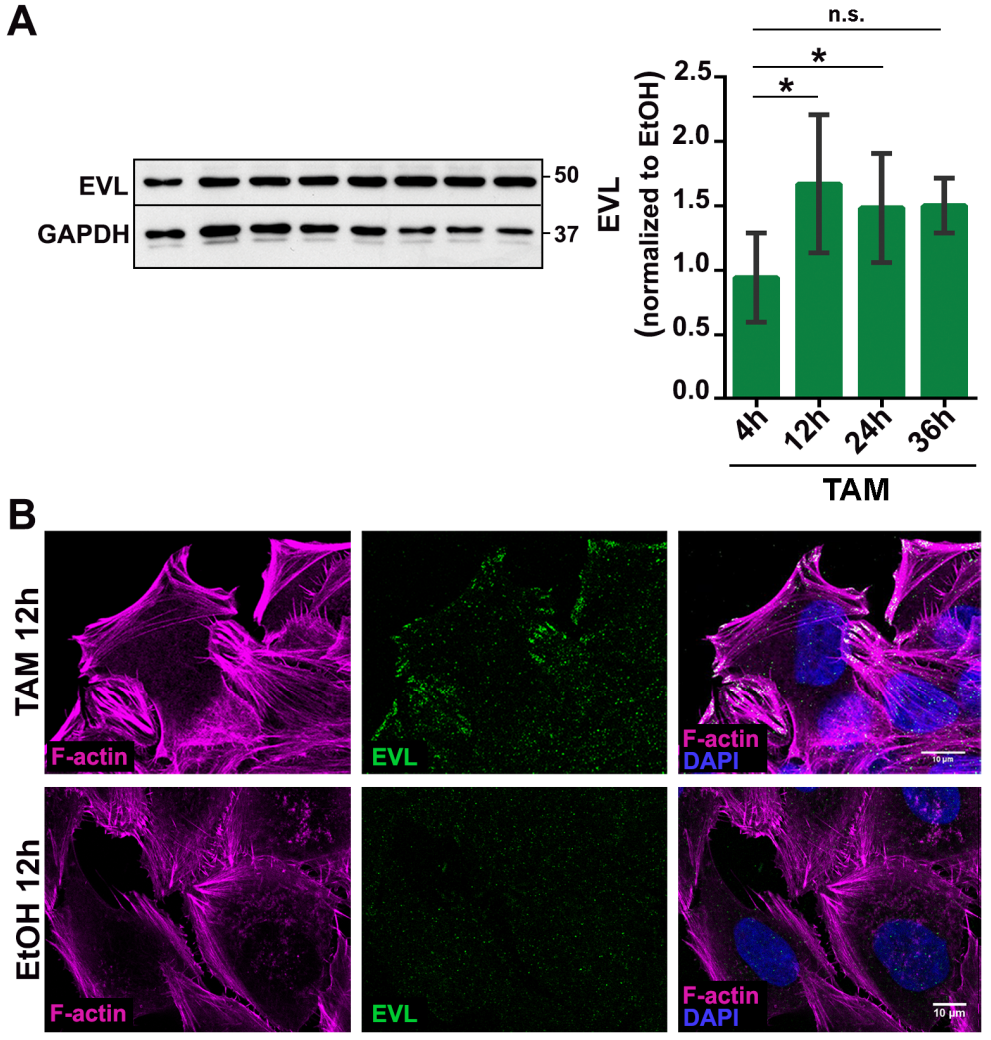

Figure 4.1: EVL accumulates in TAM-induced MCF10A-ER-Src cells and localizes at the tips of actin filaments. (A) (left panel) Western blot on protein extracts from ER-Src cells treated with EtOH for 4 (lane 1), 12 (lane 2), 24 (lane 3) or 36 (lane 4) hours or with TAM for 4 (lane 5), 12 (lane 6), 24 (lane 7) or 36 (lane 8) hours, blotted with anti-EVL (upper band) and anti-GAPDH (lower band) used as control. (right panel) Quantification of total EVL levels in ER-Src cells treated with TAM for 4 (lane 1), 12 (lane 2), 24 (lane 3) or 36 (lane 4) hours, normalized to EVL levels in EtOH-treated ER-Src cells for the same time points. Error bars indicate SD. ns indicates non-significant. * indicate P<0.05**. (B)** Standard confocal sections of ER-Src cells induced with TAM or EtOH for 12 hours and stained with Phalloidin (magenta) to mark F-actin, anti-EVL (green) and DAPI (blue) to mark nuclei. Scale bar represents 10 µm.

4.4.2 SRC-INDUCED TRANSFORMATION IS DEPENDENT ON EVL

To evaluate the importance of EVL in malignant transformation, I used short-hairpin RNA to knock down EVL in ER-Src cells. Knocking down EVL using two independent short-hairpin RNA (shEVL) significantly reduced EVL mRNA levels in TAM- or EtOH-treated ER-Src cells compared to cells transfected with a scrambled short-hairpin RNA (shScr) (Figure 4.2.A and C). The two sequences of shEVL achieved significant knockdown levels (50-70 %), leading to reduced levels of protein (Figure 4.2.E and F). As shown by Figure 4.2, low levels of EVL mRNA leads to decreased number of cells. The numbers of ER-Src cells treated with EtOH or TAM for 36 hours were significantly reduced when knocked down for EVL (EVL KD), compared to shScr-treated cells (Figure 4.2.B and D). Previously has been reported that EVL KD significantly weakened matrix adhesion, especially in cells strongly depleted of EVL (Mouneimne et al. 2012). Since Focal Adhesion maturation rely on stress fibres assembly (Oakes et al. 2012; Petit & Thiery 2000), these data suggest that EVL might promote cell growth through the regulation of actin stress fibres, which impacts on cells adhesion properties.

In order to validate the role of EVL in cell growth, cells were cultured in Matrigel, which mimics the *in vivo* context. Surprisingly, knocking down EVL had no visible effect on the size of EtOH-treated ER-Src acini cultured for 14 days, suggesting that EVL-depleted cells that had survived proliferate at a similar rate than control EtOH and shScrambled-treated ER-Src cells. In contrast, knocking down EVL delayed the growth of TAM-treated ER-Src acini. Even though, there was a decrease in acini size, TAM-treated ER-Src acini were spherical with smooth outer edges (Figure 4.3.A), suggesting that reduced levels of EVL fully suppressed their invasive spike-like phenotype.

To better characterize the importance of EVL in the tumourigenic process, we tested the effect of reducing EVL expression on the ability of TAM-treated ER-Src cells to form colonies in soft agar, a property that frequently correlates with tumorigenicity. As expected (Figure 3.9), TAM treatment

significantly enhanced the ability of ER-Src cells transfected with shScrambled to produce anchorage-independent colonies in the absence of EGF (Figure 4.3.B). Excitingly, knocking down EVL in these cells almost completely inhibited this ability to levels comparable to EtOH-treated cells. Altogether, our results show that EVL is required to promote Src-dependent cellular transformation.

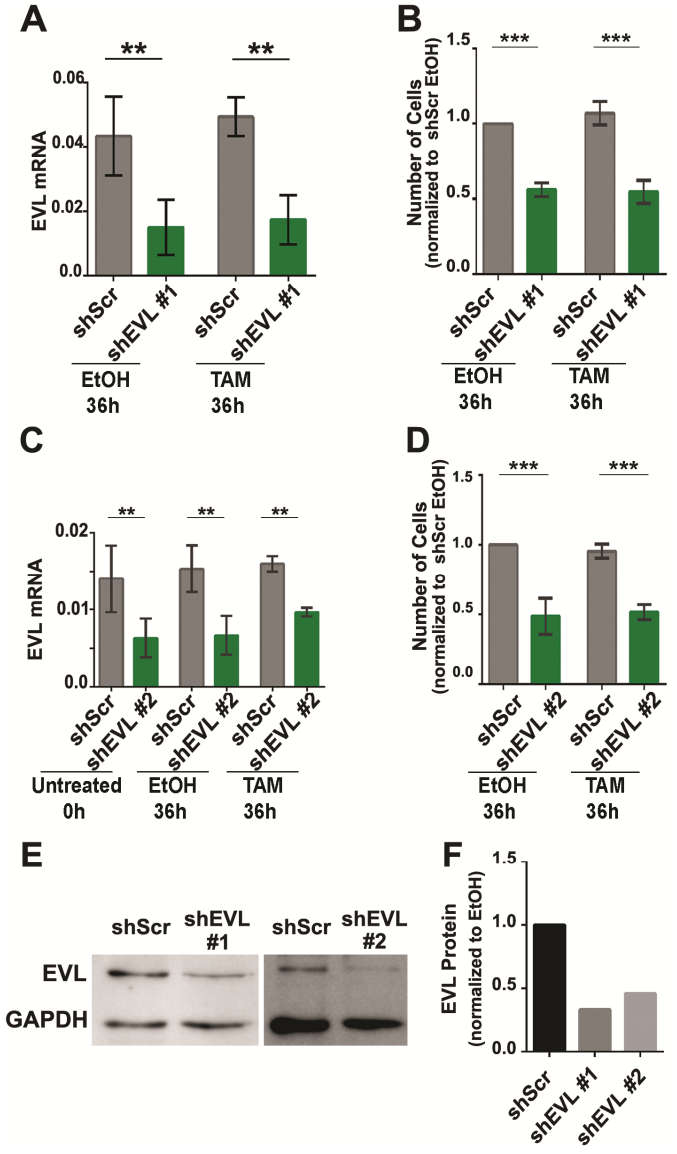

Figure 4.2: Knocking down EVL reduces EVL levels and affects cell growth. (A) and **(C)** Graphs of EVL mRNA levels measured by qRT-PCR in extracts from untreated ER-Src cells

expressing shScrambled (ShScr; lane 1) or shEVL (lane 2) or 36 hours EtOH-treated ER-Src cells expressing shScr (lane 3) or shEVL (lane 4) or 36 hours TAM-treated ER-Src cells expressing shScr (lane 5) or shEVL (lane 6). **(B)** and **(D)** Graph of the total number of ER-Src cells expressing shScr or shEVL, treated with EtOH (lane 1 and 2, respectively) or TAM (lane 3 and 4, respectively), for 36h, measured by an automated cell counter. Numbers of cells in each experimental condition are normalized to those of EtOH-treated ER-Src, expressing shScr. Graphs in (A) and (B), correspond to experiments using shEVL#1, while and **(C)** and **(D)** correspond to shEVL#2. Error bars indicate SD. ** indicate P<0,01Error bars indicate SD. **** indicate P<0.0001. **(E)** Western blot on protein extracts from ER-Src cells treated with shScr (lanes 1) or shEVL#1 (lane 2), or shEVL#2 (lane 4) blotted with (upper panel) anti-EVL (upper band) and anti-GAPDH (lower band). **(F)** Quantification of total EVL levels in 36 hours TAM-induced ER-Src cells treated with shScr or shEVL#1 or shEVL#2, normalized to EVL levels in EtOH-treated ER-Src cells for the same time point.

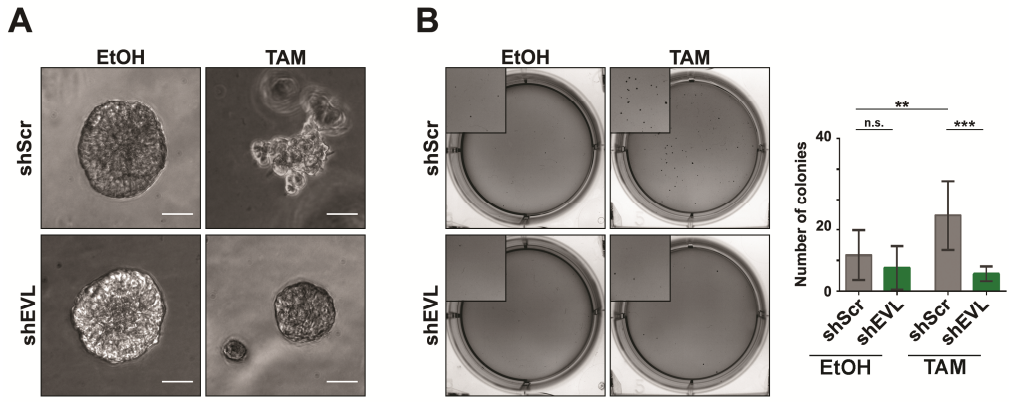

Figure 4.3: EVL is required for Src-induced cellular transformation. (A) 3D, 14 days cultures on Matrigel of shScr- or shEVL-treated ER-Src cells after induction with EtOH or TAM. Note that knocking down EVL restores the spherical acinar-like structures of TAM-induced ER-Src cells**. (B)** (left panels) representative phase-contrast images of colonies grown in soft agar in the absence of EGF of shScr- or shEVL-treated ER-Src cells after induction with EtOH or TAM. (right panel) Quantification of the number of colonies for the four experimental conditions. Error bars indicate SD. ns indicates non-significant, ** indicate P<0.01.

4.4.3 EVL IS NECESSARY TO ORIENTATE STRESS FIBRES FORMED TRANSIENTLY IN SRC-TRANSFORMED CELLS

Previously, I have shown that EVL is required for Src-induced cell transformation and its levels are increased in the first phase of tumourigenesis (Figure 4.3). To investigate if EVL sustains cellular transformation through the control of F-actin, we first analyzed the actin cytoskeleton features previously

associated with transformation, after 12 hours of EtOH or TAM treatment (Figure 3.12).

Since, Focal Adhesion (FA) are large adhesion contacts found at the ends of actin stress fibres, relying on these actin structures and on Src activity for proper maturation (Petit & Thiery 2000; Oakes et al. 2012; Frame et al. 2002); we started by analysing EVL KD effect on FA structures. It has been reported that EVL KD significantly weakens matrix adhesion, especially in cells strongly depleted of EVL (Mouneimne et al. 2012). Additionally, decreased adhesion in EVL KD conditions has been associated to increased migratory potential. Both SUM 159 cells and MCF10A show increased speed when knocked down EVL (Mouneimne et al. 2012). FAs were larger in TAM-induced ER-Src cells and interestingly, the EVL knock down did not affect their length (Figure 4.4.A), but a significant decrease was observed in the migration track length (Figure 4.4.B). These observations are in agreement with previous reports (Mouneimne et al. 2012). So, next we investigated the impact of EVL inhibition on the ability of Src-transformed cells to accumulate stress fibres. Although EVL has been shown to promote actin filament elongation (Chesarone & Goode 2009), quantification of the F and G actin pools in each experimental condition showed that knocking down EVL did not suppress the increased in F/G-actin ratio of TAM-treated ER-Src cells at 12 hours. In contrast, knocking down EVL in EtOH-treated ER-Src cells significantly triggered higher amounts of the F-actin pool (Figure 4.4.C). These results show that EVL does not trigger cellular transformation by promoting FA formation and stress fibres accumulation.

From the images acquired to characterize FA (Figure 4.4.A), we noticed that the Src-dependent stress fibres knocked down for EVL appeared to have lost their parallel organization. Accordingly, quantification of the stress fibres orientation revealed that shScrambled-treated ER-Src cells induced with TAM showed a more nematic arrangement of fibres at 12 hours when compared to EtOH treated cells (Figure 4.4.A). Knocking down EVL fully suppressed the increase in fibre anisotropy of TAM-induced ER-Src to levels comparable to those

of EtOH-treated ER-Src cells (Figure 4.4.D). All the observations made in this section strongly suggest that EVL acts as an oncogene downstream of Src, mainly through the promotion of an orientational order in the actin stress fibres.

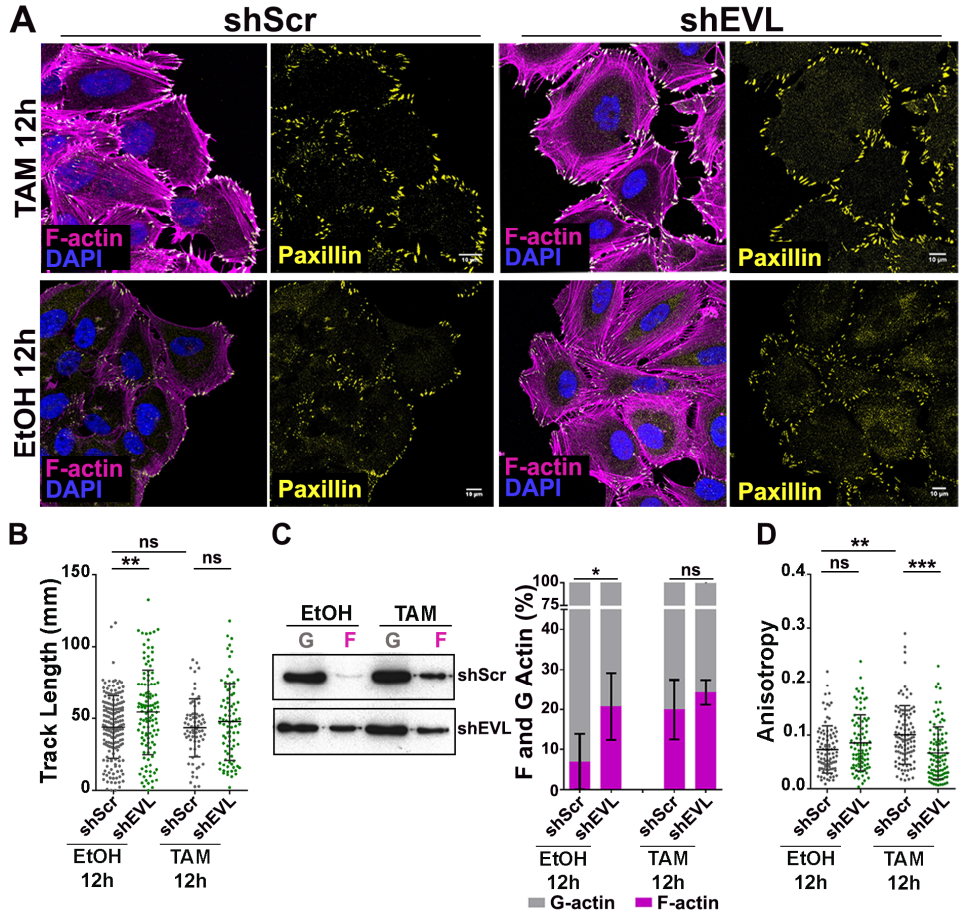

Figure 4.4: EVL controls Src-dependent stress fibres orientation. (A) Standard confocal sections of ER-Src treated with shambled or shEVL and induced with TAM or EtOH for 12 hours, stained with Phalloidin (magenta) to mark F-actin, anti-Paxillin (yellow) and DAPI (blue) to mark nuclei. Scale bars represent 10 μm. **(B)** Quantification of migration track length of ER-Src cells transfected with shScr or shEVL and treated with EtOH or TAM for 12h. At least 70 cells were tracked per condition. ns indicates non-significant. Error bars indicate SD. ** indicate P<0.01. **(C)** (left panel) Western blot on protein extracts from ER-Src cells treated with shScr (upper blot) or shEVL (lower blot) and induced with EtOH (lane 1 and 2) or TAM (lane 3 and 4) for 12h, blotted with anti-actin to visualize the G- (lane 1 and 3) and F-actin (lane 2 and 4) pools. (right panel) Quantification of the percentage of G- (grey) and F-actin (magenta) ratio between shScr or shEVL-treated ER-Src cells induced with EtOH- or TAM-for 12 hours. Error bars indicate SD. *** indicate P<0.001**. (D)** Quantification of the anisotropy of stress fibres in shScr or shEVL-treated ER-Src cells induced with EtOH- or TAM-for 12 hours. Error bars indicate SD. ns indicates non-significant. **** indicates P<0.0001.

4.4.4 EVL INHIBITS THE SRC-DEPENDENT INCREASE IN CELL STIFFNESS.

We next investigated the mechanism by which the EVL-dependent polarized stress fibres promote cellular transformation. Higher absolute amount of F-actin or stress fibres formation have been associated with increased cell stiffness, whereas a reduction in F-actin or stress fibre disassembly correlates with lower cell stiffness (Doornaert 2003; Bhadriraju & Hansen 2002). Atomic Force Microscopy (AFM) based indentation measurements revealed that ER-Src cells were significantly stiffer 12 hours after TAM treatment compared to EtOH-treated ER-Src cells, in 2D and 3D culture conditions (Figure 3.15). Excitingly, quantification of the elasticity of ER-Src cells knocked down for EVL by AFM showed similar levels of elasticity between TAM and EtOH treated cells (Figure 4.5.B). TAM-treated Er-Src cells expressing shScr sequence presented an increase in stiffness similar as previously observed (Figure 3.15 and Figure 4.5.B). As described in the previous chapter, the increase in cell stiffness was associated with higher Myosin II activity, as phospho-Myosin light chain (pMLC) was recruited to the Src-dependent polarized stress fibres 12 hours after TAM treatment (Figure 3.13 and Figure 4.5.A). Consistent with these observations, pMLC decreased its accumulation on the Src-dependent stress fibres that has lost their polarized organization (Figure 4.5). In conclusion, Src-dependent changes in cell mechanical properties require the EVL-mediated orientation of stress fibres and their crosslinking and contractility properties, mediated by pMLC.

To evaluate the impact of reduced levels of EVL in the first phase of malignant transformation, I assess cell growth, using as read-out the DNA content of cells in shScr and shEVL conditions, with EtOH or TAM treatment. Knocking down EVL reduced the growth ER-Src cells treated with TAM for 12 hours, but had no significant effect on EtOH-treated ER-Src cells (Figure 4.5.C). Taken together, we conclude that during the first 12 hours of cellular transformation, EVL polarizes the Src-dependent stress fibres, increasing cells stiffness and promoting Src-mediated cell growth and transformation.

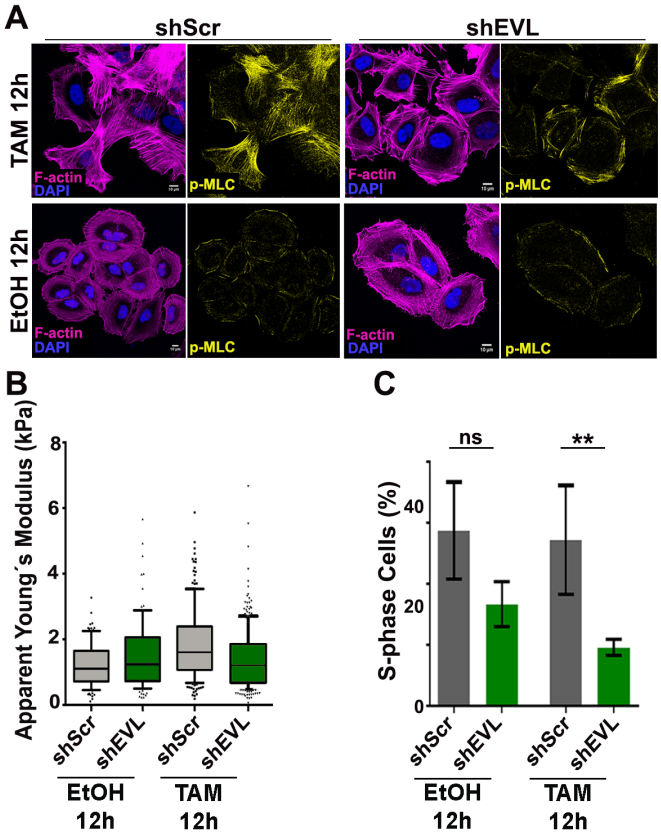

Figure 4.5: Knocking down of EVL leads to decreased cell stiffness and decreased cell growth. (A) Standard confocal sections of scrambled or shEVL treated ER-Src cells, induced with EtOH or TAM for 12 hours, stained with Phalloidin (magenta) to mark F-actin, anti-pMLC (yellow) and DAPI (blue) to mark nuclei. Scale bars correspond to 10 μm. **(B)** Apparent Young' moduli of ER-Src of scrambled or shEVL treated ER-Src cells, induced with EtOH or TAM for 12 hours. **(C)** Quantification of the number of cells in S-phase in shScr or shEVL treated ER-Src cells induced with EtOH or TAM for 12 hours. Error bars indicate SD. ns indicates non-significant. ** indicates P<0.01.

4.4.5 EVL ACCUMULATES IN PRE-MALIGNANT OESTROGEN RECEPTOR POSITIVE (ER+) DCIS

To evaluate EVL expression in breast cancer progression we performed immunohistochemistry in a series of human breast tissues comprising normal breast, DCIS and IDCs. Consistent with a role of EVL on F-actin regulation, EVL mainly localized to the cytoplasm in all samples analysed and could also be

observed at the cell membrane (Figure 4.6.A). In normal breast, EVL expression was low with only 4.2% (1/24 cases) of cases scored positive and was mainly found in luminal cells. Strikingly, EVL levels were significantly higher in DCIS and IDC lesions compared to normal breast tissues, with 40.7% (61/150) and 56.0% (61/150) classified as positive in DCIS and IDC respectively. Interestingly, IDC presented slightly reduced EVL expression compared to DCIS (Figure 4.6.A). Indeed, when considering cases where both *in situ* and invasive fronts were present simultaneously, we observed a significant reduction in EVL expression from the *in situ* to the invasive counterpart in 54.9% (39/71) of cases. Only 11.3% (8/71) of cases showed higher EVL levels in the invasive compartments compared and 33.8% (24/71) of cases showed no change in EVL expression between both components (Figure 4.6.B).

We then investigated in this series of human breast tumours, if the presence of high EVL levels correlates with specific clinicopathological features. Consistent with our microarray analysis of breast tumour samples, in which EVL was found up-regulated in ER+ breast lesions but not ER- (Figure 2.5 and Supplementary Fig. S1), high EVL expression was positively associated with the expression of ER, in both DCIS and IDC (P=0.008 and P=0.001, respectively). Higher EVL levels was also significantly associated with the luminal A molecular subtype (P=0.002 and P=0.008, respectively), the absence of HER2 expression, the negative expression of the two basal markers CK5 and P-cadherin in DCIS lesions, and with low grade DCIS and grade I IDC (Table 4. and Table 4.). No association was found with lymph node status or patient's age (data not shown). Taken together, these observations are consistent with a requirement of high EVL levels for the development of ER+ pre-malignant breast lesions.

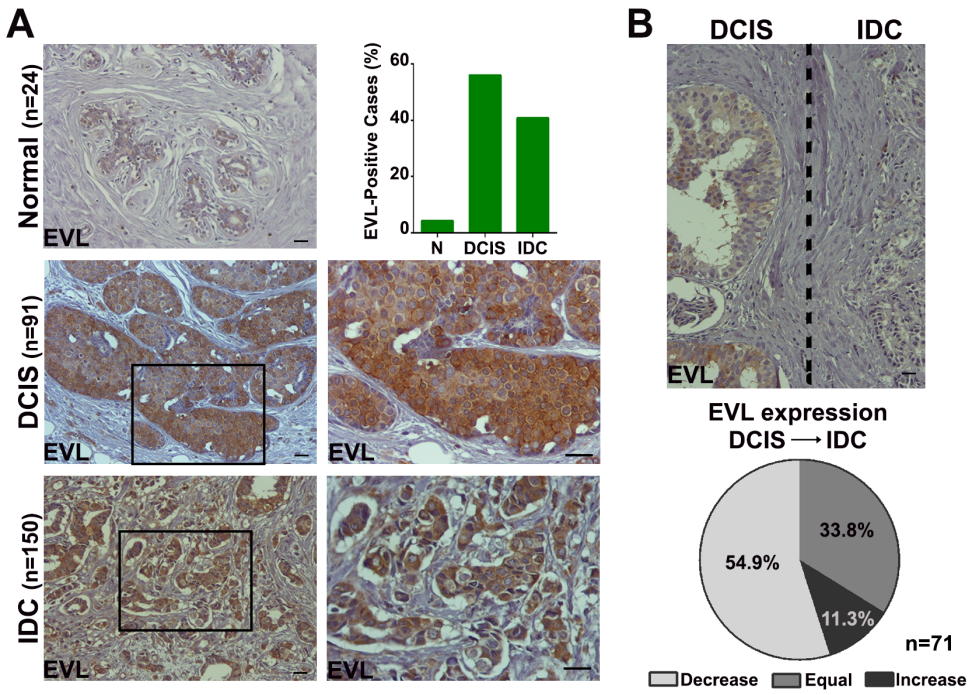

Figure 4.6: EVL is highly expressed in DCIS. (A) Representative images of EVL staining by IHC in normal human breast tissue (Normal), DCIS and IDC tissue and quantification of EVL protein expression at each stage (n is the number of patients per group). Values are from visual scores ± SEM. Scale bars represent 100 μm. Images on the right are magnifications of the boxed areas. EVL is highly expressed in human breast carcinomas but show lower accumulation in IDC than in DCIS**. (B)** Representative image of EVL staining by IHC from the same breast carcinoma sample containing both an in situ and invasive components and quantification (71 cases). DCIS samples show a significant increase in EVL levels compared to the IDC counterpart. Scale bar represents 100 μm.

Table 4.A: EVL expression is associated with Luminal A molecular subtype in DCIS. Association of EVL expression with clinicopathological features, including ER status, basal markers (CK5 and P-cad) expression, and breast carcinomas molecular subtypes.

		EVL Classification - DCIS		
		Count (%)		p-Value
		Neg	Pos	
ER	Neg	15 (38.5)	7 (14.0)	0.008
	Pos	24 (61.5)	43 (86.0)	
	Total	39 (100)	50 (100)	
HER2	Neg	29 (74.4)	48 (96.0)	0.003
	Pos	10 (25.6)	2 (4.0)	
	Total	39 (100)	50 (100)	
CK5	Neg	34 (87.2)	49 (98.0)	0.043
	Pos	5 (12.8)	1 (2.0)	
	Total	39 (100)	50 (100)	
P-Cad	Neg	27 (69.2)	49 (98.1)	0.001
	Pos	12 (30.8)	1 (2.0)	
	Total	39 (100)	50 (100)	
Subtype	Luminal A	21 (53.8)	46 (92.0)	0.002
	Luminal B	5 (12.8)	1 (2.0)	
	HER-2 OE	5 (12.8)	1 (2.0)	
	Basal	6 (15.4)	1 (2.0)	
	Ind.	2 (5.1)	1 (2.0)	
	Total	39 (100)	50 (100)	
Grade	Low	10 (25.6)	20 (40.0)	0.016
	Inter	11 (28.2)	21 (42.0)	
	High	18 (46.2)	9 (18.0)	
	Total	39 (100)	50 (100)	
Inflammation	0	1 (5.3)	7 (30.4)	0.091
	1	13 (68.4)	13 (56.5)	
	2	5 (26.3)	2 (8.7)	
	3	0 (0.0)	0 (0.0)	
	Total	19 (100)	23 (100)	

Table 4.B: EVL expression is associated with Luminal A molecular subtype in IDC. Association of EVL expression with clinicopathological features, including ER status, basal markers (CK5 and P-cad) expression, and breast carcinomas molecular subtypes.

		EVL Classification - IDC		
		Count (%)		p-Value
		Neg	Pos	
ER	Neg	29 (36.3)	6 (10.9)	0.037
	Pos	51 (63.8)	49 (89.1)	
	Total	80 (100)	55 (100)	
HER2	Neg	63 (78.8)	46 (83.6)	0.001
	Pos	17 (21.3)	9 (16.4)	
	Total	80 (100)	55 (100)	
CK5	Neg	75 (93.8)	54 (98.2)	0.479
	Pos	5 (6.3)	1 (1.8)	
	Total	80 (100)	55 (100)	
P-Cad	Neg	55 (68.8)	52 (94.5)	0.0002
	Pos	25 (31.3)	3 (5.5)	
	Total	80 (100)	55 (100)	
Subtype	Luminal A	50 (62.5)	46 (83.6)	0.008
	Luminal B	4 (5.0)	5 (9.1)	
	HER-2 OE	13 (16.3)	4 (7.3)	
	Basal	10 (12.5)	0 (0.0)	
	Ind.	3 (3.8)	0 (0.0)	
	Total	80 (100)	55 (100)	
Grade	Low	28 (35.0)	27 (49.1)	0.020
	Inter	21 (26.3)	19 (34.5)	
	High	31 (38.8)	9 (16.4)	
	Total	80 (100)	55 (100)	
Inflammation	0	10 (22.7)	5 (15.6)	0.037
	1	22 (50.0)	25 (78.1)	
	2	11 (25.0)	1 (3.1)	
	3	1 (2.3)	1 (3.1)	
	Total	44 (100)	32 (100)	

4.5 DISCUSSION

In this chapter, I used one of the ABPs identified as being differentially expressed in ER+ DCIS and in Src-dependent transformation (Figure 2.5) to understand impact of the transient stress fibres in the first phase of malignant transformation (Figure 3.12).

EVL acts as an oncogene downstream of Src.

From the set of 6 ABPs defined before (Figure 2.5) I have decided to study specifically EVL based on our previous *in vivo* and *in vitro* evidences. Ena, the EVL orthologue in *Drosophila,* acts as an oncogene downstream of Src (Figure 2.7 and Figure 2.8). In ER-Src cells, I have identified an accumulation of transient stress fibres in the first phase of transformation. Additionally, EVL is the only up-regulated ABP, from the 6 identified, that belongs to a family of proteins that have been associated with long, straight, rapidly elongating, bundled actin filaments, such as stress fibres (Winkelman et al. 2014).

As in fly, EVL KD completely blocks the Src-induced malignant transformation (Figure 4.3). In matrigel, as in soft agar, EVL KD cells treated with TAM presented a phenotype similar to EtOH-treated ones. In 3D culture, EVL KD cells treated with TAM formed smooth edges acini, while the ones expressing scrambled sequences and treated with TAM presented a typical invasive phenotype. In the anchorage-independent assay, also known as soft agar assay, only shScr cells treated with TAM were able to survive and form colonies. Once again, EVL KD treated with TAM behaved as non-transformed cells. With these results we were able to confirm in the human context, that EVL is required for Src-dependent full transformation.

Besides, the phenotypes associated to fully transformed cells, EVL KD also showed impaired proliferation ability (Figure 4.2). This observation might be related with the altered adhesion properties described by Mouneimne et al. 2012. Furthermore, the weaken adhesion observed had such an impact on tumor initiation and growth that made the authors design an inducible EVL KD system

to enable the study of invasive phenotypes (Mouneimne et al. 2012). Taking all this arguments in consideration, we confirmed EVL as a good candidate to study the role of the Src-dependent actin structures in cell transformation, particularly in early stages.

EVL sustains Src-dependent tumour growth through the promotion of stress fibres orientation.

Consistent with the previous observations in fly (Figure 2.9) in the first 12 hours of ER-Src cells transformation, increased levels of active Src, leads to is an increase EVL's protein levels. In agreement with the function attributed to members of the Ena/VASP family (Winkelman et al. 2014; Barzik et al. 2005), 12 hours after treatment, EVL is localized at the tips of stress fibres that accumulate transiently upon Src activation (Figure 4.1). As mentioned in previous chapter, stress fibres are key components in assembly and maturation of Focal Adhesions (FAs) (Petit & Thiery 2000; Oakes et al. 2012). According to Mouneimne et al., EVL KD supresses stress fibres formation and is correlated with weakened adhesion properties (Mouneimne et al. 2012). Therefore, I would expect a significant change in FAs length in EVL KD cells. Intriguingly, EVL KD and Scrambled cells present FAs with similar lengths, upon TAM treatment (Figure 4.4.A). To further understand this observation I searched for possible changes F and G actin pools in the different conditions. EVL has been proposed as a regulator the assembly of F-actin filaments by preventing the activity of capping proteins, favouring actin filaments elongation (Chesarone & Goode 2009). Surprisingly, knocking down EVL increases the F-actin pool in non-transformed ER-Src cells and does not block its increase in transforming conditions (Figure 4.4.C). So far, these results suggest that EVL KD does not block stress fibres formation in Src-induced transformation and in addition induces the formation of other types of F-actin structures that are not associated with FAs. Ena/VASP proteins not only possess anti-capping activity but also inhibits actin filament branching by the Arp2/3 complex and bundle actin filaments (Skoble et al. 2001;

Winkelman et al. 2014). Therefore, observed increase in the F-actin pool of untransformed EVL KD might be explained by the accumulation of Arp2/3-dependent actin-filament branches due to decreased levels of EVL. In contrast, in TAM-induced ER-Src cells knocked down for EVL, Arp2/3 activity could be antagonized by the nucleating factor activated by Src that promotes stress fibres formation.

Knocking down EVL induces a very striking and interesting feature of the stress fibres transiently formed upon Src activation. In this cellular context, the actin filaments connected to the FAs completely lose their orientational order (Figure 4.4.C). Our results suggest that the main role of EVL in Src-dependent transformation is not the filaments elongation, but the bundling or clustering of stress fibres at their barbed ends.

EVL promotes cell stiffening and proliferation in Src-dependent transformation.

In the previous chapter, I have presented the deregulation of the acto-myosin system as a feature of the first phase of transformation. In support of this statement, I have shown that ER-Src cells treated with TAM, after 12 hours, present an increase in their stiffness correlated with stress fibres highly decorated with pMLC (Figure 3.13). As reported and reviewed before (Blanchoin et al. 2014), the presence of cross-linkers bridging actin filaments together, increases cells elastic modulus. In agreement, when EVL KD cells treated with TAM show a decrease in the pMLC localization at the stress fibres there is also a decrease in cell stiffness (Figure 4.5). This was only observable in EVL KD cells treated with TAM, the same condition in which it was observable the loss of stress fibres polarization. These observations argue that increases in F-actin content *per se* or the stress fibre formation are not sufficient to predict an increase in cell stiffness. Instead, our results are consistent with previous reports suggesting that EVL-mediated contractibility is also dependent of the spatial organization of actin fibres (Mouneimne et al. 2012; Jalilian et al. 2015; Roca-Cusachs et al. 2008; Yim et

al. 2010). Consequently, EVL-dependent anisotropic stress fibres organization favours contractibility, as opposed to an isotropic organization.

Polarization of actin fibres and cells stiffening by EVL play a role in cellular transformation (Figure 4.5.C) via acto-myosin contractibility. Particularly, EVL KD cells under transforming conditions show impairment in proliferation (Figure 4.5.C). Altogether, the results in ER-Src cell line show that Src requires EVL in the early events of tumourigenesis. In the first phase of Src-dependent transformation, EVL is upregulated and mobilized to actin filaments barbed ends. Once in the tips of actin fibres, EVL promotes polarization of the filaments increasing their cross-linking and contractility. As a result, in this first phase of transformation cells exhibit increased stiffness and proliferative advantage when compared to their non-induced counterparts (Figure 4.7).

EVL, a marker of pre-malignant Luminal A breast lesions

Although our results from the in silico and *in vitro* system were coherent, I decided to validate my results, assessing EVL protein levels in human tissue from patients. Consistent with a role of the EVL-dependent polarized stress fibres in tumour growth, we found that EVL protein levels were specifically elevated in ER+ DCIS, associated with the Luminal A molecular subtypes (Figure 4.6). However, IDC invasive fronts exhibit significant lower EVL levels, compared to the in situ counterpart (Figure 4.6). Accordingly, highly invasive breast tumours and poor survival outcomes have been previously reported associated with reduced EVL transcript and proteins (Mouneimne et al. 2012; Hu et al. 2008). Consistent with previous observations (Mouneimne et al. 2012), we also found that EVL limits the migratory ability of MCF10A cells (Figure 4.4.B) , in line with the results regarding the invasive properties of the SUM159 beast tumour cell line (Mouneimne et al. 2012).

4.6 CONCLUSIONS

In conclusion, EVL-dependent stress fibres would play a dual role in tumour progression. In the first phase, it would be required their assembly and accumulation to promote Src-mediated transformation. In the second phase, the stiff F-actin structures are no longer compatible with the migratory and invasive phenotypes triggered by high levels of Src activity. Therefore, its necessary that EVL levels decrease, stress fibres get dismantled and cells become softer to achieve the higher invasive potential. Thus, in the multistep development of breast tumours EVL-dependent polarized stress fibres might be tumour promoters, while in late stages they might behave as suppressors of cancer cell migration and invasion (Figure 4.7).

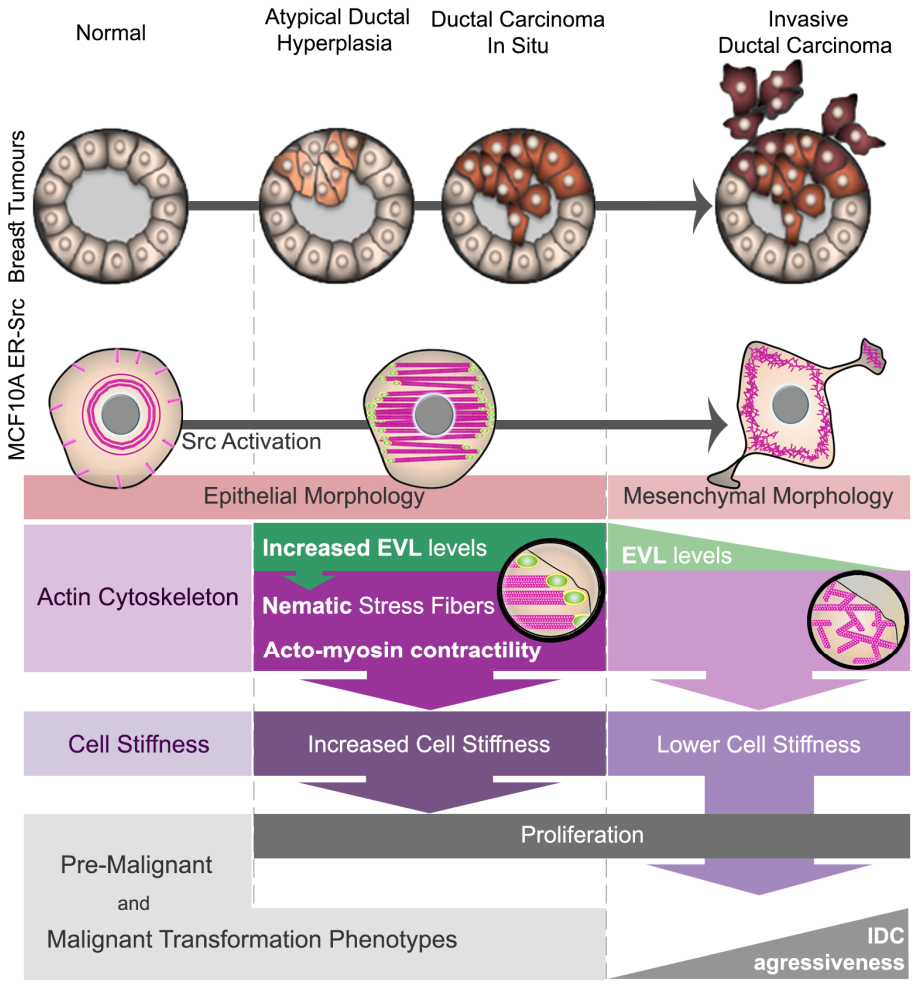

Figure 4.7: Model by which EVL promotes cell stiffening and proliferation in early stages of breast cancer progression. EVL is upregulated and mobilized to actin filaments barbed ends to promote polarization of the filaments. The high orientation of the stress fibres leads to increased cell stiffness and proliferative advantage when compared to normal cells. In invasive stages, high levels of EVL are correlated with decreased aggressiveness

4.7 ACKNOWLEDGEMENTS

I would like to acknowledge the people who have contributed to the work described in this chapter, including Anna Taubenberger for her measurements in EVL KD cells and Nuno Pimpão Martins for the help in live-imaging and quantification of cells migration. I would also like to thank André Vieira and António Polónia for the analysis of EVL levels in human tumour samples.

Chapter 5

General Discussion

"Abram-me todas as portas!
Por força que hei-de passar!
Minha senha? Walt Whitman!
Mas não dou senha nenhuma...
Passo sem explicações...
Se for preciso meto dentro as portas...
Sim — eu franzino e civilizado, meto dentro as portas,
Porque neste momento não sou franzino nem civilizado,
Sou EU, um universo pensante de carne e osso, querendo passar,
E que há-de passar por força, porque quando quero passar sou Deus!"

Álvaro de Campos, Livro de Versos.

In this thesis, I investigated if F-actin plays a role downstream of Src activation in the earlier events of tumour progression. I first identified ABPs misregulated in both pre-malignant breast lesions and TAM-induced ER-Src cells, and involved in Src-induced tissue overgrowth in Drosophila melanogaster (Chapter 2). Then, I showed that earlier during cellular transformation, low Src induction induces the transient polymerization of polarized stress fibres that correlate with an increase in cell stiffness and the acquisition of self-sufficiency in growth properties, prior cells acquire malignant phenotypes (Chapter 3). Finally, I tested the role of EVL for transformation of the TAM-induced ER-Src cell line. I found that Src induces the upregulation of EVL and its localization to the tips of the transient Src-dependent actin stress fibres. Polarization of these fibres by EVL is required to promote cell stiffening, cell growth and the progression toward malignancy. Later during transformation, higher Src activity, in addition to a reduction in EVL levels may disassemble stress fibres to facilitate cell invasion (Chapter 4).

5.1 SRC PATHWAY TRIGGERS FULL TRANSFORMATION OF HUMAN BREAST CELLS

Higher levels of Src expression are associated with breast cancer aggressiveness

Several players are known to contribute to the malignant transformation of cells. In particular, over-expression and/or over-activation of Src-family kinases have been described in several human solid cancers (Irby & Yeatman 2000). (Zhang et al. 2009; Bild et al. 2006). I found that high grade malignant tumours, known to be associated with poorer prognosis (Elston & Ellis 1991), over-express Src (Figure 2.2). In agreement with my observations, previous studies have observed increased Src expression levels in malignant breast tumours (Elsberger et al. 2010). Moreover, two distinct studies have shown that

ER+ breast tumours presenting a gene expression signature associated with an increase in Src activity also exhibit worse clinical outcomes. Although, in my pre-malignant breast tumour samples, Src expression is not significant affected compared to normal breast tissues, its activity levels could be increased. Consistent with this possibility, I found that some ABPs deregulated by Src activation in TAM-induced ER-Src cells are also deregulated in these pre-malignant breast tumour samples (Figure 2.5).

Altogether, these observations suggest that while deregulation of Src activity could be a feature of pre-malignant tumours, an increase in Src expression levels could characterize the later stages of breast cancer progression.

The acquisition of distinct transformation features depends on the stepwise increase in Src activity.

So far, it has been established that Src controls different aspects of cancer progression. It is involved in cellular proliferation and EMT, and also acts as a trigger of cancer cell migration and invasion (Guarino 2010). However, the mechanisms by which Src impacts on these distinct cancer-associated features remain unclear. In this study, my cell model with inducible Src activation gave us the opportunity to investigate these mechanisms in the context of breast cancer progression. My work shows that low Src activity that occurs during the first phase of Src-induced cellular transformation triggers the acquisition of self-sufficiency in growth properties (Figure 3.11). Further Src activation induces the second phase in malignant transformation. Higher levels of high Src activation induces the development of malignant features already previously associated with Src pathway, such as the promotion of scattering of cells (Figure 3.4(Boyer et al. 1997; Avizienyte & Frame 2005) and/or cells with CSC identity (Figure 3.7and (Iliopoulos et al. 2011). A similar level-dependence of Src function has been described in other types of epithelial cancers, like colorectal cancer progression (Yeatman 2004; Mark S. Talamonti et al. 1993; Cartwright et al. 1994; Jones et al. 2002). Thus, the effects of Src activation on distinct cancer associated

features might be dependent on Src activity levels, with low or high levels associated with proliferation or invasiveness, respectively.

5.2 SRC HAS DISTINCT EFFECTS ON F-ACTIN-MEDIATED CELL STIFFENING TO PROMOTE PROLIFERATION AND INVASIVENESS

Src assembles distinct F-actin networks to promote proliferation or invasiveness

In this study I present strong evidences consistent with a model by which the control of F-actin by Src activation not only facilitate malignancy-associated properties (Zhang & Yu 2012), but is also required for Src-induced tumour growth earlier during tumour progression. To perform these different functions, Src appears to build distinct F-actin networks depending on the cellular context. In malignant lesions, Src-mediated cell invasion is linked to its ability to disassemble stress fibres, while to promote the formation of actin-rich structures called invadopodia, required for invasion (Eckert & Yang 2011; Murphy & Courtneidge 2011). In contrast, I show that in pre-malignant lesions, Src induction induces the transient accumulation of stress fibres (Figure 3.12). These observations are in agreement with a previous report from late 1970s, in which the activation of Src in chick embryo fibroblasts also triggers the assembly of actin-containing microfilament bundles in the first 24 hours of activation (Wang & Goldberg 1976). I show that stress fibre assembly correlates with the acquisition of self-sufficiency in growth (Figure 3.11). Because I demonstrate that EVL is required to polarize these actin fibres and to promote cell growth (Figure 4.4), accumulation of these longitudinal stress fibres likely mediates Src-induced proliferation. Although the nucleating-promoting factor, which induces stress fibre formation downstream of Src is yet to be identified, I identified a battery of other ABPs that might be involved in the regulation of these actin structures and in Src-induced tissue growth. For instance, the down-regulation of DST, FHOD3 and TPM2 (Figure 2.5

and Hirsch et al. 2010) could be required for tumour growth, as all are down-regulated in pre-malignant lesions (Figure 2.5) and restrict the pro-growth function of Src in vivo (Figure 2.8). In agreement with this hypothesis, a large number of cancers, including those of the breast down-regulate TPM2 (Stehn et al. 2006). Moreover, TPM1 and 2 have been proposed to act as tumour suppressors, as restoration their expression in Ras-transformed cells suppresses the transformed Figure 4.4phenotype (Prasad et al. 1993; Shah et al. 1998). DST was also found down-regulated in transformed fibroblasts expressing the RasV12 oncogene, in melanoma, and breast cancer-stem cells (Hirsch et al., 2009; Shimbo et al., 2010). Surprisingly, the two Arp2/3 components ACTR3 and ARPC5L are up-regulated in TAM-induced ER-Src cells and in DCIS (Figure 2.5 and Hirsch et al. 2010), but restrict Src-induced overgrowth of Drosophila epithelia (Figure 2.8). Consistent with a tumour suppressor function of Arp2/3, overexpression of the Arp2/3 regulator N-WASP decreases growth of the breast cancer cell line MDAMB231 in animals (Martin et al. 2008). However, N-WASP and Arp2/3 have also been implicated in cancer cell mobility and invasiveness (Martin et al. 2008; Gligorijevic et al. 2012; Kim et al. 2009; Kinoshita et al. 2012; Wang et al. 2010). Thus, Arp2/3 may have opposite functions in tumour growth and metastasis respectively. Whether Arp2/3-dependent branched actin filaments, stabilized by TPM2 and DST, counteract the formation of the Src-mediated stress fibres to limit cellular transformation remains to be determined.

Src promotes proliferation or invasiveness via changes in cell stiffening

My work reveals that during transformation, Src has opposite effects on stress fibre assembly and cell stiffening accompanying the acquisition of proliferative or invasiveness abilities, respectively (Figure 3.16). Low Src activity induced during the first phase of Src-induced cellular transformation triggers the transient polymerization of parallel actin stress fibres, which may induce an increase in cell stiffness. Accordingly, these cells assemble larger FAs (Gupta et al. 2015 and Figure 4.4). Moreover, the parallel actin fibres are highly enriched in

Myosin II activity (Figure 3.13 and Figure 4.5). Furthermore, Src is known to activate the Rho kinase (ROCK), which promotes acto-myosin contractility via Myosin II phosphorylation (Eckert & Yang 2011).

Cell stiffening, in turn, could sustain self-sufficiency in growth property (Figure 3.16). In agreement with a role of cell stiffening in providing a proliferative advantage, cell stiffening has been shown to enhance the activity of mitogen factors, such as YAP/TAZ and ERK (Aragona et al. 2013; Paszek et al. 2005; Aplin et al. 2001; Aplin & Juliano 2001).Src is also activated in response to F-actin-mediated mechanical stretches in mammals (Sniadecki 2010). Moreover, Src translocation and activation to focal adhesion has been shown to be dependent on acto-myosin stress fibres (Fincham et al. 1996; Fincham et al. 2000). Thus, Src-dependent cell stiffening may also act as part of a positive feedback mechanism to further enhance Src activation. Accordingly, I found that activation of ER-Src cells induces the activation of endogenous Src (Figure 3.2).

In agreement with previously observations showing that Src activation promotes stress fibre disassembly (Frame 2004), which allows for cell migration and invasion (Gross 2013; Machesky 2008; Barry et al. 2010; Vignjevic & Montagnac 2008; Guck et al. 2005; Remmerbach et al. 2009), TAM-induced ER-Src cells with higher Src activity disassemble the longitudinal stress fibres (Figure 3.12), show a reduction in cellular stiffness (Figure 3.15) and acquire migrating ability (Movie 4). The apparently opposite effects of Src on stress fibres and cell stiffening correlates with a stepwise increase in Src activity levels and the successive acquisition of pre-malignant and malignant features in ER-Src cells, as well as in some cancers, such as those of the colon (Cartwright et al. 1994; M S Talamonti et al. 1993; Jones et al. 2002).

Thus, while low Src activity would promote stress fibre-mediated cell stiffening accompanying tumour growth, higher levels would have the opposite effect, allowing for cell invasion.

5.3 EVL ORGANIZES STRESS FIBRES TO CONTROL CELL STIFFNESS AND TUMOUR GROWTH.

EVL regulates the orientation of stress fibres to promote cell stiffening

I have identified EVL as a key F-actin regulator required downstream of Src. Ena/VASP proteins have been shown to promote actin filament elongation through an anti-capping activity (Bear et al. 2002). However, my observations are consistent with a model by which EVL is recruited at the tips of the Src-dependent stress fibres (Figure 4.1) to polarize them (Figure 4.4). In turn, polarization of these fibres increases cell stiffening (Figure 4.5). Thus, like Drosophila Ena, upon Src activation, EVL may promote the clustering of actin filaments at their polymerizing ends to favour the bundling along filament length (Winkelman et al. 2014; Lanier et al. 1999)(Bear & Gertler 2009). Surprisingly, I also observed that knocking down EVL increases the F-actin pool in non-transformed ER-Src cells (Figure 4.4). As, Ena/VASP proteins also appear to display an anti-branching activity by inhibiting Arp2/3 activity (Bear & Gertler 2009).(Bear et al. 2002), the absence of EVL in un-transformed ER-Src cells may de-repress Arp2/3 activity, allowing for F-actin accumulation. Thus EVL seems to have distinct effects on F-actin depending on the cellular context.

Interestingly, increase in cell stiffness does not dependent exclusively on stress fibre formation or increase in F-actin content, since knocking down EVL prevents the increase in cell stiffness of TAM-induced ER-Src cells (Figure 4.5) but has no effect on F-actin accumulation (Figure 4.4). Instead, as previously reported (Jalilian et al. 2015; Roca-Cusachs et al. 2008; Yim et al. 2010), my study shows that cellular contractibility is also dependent of the spatial organization of actin fibres. So, EVL-dependent anisotropic stress fibres organization would promote contractibility, as opposed to an isotropic organization.

5.4 EVL ACTS AS AN ONCOGENE DOWNSTREAM OF SRC

Consistent with a role of the EVL-dependent polarized stress fibres in tumour growth, I found that EVL is required for the growth of TAM-induced ER-Src cells and cellular transformation (Figure 4.5). Moreover, EVL mRNA and protein levels were elevated specifically in ER+ DCIS (Figure 2.5 and Figure 4.6). However, IDC invasive fronts exhibit significant lower EVL levels, compared to the in situ counterpart (Figure 4.6). In addition, low EVL levels were shown to be predictive of highly invasive tumours and poor prognosis (Mouneimne et al., 2012). Thus, the multistep development of breast tumours may involve first an accumulation of EVL-dependent polarized actin fibres, involved in tumour growth, followed by a subsequent decrease, which would allow for cell migration and invasion.

How the EVL-dependent polarized actin fibres promote Src-mediated transformation remains to be determined. As previously mentioned, some oncogenes, like ERK and YAP/TAZ, are activated in response to mechanical forces through cytoskeleton changes So, one exiting possibility is that the F-actin-mediated increase in intracellular mechanical properties triggers a boost of oncogenic activity, which leads to sustained proliferation and tumour growth (Aragona et al. 2013; Paszek et al. 2005; Aplin et al. 2001; Aplin & Juliano 2001).

Interestingly, high EVL levels are mainly associated with the Luminal A molecular subtype (Table 4. and Table 4.). Although higher Src levels or activity have been observed in diverse breast cancer subtypes, correlations have been reported between these subtypes, disease survival and Src activity levels and/or localization (Anbalagan et al. 2012; Campbell et al. 2008; Stover et al. 1996). Thus, this raises the possibility that the requirement of EVL for the growth of the Luminal A subtype is determined by the activation status of Src and/or its subcellular location. Since increased rigidity and acto-myosin contractibility are general properties of tumours (Beil et al. 2003), Src may also promote growth of

other breast cancer molecular subtypes through the control on F-actin. Whether Src affects other ABPs in these molecular subtypes remained to be determined.

5.5 EVL IS PART OF A FEED-FORWARD SELF-REINFORCING MECHANO-TRANSDUCER LOOP

The positive correlation between age and tumour development has long been recognized. In addition, increased breast density has also been associated with an increased risk of breast cancer development (Martin & Boyd 2008). Older tissues show a loss of collagen and an increase in fatty tissue content (Li et al. 2005). Moreover, as women age and therefore cancer incidence rises, the mammographic density decreases (Li et al. 2005). Therefore, it would be expected that older tissues are softer. But actually, this is not the case. Aged tissues have a stiffer, less organized and less functional ECM, probably due to aberrant collagen cross-linkage (Levental et al. 2009). Thus, there is a positive association between age, matrix crosslinking, tissue stiffening and increased risk of malignancy.

It has been suggested that sustained stiffening of the ECM would take place through an exogenous and endogenous force continuum (Paszek et al. 2005). The increase of endogenous and exogenous force can lead to integrin activation, Src activation, focal adhesions formation and to a chronic increase in cytoskeletal tension (Paszek et al. 2005; Butcher et al. 2009). My study suggests that during tumorigenesis, Src could respond to an increase in ECM-dependent stiffening, mediating a mechano-transduction pathway via the EVL-mediated longitudinal actin stress fibres. Accordingly, chronic ECM stiffening triggers the development of benign lesions through the activation of Src and Rho GTPase function (Paszek et al. 2005). The EVL-dependent nematic stress fibres would enhance tumour growth, possibly through Cyclin D1 expression, YAP/TAZ, or ERK signalling (Paszek et al. 2005; Klein et al. 2009). Activation of YAP downstream of Src has been shown to alter the ECM composition (Calvo et al.,

2013). Thus, further stiffening of the ECM would lead to a feed-forward self-reinforcing loop, which would further increase Src activation. This would, in turn, inactivate RhoA (Frame et al. 2002), decrease EVL levels, disassemble the stress fibres for cells to progress into malignancy.

Altogether, my observations are in agreement with a model by which increased rigidity of the matrix would enhance Src activity. In turn, Src would stiffer cell via the assembly of stress fibres, polarized by EVL and consequently breast tumour growth (Figure 5.1). Given that mechano-transduction signalling mechanisms have been described in a broad spectrum of tissue and cell types (Jaalouk & Lammerding 2009), I believe that these findings may have significant impacts for the development of new diagnostic tools not only for breast cancer but also for most of epithelial cancers.

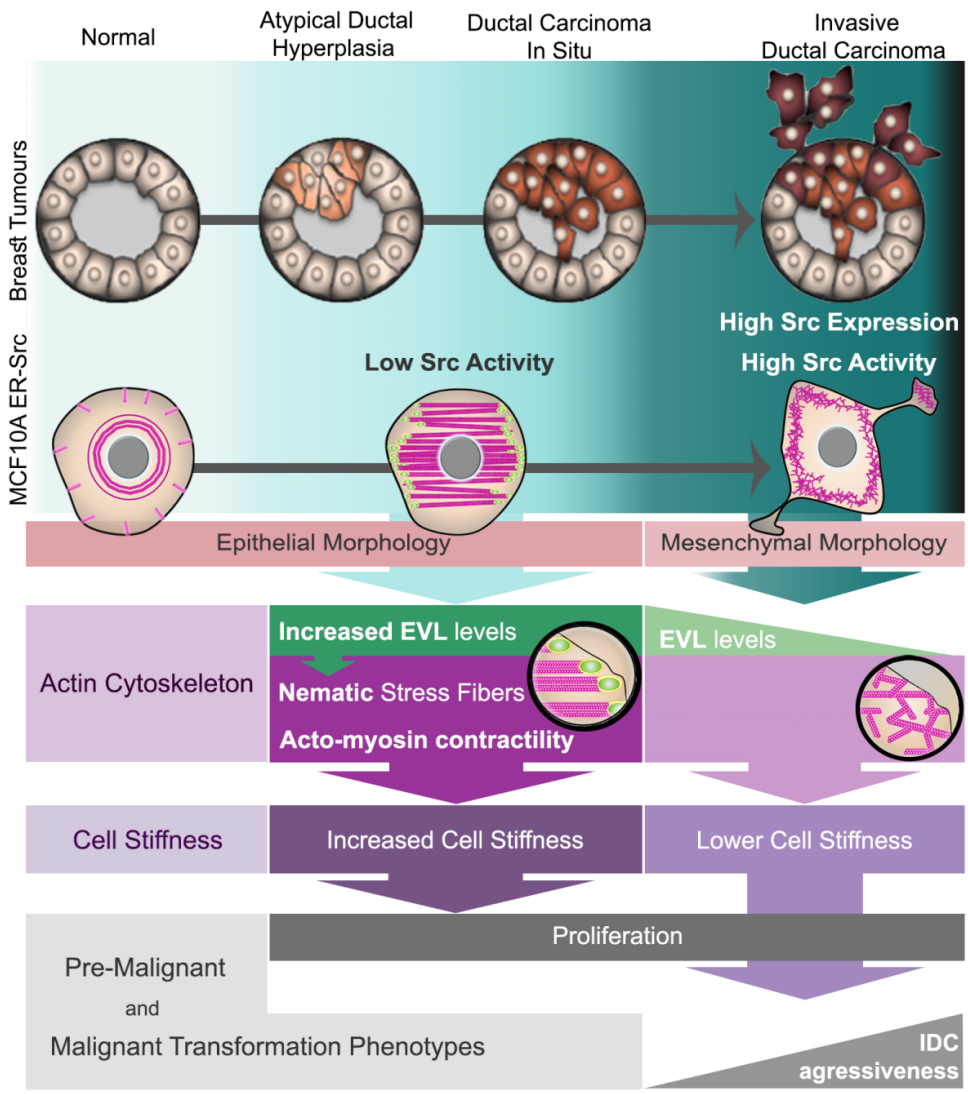

Figure 5.1: Model by which Src controls EVL and stress fibre-dependent cell stiffening to promote tumour growth during transformation.

Bibliography

Abella, J.V.G. et al., 2015. Isoform diversity in the Arp2/3 complex determines actin filament dynamics. *Nature cell biology*, 18(1), pp.76–86.

Abram, C.L. & Courtneidge, S.A., 2000. Src Family Tyrosine Kinases and Growth Factor Signaling. *Experimental Cell Research*, 254(1), pp.1–13.

Ahern-Djamali, S.M. et al., 1998. Mutations in Drosophila enabled and rescue by human vasodilator-stimulated phosphoprotein (VASP) indicate important functional roles for Ena/VASP homology domain 1 (EVH1) and EVH2 domains. *Molecular biology of the cell*, 9(8), pp.2157–2171.

Alberts, B. et al., 2002. *Molecular Biology of the Cell*,

Aleshin, A. & Finn, R.S., 2010. SRC : A Century of Science Brought to the Clinic. , 12(8), pp.599–607.

Alimonti, A. et al., 2010. Subtle variations in Pten dose determine cancer susceptibility. *Nature genetics*, 42, pp.1–6.

Anbalagan, M. et al., 2012. Subcellular localization of total and activated Src kinase in African American and Caucasian breast cancer. *PLoS ONE*, 7(3).

Anderson, W.F. et al., 2014. How many etiological subtypes of breast cancer: Two, three, four, or more? *Journal of the National Cancer Institute*, 106(8).

Androic, I. et al., 2008. Targeting cyclin B1 inhibits proliferation and sensitizes breast cancer cells to taxol. *BMC cancer*, 8(1), p.391.

Aplin, A.E. et al., 2001. Integrin-mediated adhesion regulates ERK nuclear translocation and phosphorylation of Elk-1. *Journal of Cell Biology*, 153(2), pp.273–281.

Aplin, A.E. & Juliano, R.L., 2001. Regulation of nucleocytoplasmic trafficking by

cell adhesion receptors and the cytoskeleton. *Journal of Cell Biology*, 155(2), pp.187–191.

Aragona, M. et al., 2013. A mechanical checkpoint controls multicellular growth through YAP/TAZ regulation by actin-processing factors. *Cell*, 154(5), pp.1047–1059.

Avizienyte, E. & Frame, M.C., 2005. Src and FAK signalling controls adhesion fate and the epithelial-to- mesenchymal transition. *Current Opinion in Cell Biology*, 17(5 SPEC. ISS.), pp.542–547.

Bandaru, S. et al., 2014. Targeting filamin B induces tumor growth and metastasis via enhanced activity of matrix metalloproteinase-9 and secretion of VEGF-A. *Oncogenesis*, 3(9), p.e119.

Baranwal, S. et al., 2012. Nonredundant roles of cytoplasmic β- and γ-actin isoforms in regulation of epithelial apical junctions. *Molecular biology of the cell*, 23(18), pp.3542–53.

Barry, W.T. et al., 2010. Intratumor heterogeneity and precision of microarray-based predictors of breast cancer biology and clinical outcome. *Journal of Clinical Oncology*, 28, pp.2198–2206.

Barzik, M. et al., 2005. Ena/VASP proteins enhance actin polymerization in the presence of barbed end capping proteins. *Journal of Biological Chemistry*, 280(31), pp.28653–28662.

Bear, J.E. et al., 2002. Antagonism between Ena/VASP proteins and actin filament capping regulates fibroblast motility. *Cell*, 109(4), pp.509–521.

Bear, J.E. & Gertler, F.B., 2009. Ena/VASP: towards resolving a pointed controversy at the barbed end. *Journal of cell science*, 122(Pt 12), pp.1947–1953.

Beil, M. et al., 2003. Sphingosylphosphorylcholine regulates keratin network architecture and visco-elastic properties of human cancer cells. *Nature cell biology*, 5(9), pp.803–811.

Belsches, A.P., Haskell, M.D. & Parsons, S.J., 1997. Role of c-Src tyrosine kinase in EGF-induced mitogenesis. *Frontiers in Bioscience*, 2, pp.d501–18.

Bhadriraju, K. & Hansen, L.K., 2002. Extracellular matrix- and cytoskeleton-dependent changes in cell shape and stiffness. *Experimental cell research*, 278(1), pp.92–100.

Bild, A.H. et al., 2006. Oncogenic pathway signatures in human cancers as a guide to targeted therapies. *Nature*, 439(7074), pp.353–357.

Biscardi, J.S. et al., 2000. Tyrosine kinase signalling in breast cancer: Epidermal growth factor receptor and c-Src interactions in breast cancer. *Breast Cancer Research*, 2(3), pp.203–210.

Bjorge, J.D., Jakymiw, a & Fujita, D.J., 2000. Selected glimpses into the activation and function of Src kinase. *Oncogene*, 19(49), pp.5620–5635.

Blanchoin, L. et al., 2014. Actin dynamics, architecture, and mechanics in cell motility. *Physiological reviews*, 94(1), pp.235–63.

Bombonati, A. & Sgroi, D.C., 2011. The molecular pathology of breast cancer progression. *The Journal of pathology*, 223, pp.307–317.

Boudaoud, A. et al., 2014. FibrilTool, an ImageJ plug-in to quantify fibrillar structures in raw microscopy images. *Nature protocols*, 9(2), pp.457–463.

Boudreau, A., Van't Veer, L.J. & Bissell, M.J., 2012. An "elite hacker": Beast tumors exploit the normal microenvironment program to instruct their progression and biological diversity. *Cell Adhesion and Migration*, 6(3), pp.236–248.

Boyer, B. et al., 1997. Src and Ras are involved in separate pathways in epithelial cell scattering. *EMBO Journal*, 16(19), pp.5904–5913.

Braverman, R.H. et al., 1996. Anti-oncogenic effects of tropomyosin: Isoform specificity and importance of protein coding sequences. *Oncogene*, 13(3), pp.537–545.

Bromann, P. a, Korkaya, H. & Courtneidge, S. a, 2004. The interplay between Src family kinases and receptor tyrosine kinases. *Oncogene*, 23(48), pp.7957–7968.

Butcher, D.T., Alliston, T. & Weaver, V.M., 2009. A tense situation: forcing tumour progression. *Nature reviews. Cancer*, 9(2), pp.108–22.

Calleja, M. et al., 1996. Visualization of gene expression in living adult Drosophila. *Science (New York, N.Y.)*, 274(5285), pp.252–255.

Campbell, E.J. et al., 2008. Phosphorylated c-Src in the nucleus is associated with improved patient outcome in ER-positive breast cancer. *British journal of cancer*, 99, pp.1769–1774.

Campellone, K.G. & Welch, M.D., 2010. A nucleator arms race: cellular control of actin assembly. *Nature reviews. Molecular cell biology*, 11(4), pp.237–51.

Cantley, L.C., 2002. The Phosphoinositide 3-Kinase Pathway. *Science*, 296(5573), pp.1655–1657.

Carmeci, C. et al., 1998. Moesin expression is associated with the estrogen

receptor-negative breast cancer phenotype. *Surgery*, 124(2), pp.211–217.

Cartwright, C.A., Coad, C.A. & Egbert, B.M., 1994. Elevated c-Src tyrosine kinase activity in premalignant epithelia of ulcerative colitis. *Journal of Clinical Investigation*, 93(2), pp.509–515.

Chen, D.-T. et al., 2010. Proliferative genes dominate malignancy-risk gene signature in histologically-normal breast tissue. *Breast Cancer Research and Treatment*, 119, pp.335–346.

Chesarone, M. a. & Goode, B.L., 2009. Actin nucleation and elongation factors: mechanisms and interplay. *Current Opinion in Cell Biology*, 21(1), pp.28–37.

Colombo, P.-E. et al., 2011. Microarrays in the 2010s: the contribution of microarray-based gene expression profiling to breast cancer classification, prognostication and prediction. *Breast Cancer Research*, 13(3), p.212.

Cooper, J.A. & Sept, D., 2008. New Insights into Mechanism and Regulation of Actin Capping Protein. *International Review of Cell and Molecular Biology*, 267, pp.183–206.

Damonte, P. et al., 2008. Mammary carcinoma behavior is programmed in the precancer stem cell. *Breast cancer research : BCR*, 10(3), p.R50.

Debnath, J. et al., 2002. The role of apoptosis in creating and maintaining luminal space within normal and oncogene-expressing mammary acini. *Cell*, 111(1), pp.29–40.

Debnath, J., Muthuswamy, S.K. & Brugge, J.S., 2003. Morphogenesis and oncogenesis of MCF-10A mammary epithelial acini grown in three-dimensional basement membrane cultures. *Methods San Diego Calif*, 30(3), pp.256–268.

Decaestecker, C. et al., 2007. Can anti-migratory drugs be screened in vitro? A review of 2D and 3D assays for the quantitative analysis of cell migration. *Medicinal Research Reviews*, 27(2), pp.149–176.

Desmedt, C. et al., 2007. Strong time dependence of the 76-gene prognostic signature for node-negative breast cancer patients in the TRANSBIG multicenter independent validation series. *Clinical Cancer Research*, 13, pp.3207–3214.

Dhillon, a S. et al., 2007. MAP kinase signalling pathways in cancer. *Oncogene*, 26(22), pp.3279–3290.

Doornaert, B., 2003. Time course of actin cytoskeleton stiffness and matrix adhesion molecules in human bronchial epithelial cell cultures. *Exp Cell Res*,

287(2), pp.199–208.

Draghici, S. et al., 2007. A systems biology approach for pathway level analysis. *Genome research*, 17(10), pp.1537–45.

Dugina, V. et al., 2009. Beta and gamma-cytoplasmic actins display distinct distribution and functional diversity. *Journal of cell science*, 122(Pt 16), pp.2980–8.

Eckert, M. a & Yang, J., 2011. Targeting invadopodia to block breast cancer metastasis. *Oncotarget*, 2(7), pp.562–568.

Ellis, I.. et al., 2003. CHAPTER 1 WHO histological classification of tumours of the breast. *Pathology and Genetics of the Breast and Female Genital Organs*, p.432.

Elsberger, B. et al., 2010. Breast cancer patients' clinical outcome measures are associated with Src kinase family member expression. *British journal of cancer*, 103(6), pp.899–909.

Elsberger, B. et al., 2009. Is expression or activation of Src kinase associated with cancer-specific survival in ER-, PR- and HER2-negative breast cancer patients? *The American journal of pathology*, 175(4), pp.1389–97.

Elston, C.W. & Ellis, I.O., 1991. Pathological prognostic factors in breast cancer. I. The value of histological grade in breast cancer: experience from a large study with long-term follow up. *Histopathology*, 19, pp.403–410.

Emery, L. a et al., 2009. Early dysregulation of cell adhesion and extracellular matrix pathways in breast cancer progression. *The American journal of pathology*, 175(3), pp.1292–1302.

Feng, Y. & Walsh, C.A., 2004. The many faces of filamin: a versatile molecular scaffold for cell motility and signalling. *Nat Cell Biol*, 6(11), pp.1034–1038.

Ferlay, J. et al., 2014. Cancer incidence and mortality worldwide: sources, methods and major patterns in GLOBOCAN 2012. *Int J Cancer*, 136(5), pp.E359–86.

Fernández, B.G. et al., 2011. Actin-Capping Protein and the Hippo pathway regulate F-actin and tissue growth in Drosophila. *Development (Cambridge, England)*, 138(11), pp.2337–46.

Fernández, B.G., Jezowska, B. & Janody, F., 2013. Drosophila actin-Capping Protein limits JNK activation by the Src proto-oncogene. *Oncogene*, pp.1–13.

Fincham, V.J. et al., 1996. Translocation of src kinase to the cell periphery is

mediated by the actin cytoskeleton under the control of the Rho family of small G proteins. *Journal of Cell Biology*, 135(6), pp.1551–1564.

Fincham, V.J., Brunton, V.G. & Frame, M.C., 2000. The SH3 domain directs acto-myosin-dependent targeting of v-Src to focal adhesions via phosphatidylinositol 3-kinase. *Molecular and cellular biology*, 20(17), pp.6518–36.

Finn, R.S., 2008. Targeting Src in breast cancer. *Annals of oncology : official journal of the European Society for Medical Oncology / ESMO*, 19(8), pp.1379–86.

Frame, M.C., 2004. Newest findings on the oldest oncogene; how activated src does it. *Journal of cell science*, 117(Pt 7), pp.989–98.

Frame, M.C. et al., 2002. v-Src's hold over actin and cell adhesions. *Nature reviews. Molecular cell biology*, 3(4), pp.233–45.

Gaspar, P. et al., 2015. Zyxin antagonizes the FERM protein expanded to couple f-actin and yorkie-dependent organ growth. *Current Biology*, 25(6), pp.679–689.

Gentry, B.S. et al., 2012. Multiple actin binding domains of Ena/VASP proteins determine actin network stiffening. *European Biophysics Journal*, 41(11), pp.979–990.

Gligorijevic, B. et al., 2012. N-WASP-mediated invadopodium formation is involved in intravasation and lung metastasis of mammary tumors. *Journal of Cell Science*, 125(3), pp.724–734.

Gonzalez, C., 2013. Drosophila melanogaster: a model and a tool to investigate malignancy and identify new therapeutics. *Nature Reviews Cancer*, 13(3), pp.172–183.

Gross, S.R., 2013. Actin binding proteins: Their ups and downs in metastatic life. *Cell adhesion & migration*, 7(2), pp.199–213.

Guarino, M., 2010. Src signaling in cancer invasion. *Journal of cellular physiology*, 223(1), pp.14–26.

Guck, J. et al., 2005. Optical deformability as an inherent cell marker for testing malignant transformation and metastatic competence. *Biophysical journal*, 88(5), pp.3689–3698.

Guck, J. et al., 2001. The optical stretcher: a novel laser tool to micromanipulate cells. *Biophysical journal*, 81(2), pp.767–784.

Gudjonsson, T. et al., 2005. Myoepithelial cells: their origin and function in breast

morphogenesis and neoplasia. *Journal of mammary gland biology and neoplasia*, 10(3), pp.261–272.

Gunning, P.W. et al., 2015. Tropomyosin - master regulator of actin filament function in the cytoskeleton. *Journal of cell science*, pp.1–10.

Gupta, M. et al., 2015. Adaptive rheology and ordering of cell cytoskeleton govern matrix rigidity sensing. *Nature communications*, 6, p.7525.

Haghparast, S.M.A. et al., 2013. Actin-based biomechanical features of suspended normal and cancer cells. *Journal of Bioscience and Bioengineering*, 116(3), pp.380–385.

Hammerick, K.E. et al., 2011. Elastic properties of induced pluripotent stem cells. *Tissue engineering. Part A*, 17(3-4), pp.495–502.

Hanahan, D. & Weinberg, R.A., 2011. Hallmarks of cancer: the next generation. *Cell*, 144(5), pp.646–674.

Hansen, S.D. & Mullins, R.D., 2010. VASP is a processive actin polymerase that requires monomeric actin for barbed end association. *Journal of Cell Biology*, 191(3), pp.571–584.

Hartmann, L.C. et al., 2005. Benign Breast Disease and the Risk of Breast Cancer. *New England Journal of Medicine*, 353(3), pp.229–237.

Hawthorn, L. et al., 2010. Integration of transcript expression, copy number and LOH analysis of infiltrating ductal carcinoma of the breast. *BMC Cancer*, 10, p.460.

Hay, B. a, Wolff, T. & Rubin, G.M., 1994. Expression of baculovirus P35 prevents cell death in Drosophila. *Development (Cambridge, England)*, 120(8), pp.2121–2129.

Helfman, D.M. et al., 2008. Tropomyosin as a regulator of cancer cell transformation. *Advances in Experimental Medicine and Biology*, 644, pp.124–131.

Hirsch, H. a et al., 2010. A transcriptional signature and common gene networks link cancer with lipid metabolism and diverse human diseases. *Cancer cell*, 17(4), pp.348–61.

Hirsch, H. a et al., 2009. Metformin selectively targets cancer stem cells, and acts together with chemotherapy to block tumor growth and prolong remission. *Cancer Res*, 69(19), pp.7507–7511.

Hotulainen, P. & Lappalainen, P., 2006. Stress fibers are generated by two distinct

actin assembly mechanisms in motile cells. *Journal of Cell Biology*, 173(3), pp.383–394.

Hu, L. De et al., 2008. EVL (Ena/VASP-like) expression is up-regulated in human breast cancer and its relative expression level is correlated with clinical stages. *Oncology Reports*, 19(4), pp.1015–1020.

Hu, Z. et al., 2006. The molecular portraits of breast tumors are conserved across microarray platforms. *BMC Genomics*, 7, p.96.

Hudson, A.M. & Cooley, L., 2002. A subset of dynamic actin rearrangements in Drosophila requires the Arp2/3 complex. *Journal of Cell Biology*, 156(4), pp.677–687.

Huveneers, S. & Danen, E.H.J., 2009. Adhesion signaling - crosstalk between integrins, Src and Rho. *Journal of cell science*, 122, pp.1059–1069.

Iliopoulos, D. et al., 2011. Inducible formation of breast cancer stem cells and their dynamic equilibrium with non-stem cancer cells via IL6 secretion. *Proceedings of the National Academy of Sciences of the United States of America*, 108(4), pp.1397–402.

Iliopoulos, D., Hirsch, H. a & Struhl, K., 2009. An epigenetic switch involving NF-kappaB, Lin28, Let-7 MicroRNA, and IL6 links inflammation to cell transformation. *Cell*, 139(4), pp.693–706.

Imbalzano, K.M. et al., 2009. Increasingly transformed MCF-10A cells have a progressively tumor-like phenotype in three-dimensional basement membrane culture. *Cancer cell international*, 9, p.7.

Insall, R.H. & Machesky, L.M., 2009. Actin Dynamics at the Leading Edge: From Simple Machinery to Complex Networks. *Developmental Cell*, 17(3), pp.310–322.

Irby, R.B. & Yeatman, T.J., 2000. Role of Src expression and activation in human cancer. *Oncogene*, 19(49), pp.5636–42.

Jaalouk, D.E. & Lammerding, J., 2009. Mechanotransduction gone awry. *Nature Reviews Molecular Cell Biology*, 10(1), pp.63–73.

Jalilian, I. et al., 2015. Cell elasticity is regulated by the tropomyosin isoform composition of the actin cytoskeleton. *PLoS ONE*, 10(5).

Jezowska, B. et al., 2011. A dual function of Drosophila capping protein on DE-cadherin maintains epithelial integrity and prevents JNK-mediated apoptosis. *Developmental Biology*, 360(1), pp.143–159.

Johnson, W.E., Li, C. & Rabinovic, A., 2007. Adjusting batch effects in microarray expression data using empirical Bayes methods. *Biostatistics (Oxford, England)*, 8(1), pp.118–27.

Jones, R.J. et al., 2002. Elevated c-Src is linked to altered cell-matrix adhesion rather than proliferation in KM12C human colorectal cancer cells. *British journal of cancer*, 87(10), pp.1128–1135.

Kanaan, Z. et al., 2010. The actin-cytoskeleton pathway and its potential role in inflammatory bowel disease-associated human colorectal cancer. *Genetic testing and molecular biomarkers*, 14(3), pp.347–53.

Kanomata, N. et al., 2011. Clinicopathological significance of Y416Src and Y527Src expression in breast cancer. *Journal of clinical pathology*, 64(7), pp.578–86.

Kao, J. et al., 2009. Molecular profiling of breast cancer cell lines defines relevant tumor models and provides a resource for cancer gene discovery. *PLoS ONE*, 4(7).

Keefer, C.L. & Desai, J.P., 2011. Mechanical phenotyping of stem cells. *Theriogenology*, 75(8), pp.1426–1430.

Kim, D.H. et al., 2009. Proteomic analysis of breast cancer tissue reveals upregulation of actin-remodeling proteins and its relevance to cancer invasiveness. *Proteomics - Clinical Applications*, 3(1), pp.30–40.

Kinoshita, T. et al., 2012. Actin-related protein 2/3 complex subunit 5 (ARPC5) contributes to cell migration and invasion and is directly regulated by tumor-suppressive microRNA-133a in head and neck squamous cell carcinoma. *International Journal of Oncology*, 40(6), pp.1770–1778.

Kirkbride, K.C. et al., 2011. Cortactin: A multifunctional regulator of cellular invasiveness. *Cell Adhesion and Migration*, 5(2), pp.187–198.

Klein, E.A. et al., 2009. Cell-Cycle Control by Physiological Matrix Elasticity and In Vivo Tissue Stiffening. *Current Biology*, 19(18), pp.1511–1518.

Knight, W.A. et al., 1977. Estrogen receptor as an independent prognostic factor for early recurrence in breast cancer. *Cancer Research*, 37(12), pp.4669–4671.

Kotiyal, S. & Bhattacharya, S., 2014. Breast cancer stem cells, EMT and therapeutic targets. *Biochemical and Biophysical Research Communications*, 453(1), pp.112–116.

Kretschmer, C. et al., 2011. Identification of early molecular markers for breast cancer. *Molecular Cancer*, 10, p.15.

Lamouille, S., Xu, J. & Derynck, R., 2014. Molecular mechanisms of epithelial-mesenchymal transition. *Nature reviews. Molecular cell biology*, 15(3), pp.178–96.

Lanier, L.M. et al., 1999. Mena is required for neurulation and commissure formation. *Neuron*, 22(2), pp.313–325.

Lebrand, C. et al., 2004. Critical role of Ena/VASP proteins for filopodia formation in neurons and in function downstream of netrin-1. *Neuron*, 42(1), pp.37–49.

Lee, S. & Kolodziej, P. a, 2002. Short Stop provides an essential link between F-actin and microtubules during axon extension. *Development (Cambridge, England)*, 129, pp.1195–1204.

Lee, S.H. & Dominguez, R., 2010. Regulation of actin cytoskeleton dynamics in cells. *Molecules and cells*, 29(4), pp.311–325.

Levental, K.R. et al., 2009. Matrix Crosslinking Forces Tumor Progression by Enhancing Integrin Signaling. *Cell*, 139(5), pp.891–906.

Li, T. et al., 2005. The association of measured breast tissue characteristics with mammographic density and other risk factors for breast cancer. *Cancer Epidemiology Biomarkers and Prevention*, 14(2), pp.343–349.

Li, X. et al., 2008. Intrinsic resistance of tumorigenic breast cancer cells to chemotherapy. *Journal of the National Cancer Institute*, 100(9), pp.672–679.

Li, Y. et al., 2010. Amplification of LAPTM4B and YWHAZ contributes to chemotherapy resistance and recurrence of breast cancer. *Nature Medicine*, 16, pp.214–218.

Lin, Y. et al., 2010. Predicting features of breast cancer with gene expression patterns. *Breast Cancer Research and Treatment*, 108, pp.691–699.

Lindberg, U. et al., 2008. The microfilament system and malignancy. *Seminars in Cancer Biology*, 18(1), pp.2–11.

Liu, S. et al., 2014. Breast cancer stem cells transition between epithelial and mesenchymal states reflective of their normal counterparts. *Stem Cell Reports*, 2(1), pp.78–91.

Lopez-Garcia, M. a et al., 2010. Breast cancer precursors revisited: molecular features and progression pathways. *Histopathology*, 57(2), pp.171–92.

Lu, Y. et al., 2003. Src family protein-tyrosine kinases alter the function of PTEN to regulate phosphatidylinositol 3-kinase/AKT cascades. *Journal of Biological Chemistry*, 278(41), pp.40057–40066.

Lynch, C.D. et al., 2011. Filamin depletion blocks endoplasmic spreading and destabilizes force-bearing adhesions. *Molecular biology of the cell*, 22(8), pp.1263–73.

MacGrath, S.M. & Koleske, A.J., 2012. Cortactin in cell migration and cancer at a glance. *Journal of Cell Science*, 125(7), pp.1621–1626.

Machesky, L.M., 2008. Lamellipodia and filopodia in metastasis and invasion. *FEBS Letters*, 582(14), pp.2102–2111.

Mahadev, K. et al., 2002. Suppression of the Transformed Phenotype of Breast Cancer by Tropomyosin-1. *Experimental Cell Research*, 279(1), pp.40–51.

Malhotra, G.K. et al., 2010. Histological, molecular and functional subtypes of breast cancers. *Cancer Biology and Therapy*, 10(10), pp.955–960.

Malzahn, K. et al., 1998. Biological and prognostic significance of stratified epithelial cytokeratins in infiltrating ductal breast carcinomas. *Virchows Archiv : an international journal of pathology*, 433(2), pp.119–29.

Martin, L.J. & Boyd, N.F., 2008. Mammographic density. Potential mechanisms of breast cancer risk associated with mammographic density: hypotheses based on epidemiological evidence. *Breast cancer research : BCR*, 10(1), p.201.

Martin, T. a et al., 2008. N-WASP is a putative tumour suppressor in breast cancer cells, in vitro and in vivo, and is associated with clinical outcome in patients with breast cancer. *Clinical & experimental metastasis*, 25(2), pp.97–108.

Martin, T.A. & Jiang, W.G., 2008. Loss of tight junction barrier function and its role in cancer metastasis. *BBA - Biomembranes*, 1788, pp.872–891.

Masood, S. & Kameh, D., 2005. Breast. In *The Cancer Handbook*. John Wiley & Sons, Ltd.

May, C.D. et al., 2011. Epithelial-mesenchymal transition and cancer stem cells: a dangerously dynamic duo in breast cancer progression. *Breast cancer research : BCR*, 13(1), p.202.

McCall, M.N., Bolstad, B.M. & Irizarry, R. a, 2010. Frozen robust multiarray analysis (fRMA). *Biostatistics (Oxford, England)*, 11(2), pp.242–53.

McLean, G.W. et al., 2005. The role of focal-adhesion kinase in cancer - a new therapeutic opportunity. *Nature reviews. Cancer*, 5(7), pp.505–515.

Michelot, A. & Drubin, D.G., 2011. Building distinct actin filament networks in a common cytoplasm. *Current Biology*, 21(14).

Milan, M., Campuzano, S. & Garcia-Bellido, A., 1996. Cell cycling and patterned

cell proliferation in the Drosophila wing during metamorphosis. *Developmental Biology*, 93(October), pp.11687–11692.

Miralles, F. et al., 2003. Actin dynamics control SRF activity by regulation of its coactivator MAL. *Cell*, 113(3), pp.329–342.

Di Modugno, F. et al., 2007. Molecular cloning of hMena (ENAH) and its splice variant hMena+11a: epidermal growth factor increases their expression and stimulates hMena+11a phosphorylation in breast cancer cell lines. *Cancer research*, 67(6), pp.2657–2665.

Di Modugno, F. et al., 2012. Splicing program of human MENA produces a previously undescribed isoform associated with invasive, mesenchymal-like breast tumors. *Proceedings of the National Academy of Sciences of the United States of America*, 109(47), pp.19280–5.

Di Modugno, F. et al., 2006. The cytoskeleton regulatory protein hMena (ENAH) is overexpressed in human benign breast lesions with high risk of transformation and human epidermal growth factor receptor-2-positive/hormonal receptor-negative tumors. *Clinical Cancer Research*, 12(5), pp.1470–1478.

Mouneimne, G. et al., 2012. Differential Remodeling of Actin Cytoskeleton Architecture by Profilin Isoforms Leads to Distinct Effects on Cell Migration and Invasion. *Cancer Cell*, 22(5), pp.615–630.

Murphy, D.A. & Courtneidge, S.A., 2011. The "ins" and "outs" of podosomes and invadopodia: characteristics, formation and function. *Nature reviews. Molecular cell biology*, 12(7), pp.413–26.

Muthuswamy, S.K. et al., 2001. ErbB2, but not ErbB1, reinitiates proliferation and induces luminal repopulation in epithelial acini. *Nature Cell Biology*, 3(9), pp.785–792.

Nakamura, F., Stossel, T.P. & Hartwig, J.H., 2011. The filamins: Organizers of cell structure and function. *Cell Adhesion and Migration*, 5(2), pp.160–169.

Nicolaï, M., Lasbleiz, C. & Dura, J.M., 2003. Gain-of-Function Screen Identifies a Role of the Src64 Oncogene in Drosophila Mushroom Body Development. *Journal of Neurobiology*, 57(3), pp.291–302.

Oakes, P.W. et al., 2012. Tension is required but not sufficient for focal adhesion maturation without a stress fiber template. *Journal of Cell Biology*, 196(3), pp.363–374.

Paredes, J. et al., 2005. P-cadherin overexpression is an indicator of clinical outcome in invasive breast carcinomas and is associated with CDH3

promoter hypomethylation. *Clinical Cancer Research*, 11(16), pp.5869–5877.

Parsons, J.T., Horwitz, A.R. & Schwartz, M. a, 2010. Cell adhesion: integrating cytoskeletal dynamics and cellular tension. *Nature reviews. Molecular cell biology*, 11(9), pp.633–43.

Paszek, M.J. et al., 2005. Tensional homeostasis and the malignant phenotype. *Cancer Cell*, 8(3), pp.241–254.

Patsialou, A. et al., 2012. Selective gene-expression profiling of migratory tumor cells in vivo predicts clinical outcome in breast cancer patients. *Breast cancer research : BCR*, 14(5), p.R139.

Pau Ni, I.B. et al., 2010. Gene expression patterns distinguish breast carcinomas from normal breast tissues: the Malaysian context. *Pathology research and practice*, 206, pp.223–228.

Pawlak, G. et al., 2004. Alterations in tropomyosin isoform expression in human transitional cell carcinoma of the urinary bladder. *Int J Cancer*, 110(3), pp.368–373.

Pedraza, V. et al., 2010. Gene expression signatures in breast cancer distinguish phenotype characteristics, histologic subtypes, and tumor invasiveness. *Cancer*, 116, pp.486–496.

Perou, C.M. et al., 2000. Molecular portraits of human breast tumours. *Nature*, 406(6797), pp.747–52.

Petit, V. & Thiery, J.P., 2000. Focal adhesions: structure and dynamics. *Biology of the cell / under the auspices of the European Cell Biology Organization*, 92(7), pp.477–494.

Phillips, T.M., McBride, W.H. & Pajonk, F., 2006. The response of CD24-/low/CD44+ breast cancer-initiating cells to radiation. *Journal of the National Cancer Institute*, 98(24), pp.1777–1785.

Pinder, S.E. & Ellis, I.O., 2003. The diagnosis and management of pre-invasive breast disease: ductal carcinoma in situ (DCIS) and atypical ductal hyperplasia (ADH)--current definitions and classification. *Breast cancer research : BCR*, 5(5), pp.254–257.

Polyak, K., 2007. Breast cancer: origins and evolution. *The Journal of clinical investigation*, 117(11), pp.3155–63.

Popovici, V. et al., 2010. Effect of training-sample size and classification difficulty on the accuracy of genomic predictors. *Breast cancer research BCR*, 12, p.R5.

Popowicz, G.M. et al., 2006. Filamins: promiscuous organizers of the cytoskeleton. *Trends in Biochemical Sciences*, 31(7), pp.411–419.

Prasad, G.L. et al., 1999. Suppression of src-induced transformed phenotype by expression of tropomyosin-1. *Oncogene*, 18(11), pp.2027–2031.

Prasad, G.L., Fuldner, R. a & Cooper, H.L., 1993. Expression of transduced tropomyosin 1 cDNA suppresses neoplastic growth of cells transformed by the ras oncogene. *Proceedings of the National Academy of Sciences of the United States of America*, 90(15), pp.7039–43.

Provenzano, P.P. & Keely, P.J., 2009. The role of focal adhesion kinase in tumor initiation and progression. *Cell adhesion migration*, 3(4), pp.347–350.

Pylayeva, Y. et al., 2009. Ras- and PI3K-dependent breast tumorigenesis in mice and humans requires focal adhesion kinase signaling. *Journal of Clinical Investigation*, 119(2), pp.252–266.

R Development Core Team, R., 2011. R: A Language and Environment for Statistical Computing R. D. C. Team, ed. *R Foundation for Statistical Computing*, 1(2.11.1), p.409.

Raval, G.N. et al., 2003. Loss of expression of tropomyosin-1, a novel class II tumor suppressor that induces anoikis, in primary breast tumors. *Oncogene*, 22, pp.6194–6203.

Dos Remedios, C.G. et al., 2003. Actin binding proteins: regulation of cytoskeletal microfilaments. *Physiological reviews*, 83(2), pp.433–73.

Remmerbach, T.W. et al., 2009. Oral cancer diagnosis by mechanical phenotyping. *Cancer Research*, 69(5), pp.1728–1732.

Ribeiro, A.S. & Paredes, J., 2014. P-Cadherin Linking Breast Cancer Stem Cells and Invasion: A Promising Marker to Identify an "Intermediate/Metastable" EMT State. *Frontiers in oncology*, 4(January), p.371.

Richardson, A.L. et al., 2006. X chromosomal abnormalities in basal-like human breast cancer. *Cancer Cell*, 9, pp.121–132.

Ridley, A.J., 2011. Life at the leading edge. *Cell*, 145(7), pp.1012–1022.

Roca-Cusachs, P. et al., 2008. Micropatterning of single endothelial cell shape reveals a tight coupling between nuclear volume in G1 and proliferation. *Biophysical journal*, 94(12), pp.4984–95.

Rous, P., 1911. A Sarcoma of the Fowl Transmissible By an Agent Separable From the Tumor Cells. *The Journal of experimental medicine*, 13(4), pp.397–411.

Roussos, E.T. et al., 2010. Mena deficiency delays tumor progression and decreases metastasis in polyoma middle-T transgenic mouse mammary tumors. *Breast cancer research : BCR*, 12(6), p.R101.

Schafer, D. a, 2004. Cell biology: barbed ends rule. *Nature*, 430(7001), pp.734–735.

Schneider, C. a, Rasband, W.S. & Eliceiri, K.W., 2012. NIH Image to ImageJ: 25 years of image analysis. *Nature Methods*, 9(7), pp.671–675.

Shah, V., Braverman, R. & Prasad, G.L., 1998. Suppression of neoplastic transformation and regulation of cytoskeleton by tropomyosins. *Somatic cell and molecular genetics*, 24(5), pp.273–80.

Sheridan, C. et al., 2006. CD44+/CD24- breast cancer cells exhibit enhanced invasive properties: an early step necessary for metastasis. *Breast cancer research : BCR*, 8(5), p.59.

Shi, L. et al., 2010. The MicroArray Quality Control (MAQC)-II study of common practices for the development and validation of microarray-based predictive models. *Nature biotechnology*, 28(8), pp.827–38.

Sigurdsson, H. et al., 1990. Indicators of prognosis in node-negative breast cancer. *New England Journal of Medicine*, 322(15), pp.1045–1053.

Sircoulomb, F. et al., 2010. Genome profiling of ERBB2-amplified breast cancers. *BMC Cancer*, 10, p.539.

Skoble, J. et al., 2001. Pivotal role of VASP in Arp2/3 complex-mediated actin nucleation, actin branch-formation, and Listeria monocytogenes motility. *Journal of Cell Biology*, 155(1), pp.89–100.

Smeets, A. et al., 2011. Prediction of lymph node involvement in breast cancer from primary tumor tissue using gene expression profiling and miRNAs. *Breast Cancer Res Treat*, 129, pp.767–776.

Smyth, G., 2005. Limma: linear models for microarray data. *Bioinformatics and computational biology solutions using R and Bioconductor*, (2005), pp.397–420.

Sniadecki, N.J., 2010. A tiny touch: activation of cell signaling pathways with magnetic nanoparticles. *Endocrinology*, 151(2), pp.451–457.

Soofi, S.S. et al., 2009. The elastic modulus of Matrigel??? as determined by atomic force microscopy. *Journal of Structural Biology*, 167(3), pp.216–219.

Sorlie, T. et al., 2003. Repeated observation of breast tumor subtypes in independent gene expression data sets. *Proceedings of the National Academy of Sciences of the United States of America*, 100(14), pp.8418–23.

Sørlie, T. et al., 2001. Gene expression patterns of breast carcinomas distinguish tumor subclasses with clinical implications. *Proceedings of the National Academy of Sciences of the United States of America*, 98(19), pp.10869–74.

Soule, H.D. et al., 1990. Isolation and Characterization of a Spontaneously Immortalized Isolation and Characterization of a Spontaneously Immortalized Human Breast. *Cancer research*, pp.6075–6086.

Stehn, J.R. et al., 2006. Specialisation of the tropomyosin composition of actin filaments provides new potential targets for chemotherapy. *Curr Cancer Drug Targets*, 6(3), pp.245–256.

Stevenson, R.P., Veltman, D. & Machesky, L.M., 2012. Actin-bundling proteins in cancer progression at a glance. *Journal of Cell Science*, 125, pp.1073–1079.

Stingl, J. & Caldas, C., 2007. Molecular heterogeneity of breast carcinomas and the cancer stem cell hypothesis. *Nature reviews. Cancer*, 7(10), pp.791–9.

Stover, D.R., Furet, P. & Lydon, N.B., 1996. Modulation of the SH2 binding specificity and kinase activity of Src by tyrosine phosphorylation within its SH2 domain. *Journal of Biological Chemistry*, 271(21), pp.12481–12487.

Stricker, J., Falzone, T. & Gardel, M.L., 2010. Mechanics of the F-actin cytoskeleton. *Journal of biomechanics*, 43(1), pp.9–14.

Takafuta, T. et al., 2003. A new member of the LIM protein family binds to filamin B and localizes at stress fibers. *Journal of Biological Chemistry*, 278(14), pp.12175–12181.

Talamonti, M.S. et al., 1993. Increase in activity and level of pp60c-src in progressive stages of human colorectal cancer. *Journal of Clinical Investigation*, 91(1), pp.53–60.

Talamonti, M.S. et al., 1993. Increase in activity and level of pp60c-src in progressive stages of human colorectal cancer. *The Journal of clinical investigation*, 91(1), pp.53–60.

Tarone, G. et al., 1985. Rous sarcoma virus-transformed fibroblasts adhere primarily at discrete protrusions of the ventral membrane called podosomes. *Experimental Cell Research*, 159(1), pp.141–157.

Tipping, M. & Perrimon, N., 2014. Drosophila as a Model for Context-Dependent Tumorigenesis. *Journal of Cellular Physiology*, 229(1), pp.27–33.

Tojkander, S. et al., 2011. A molecular pathway for myosin II recruitment to stress fibers. *Current biology : CB*, 21(7), pp.539–50.

Tojkander, S., Gateva, G. & Lappalainen, P., 2012. Actin stress fibers--assembly, dynamics and biological roles. *Journal of cell science*, 125(Pt 8), pp.1855–64.

Totsukawa, G. et al., 2000. Distinct roles of ROCK (Rho-kinase) and MLCK in spatial regulation of MLC phosphorylation for assembly of stress fibers and focal adhesions in 3T3 fibroblasts. *Journal of Cell Biology*, 150(4), pp.797–806.

Turashvili, G. et al., 2007. Novel markers for differentiation of lobular and ductal invasive breast carcinomas by laser microdissection and microarray analysis. *BMC Cancer*, 7, p.55.

Uzman, A. et al., 2000. Molecular Cell Biology (4th edition) New York, NY, 2000, ISBN 0-7167-3136-3. *Biochemistry and Molecular Biology Education*, 29, p.Section 1.2The Molecules of Life.

Vidal, M. et al., 2007. Differing Src signaling levels have distinct outcomes in Drosophila. *Cancer Research*, 67(21), pp.10278–10285.

Vidal, M., Larson, D.E. & Cagan, R.L., 2006. Csk-deficient boundary cells are eliminated from normal drosophila epithelia by exclusion, migration, and apoptosis. *Developmental Cell*, 10(1), pp.33–44.

Vieira, A.F. et al., 2014. P-cadherin signals through the laminin receptor α6β4 integrin to induce stem cell and invasive properties in basal-like breast cancer cells. *Oncotarget*, 5(3), pp.679–692.

Vignjevic, D. & Montagnac, G., 2008. Reorganisation of the dendritic actin network during cancer cell migration and invasion. *Seminars in Cancer Biology*, 18(1), pp.12–22.

Vinckier, A. & Semenza, G., 1998. Measuring elasticity of biological materials by atomic force microscopy. In *FEBS Letters*. pp. 12–16.

Wang, E. & Goldberg, A.R., 1976. Changes in microfilament organization and surface topogrophy upon transformation of chick embryo fibroblasts with Rous sarcoma virus. *Proceedings of the National Academy of Sciences of the United States of America*, 73(11), pp.4065–4069.

Wang, W. et al., 2004. Identification and testing of a gene expression signature of invasive carcinoma cells within primary mammary tumors. *Cancer Research*, 64(23), pp.8585–8594.

Wang, W.-S. et al., 2010. The expression of CFL1 and N-WASP in esophageal squamous cell carcinoma and its correlation with clinicopathological features. *Diseases of the esophagus : official journal of the International Society for Diseases of the Esophagus / I.S.D.E*, 23(6), pp.512–521.

Wear, M.A., Schafer, D.A. & Cooper, J.A., 2000. Actin dynamics: Assembly and disassembly of actin networks. *Current Biology*, 10(24).

Weigelt, B., Geyer, F.C. & Reis-Filho, J.S., 2010. Histological types of breast cancer: how special are they? *Molecular oncology*, 4, pp.192–208.

Weinberg Robert A., 2007. *The biology of Cancer*,

Wilson, G.R. et al., 2006. Activated c-SRC in ductal carcinoma in situ correlates with high tumour grade, high proliferation and HER2 positivity. *British journal of cancer*, 95(10), pp.1410–4.

Winkelman, J.D. et al., 2014. Ena/VASP Enabled is a highly processive actin polymerase tailored to self-assemble parallel-bundled F-actin networks with Fascin. *Proceedings of the National Academy of Sciences of the United States of America*, 111(11), pp.4121–6.

Winograd-Katz, S.E. et al., 2011. Analysis of the signaling pathways regulating Src-dependent remodeling of the actin cytoskeleton. *European Journal of Cell Biology*, 90(2-3), pp.143–156.

Wu, P.-H. et al., 2014. Three-dimensional cell migration does not follow a random walk. *Proceedings of the National Academy of Sciences of the United States of America*, 111(11), pp.3949–54.

Xu, W. et al., 2012. Cell Stiffness Is a Biomarker of the Metastatic Potential of Ovarian Cancer Cells. *PLoS ONE*, 7(10).

Yager, M.L. et al., 2003. Functional analysis of the actin-binding protein, tropomyosin 1, in neuroblastoma. *British journal of cancer*, 89(5), pp.860–3.

Yeatman, T.J., 2004. A renaissance for SRC. *Nature reviews. Cancer*, 4(6), pp.470–80.

Yim, E.K.F. et al., 2010. Nanotopography-induced changes in focal adhesions, cytoskeletal organization, and mechanical properties of human mesenchymal stem cells. *Biomaterials*, 31(6), pp.1299–1306.

Zhang, S. & Yu, D., 2012. Targeting Src family kinases in anti-cancer therapies: Turning promise into triumph. *Trends in Pharmacological Sciences*, 33(3), pp.122–128.

Zhang, X.H.F. et al., 2009. Latent Bone Metastasis in Breast Cancer Tied to Src-Dependent Survival Signals. *Cancer Cell*, 16(1), pp.67–78.

ITQB-UNL | Av. da República, 2780-157 Oeiras, Portugal
Tel (+351) 214 469 100 | Fax (+351) 214 411 277

www.itqb.unl.pt